# Improving lightning performance on high voltage overhead shielded networks by reducing tower footing earthing resistance

**Nivern Naidoo**

**205507095**

In fulfilment of the requirements for the degree of

MSc. Electrical Engineering,

College of Agriculture, Engineering and Science

University of KwaZulu-Natal

18 February 2019

Supervisor: Dr. A.G. Swanson

# COLLEGE OF AGRICULTURE, ENGINEERING AND SCIENCE

## DECLARATION 1 - PLAGIARISM

As the candidate's Supervisor I agree/do not agree to the submission of this dissertation.

Signed:

I, Nivern Naidoo, declare that

1. The research reported in this dissertation, except where otherwise indicated, is my original research.

2. This dissertation has not been submitted for any degree or examination at any other university.

3. This dissertation does not contain other persons' data, pictures, graphs or other information, unless specifically acknowledged as being sourced from other persons.

4. This dissertation does not contain other persons' writing, unless specifically acknowledged as being sourced from other researchers. Where other written sources have been quoted, then:
   a. Their words have been re-written but the general information attributed to them has been referenced
   b. Where their exact words have been used, then their writing has been placed in italics and inside quotation marks, and referenced.

5. This dissertation does not contain text, graphics or tables copied and pasted from the Internet, unless specifically acknowledged, and the source being detailed in the dissertation and in the References sections.

Signed…….

# DECLARATION 2 - PUBLICATIONS

Details of contributions to publications that form part and/or include research presented in this dissertation:

Conference Paper:

N Naidoo, MF Khan, AG Swanson, "Improving lightning performance on high voltage overhead shielded networks by reducing tower footing earthing resistance." *Southern African Universities Power Engineering Conference, University of the Witwatersrand,* 2018

N Naidoo, MF Khan, AG Swanson, "Improving lightning performance on high voltage overhead shielded networks by reducing tower footing earthing resistance.": *Recommended by reviewers to be submitted for further review for further publication in the SAIEE Africa Research Journal (SAIEE ARJ).*

# Acknowledgements

I would like to thank my supervisor Dr Andrew Swanson for his support and guidance from the beginning of the research till the very end. I would like to thank my industry mentor Mohamed Khan, who has guided me from my EIT mentorship and continues to do so.

I would like to thank my family and friends for their endless support during my research and long hours.

# ABSTRACT

An investigation on the use of additional earthing to improve line lightning performance of Sub-Transmission lines by reducing backflashovers was undertaken. On Sub-Transmission lines (88 kV and 132 kV) the lightning performance is very important, particularly in regions where there is a high ground flash density. Backflashovers occur when lightning strikes the shield wire or the earth tower and the voltage across the phase insulator is high enough to cause breakdown. The breakdown leads to an AC fault causing circuit breaker tripping (which may auto reclose or lockout). This results in downtime for the line and as such any improvement is important.

A section of a poorly performing line (54 Faults/100km) is simulated in TFlash based on the line parameters and measured earth electrode resistances and its base case lightning performance was found to be 22 backflashovers per year. The high earth electrode resistance was between 20 and 60 Ω which was shown to be the major cause for the backflashovers.

Various earth electrode configurations were investigated, where it was shown that a combination of shorter parallel conductors were suitable and were designed for optimal performance while also being an economical solution.

It was shown in the simulation that by decreasing the earth electrode resistance, which was the most economically feasible option, the line performance was improved to 2 backflashovers per year. This would reduce the faults that the line would experience.

The proposed earth electrodes were installed on the section of the line, resulting in a significant reduction of the tower footing resistance. Over a two year period, the faults on the line were reduced by over 81%.

# TABLE OF CONTENTS

# LIST OF FIGURES

# LIST OF TABLES

# CHAPTER 1 INTRODUCTION

## 1.1 BACKGROUND

The lightning performance of overhead power lines in South Africa is critical in ensuring continuous power delivery to customers. Power line networks of 88 kV and 132 kV voltage levels are distributed throughout South Africa using shielded overhead steel lattice towers. These networks transverse high lightning corridors and are exposed to lightning current magnitudes that when striking to or near the line may result in line insulator flashover. Lightning flashovers are the most common cause of distribution line (88 kV and 132 kV lines) outages. Lightning flashovers are a result of one of the following three mechanisms; induced overvoltages, earthwire shielding failure and backflashovers. Backflashovers is the dominant cause of lightning flashovers on 88 kV and 132 kV lines.

Backflashovers occur when lightning current strikes the shieldwire and dissipates down the tower. The earthing impedance of the tower determines the voltage rise of the tower. On a high impedance tower the subsequent voltage rise from a high current magnitude strike may cause a flashover from the tower, across the insulator, to the phase conductor [1].

The consequences of poor lightning performance of high voltage lines are a high number of flashed insulators, increased maintenance cost placed on the utility and earth faults that result in substation breaker operation. This affects the utilities supply to customers, its network performance, operating costs and degrades substation plant equipment.

This research has focussed on the backflashover mechanism and improving line performance by reducing tower footing resistance. Line simulations were done using an electromagnetic transient program to model the lightning impact on a network. Simulations were also done on various earthing electrode configurations to find a solution that reduces tower footing resistance.

On existing HV lines the current method to reduce tower footing resistance was to introduce a mixture of horizontal and vertical earth electrodes. It is common that the approach adopted is often left to the person on site to determine best orientation and placement of electrodes. The dissertation presents some theoretical understanding for the electrodes that were chosen and the resultant impact on the performance of the line.

## 1.2 REVIEW OF ESKOM STANDARDS

The Eskom earthing standard for Sub Transmission lines (33 kV to 132 kV) requires that earthing of steel tower legs be connected to the reinforcing rebar within the concrete foundation [2].

The standard stipulates that for 88 kV lines the tower footing resistance must not exceed 20 Ω. When this value is not achievable the standard prescribes remedial actions to achieve the 20 Ω target. These actions are:

Install a 15 m horizontal counterpoise, bare copper, on two opposite legs of the tower.

- If the above does not achieve the target resistance then additional counterpoises are to be installed at perpendicular angles to those already installed.
- For rocky areas, the counterpoise can be encased in conductive cement, high carbon content.
- The use of a vertical termination spike at the end of the counterpoise is only mandatory where space permits.

The standard is not descriptive on the following items:

- Counterpoise length
- Horizontal counterpoise instead of a crow's foot
- Theft deterrent materials
- Civil considerations of counterpoise installation

The standard is open ended and can lead to poor interpretation and implementation if not careful. The standard does not distinguish between a low, medium and high lightning flash density. It could be argued that in a low lightning density area a line with high tower footing resistance, but acceptable back flashover performance, does not require tower footing improvement. As such, the lightning performance and the improvement of the line should be considered in conjunction with the tower footing resistance.

## 1.3 RESEARCH PROBLEM STATEMENT

This research has focussed on reducing lightning backflashovers by improving tower footing earthing resistance. There are a number of internationally published papers and books on improving lightning performance by reducing tower footing resistance. EPRI and IEEE have contributed extensively on the theory of tower footing resistance and on electrode design. However they do not provide a preferred electrode configuration that can be used on 88 kV and 132 kV networks taking into consideration economic and practical considerations [3], [4].

This research provides practical solutions for industry and utilities to improve their lightning performance of overhead HV lines.

This research compared simulated tower footing resistance improvement, taking into account various variables, against actual improvement. It involved the design and installation of additional earth electrodes on chosen towers. It took into account practical aspects of installing earth electrodes such as the following:

- Dimensions of earth electrode
- Depth and positioning of earth electrodes in ground
- Spacing of electrodes to avoid coupling
- Theft deterrent materials – alternate material selection to a full copper solution
- Corrosion and longevity of installed earth electrodes
- Total cost of solution

This research would contribute in guiding utilities to improve their performance of existing high voltage lines and influence the design of new lines in high lightning corridors.

## 1.4 METHODOLOGY

This research is based on an Eskom 88kV line in KwaZulu-Natal. A simulation model of the line was developed in TFlash with actual measured tower footing resistance values. An electrode design was then discussed and presented, and the effect of this electrode design in improving tower footing resistance and line performance is shown in the simulation. The electrodes were then manufactured and installed on the line. The new measured tower footing resistance values were compared to the simulated improvement. The line performance was then monitored during the next storm season and compared to the simulation results.

## 1.5 OUTLINE OF CHAPTERS

Chapter 2 contains the literature review relevant for this dissertation. It describes the lightning waveform and its interaction on overhead lines. It gives a description of the lightning detection network used by Eskom and the software available to analyse lightning impact on Eskom powerlines. It presents the mechanics of the lightning flashover process in particular backflashovers. It covers wide band frequency response of the tower and the earthing system for a lightning impulse. The effect of soil ionisation is also discussed. It also introduces the simulation program, TFlash, which was used in this research.

Chapter 3 introduces a transient simulation program that is used to model lightning performance of a line. A base case simulation of a line was performed and is presented.

Chapter 4 covers the theory required to design an electrode system for high frequency applications. Various electrode configurations were simulated and a suitable design was proposed. It also covered material selection and practical design aspects for an earth electrode. The earth electrodes are manufactured and installed on towers with high tower footing resistance. The improved performance of the line is also presented.

Chapter 5 concludes the research.

# CHAPTER 2 LITERATURE REVIEW

## 2.1 INTRODUCTION

Earthing plays an important role in protection of a utility power system. Earthing is required for protection of plant equipment and safety to persons working on equipment. It does this by providing a low impedance path from the structure/substation to the mass of earth and to limit overvoltages [5].

However the topic is not widely understood and when a system is drawn on a single line diagram the earth or current return path is often overlooked and assumed to be in place and functioning correctly. There are many components to earthing on a power system grid from generator/source, substation, transmission line, distribution line, reticulation line and end user earthing.

This research concentrated on earthing of the distribution level (between 33 kV and 132 kV).

## 2.2 EARTHING ON OVERHEAD DISTRIBUTION LINES

Lightning flashovers are the most common cause of distribution line outages. There are costs involved such as damage to equipment, increase in maintenance costs and customer grievances from reduced quality of supply. There are various methods to improve line lightning performance but before exploring this, the mechanism of lightning and its impact is discussed [6].

An overhead shielded line compromises of the following earthing components (Figure 2.2-1).

- An overhead shieldwire. The function of the shieldwire is to protect the conductor from direct lightning strikes, prevent flashovers and to carry fault current back to the substation earth grid.
- The earthing conductor, on steel towers is the tower itself, connects the shieldwire to the earth electrode.
- Concrete foundation – the tower leg is connected to steel rebar and encased in a concrete foundation.
- A buried conductor (steel or copper) that extends from the concrete foundation out to the general mass of earth.

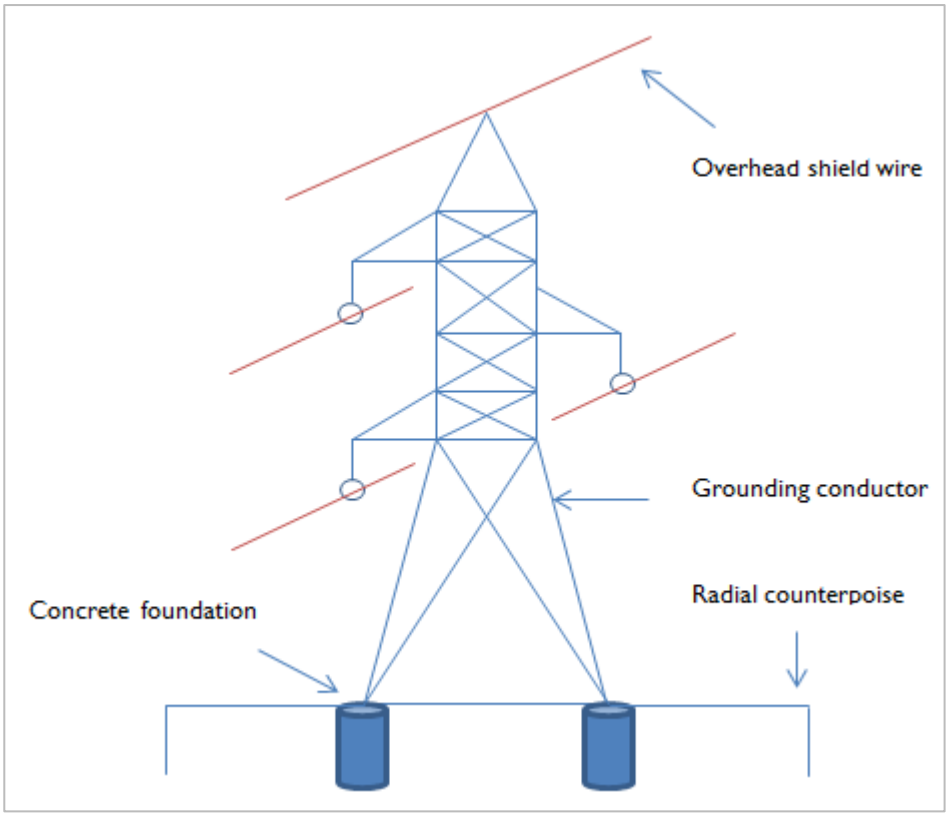


**Figure 2.2-1: Grounding components on an overhead shielded line**

## 2.3 FLASHOVER MECHANISM ON OVERHEAD LINES

The common terms used when describing lightning need to be reviewed first to better understand its impact on overhead lines [7].

- Flash – it is the entire electrical discharge from cloud to stricken object. A flash will comprise of multiple strokes.
- Stroke – the high current components in a flash. A flash will comprise of the first stroke and subsequent return stokes. The summation of these strokes will give the total flash current.
- Flashover – an electrical discharge from an energized conductor to a earthed end.
- Backflashover – an electrical discharge from a earthed end to an energized conductor. This may cause the substation feeder breaker to trip or may clear itself without tripping the substation feeder breaker.

## 2.4 THE LIGHTNING WAVEFORM

Overvoltages from lightning impulses are unipolar in nature and can be represented by the voltage waveform shown in Figure 2.4-1 [8].

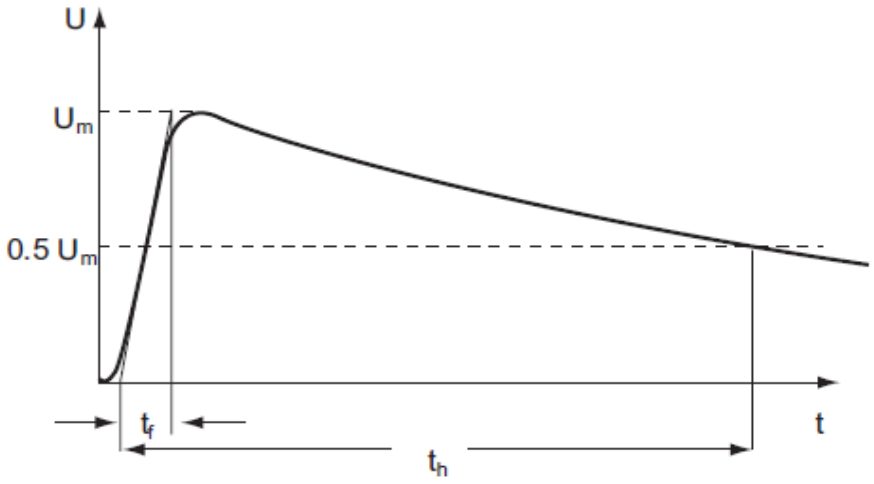


**Figure 2.4-1: Lightning impulse voltage waveform created on tower/line by lightning strike taken from [8]**

The standard lightning impulse voltage contains a fast rising front time reaching a peak, $U_{m,}$ then by a decaying tail. The front time $t_f$ is extrapolated from the 10% and 90% levels. The decay time of the tail $t_h$ is calculated as half the of the peak voltage.

Translating this into the time domain, the rise time of the standard wave is between 1-2 μs and the time to half value is between 40-60 μs. This impulse waveform is usually expressed in terms of the peak voltage $U_m$ and $t_f/t_h$. IEEE Standard 4-2000 [9] specifies the standard lightning impulse voltage as 1.2/50 μs. When lightning terminates on the shieldwire the tail time will reduce due to the impedance of the shieldwire and parallel connections of the structures to ground.

A CIGRE working group analysed various measured stroke current waveforms. From this the CIGRE waveform for lightning stroke current was proposed, Figure 2.4 2, is defined as follows [10]:

$I_p$ The peak of the stroke current

$S_m$ The maximum rate of rise (steepness) of the stoke current

$T_{eq}$ The minimum equivalent front time defined as $I_f/S_m$

$T_f$ The equivalent front duration defined as $I_f/S_{30/90}$

$T_h$ Stroke duration defined as the time between the trigger value (2 kA) on the wave front and the time on the wave tail where 50% of the peak value ($0.5I_p$) is reached.

The CIGRE waveform is preferred in calculations because the maximum steepness occurs close to the peak of the waveform.

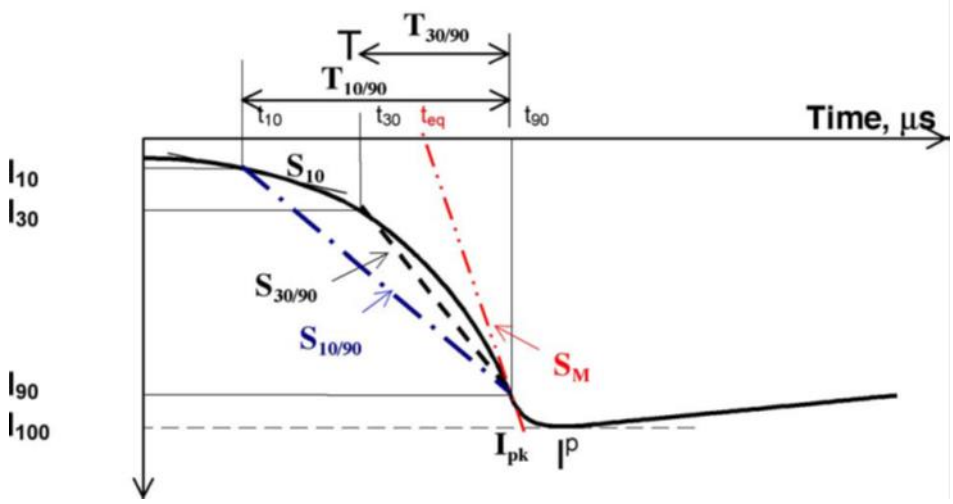


**Figure 2.4-2: Crest and front time parameters for a CIGRE current wave taken from [10]**

### 2.4.1 SUBSEQUENT STROKES

The first stroke in a lightning flash is called the return stroke and the strokes that follow are called subsequent return strokes.

Once the first lightning stroke (return stroke) in a flash terminates, the already ionised lightning channel can re illuminate with a subsequent return stroke that can terminate on or near the vicinity of the first stroke. Case studies show that the average number of strokes in a flash are between 3 -5.

Uman [11] suggests an average number of three subsequent strokes per flash, based on studies in South Africa and Florida. Anderson [12] recommended a global average ground-flash consisting of three strokes, one return stroke and two subsequent strokes, for a negative flash.

However, this number can be much higher. Hence when performing lightning studies one must consider the total lightning stroke current (in a flash) and use this to determine line lightning performance.

## 2.5 NUMBER OF LIGHTNING STROKES TO A LINE

The number of lightning strokes to a line or lightning incident rate is used to describe the probability of lightning hitting the line over a period of time. The determination of line lightning rate over a specific

area is expressed as the number of flashes per 100 km per year. There are various equations that describe the number of strokes per year experienced by a line. These equations require the area GFD (Ground Flash Density) map.

The equation used to calculate a line lightning incident rate as recommended by IEEE and CIGRE is described by Eriksson [13] in Equation 2.5-1.

$$\boldsymbol{Ns = \frac{GFD}{10}\left(28{h_t}^{0.6} + b\right)} \quad (2.5\text{-}1)$$

Where:

$N_s$ is the number of flashes to a line per 100 km per year

*GFD* is the ground flash density (flashes/km$^2$/year)

$h_t$ is the tower shieldwire height at the tower (m), and

*b* is the horizontal separation distance between shieldwires (m) – structure dependent.

Eriksson uses the shieldwire height at the connection point to the tower in his equation. More recent equations use the average height of the shieldwire above ground which is calculated by the tower height minus two thirds of sag.

## 2.6 FALLS OVERVIEW AND BRIEF DESCRIPTION OF DETECTION NETWORK

The Fault Analysis and Lightning Location System (FALLS) is a software program used by Eskom to overlay lightning events on its network infrastructure. The system gathers lightning information from South African Weather Services (SAWS). There are 22 sensors installed over South Africa and 1 in Swaziland [14] .

The lightning density map is critical in determining the exposure of line assets to lightning. It is vital in the line construction design and in determining the insulation strength, type of earthing used and even the route the line will traverse. FALLS allows the user to select their required asset for analysis. All Eskom assets i.e. substations and overhead lines are loaded onto FALLS as map data. It uses this asset info, coordinate location, to determine its lightning exposure over a selected period and for a selected analysis. There are three type of analysis available on the FALLS system namely, Gridded Exposure Analysis, Small Area Exposure analysis and Reliability Analysis.

### 2.6.1 GRIDDED EXPOSURE ANALYSIS

The Gridded Exposure Analysis is used to determine the flash or stroke density of a region or an asset over a selected time. A 5 year time period is preferred for this analysis as it takes into account seasonal weather fluctuations. The data is averaged and returned as strokes/flashes/per sq. km/year.

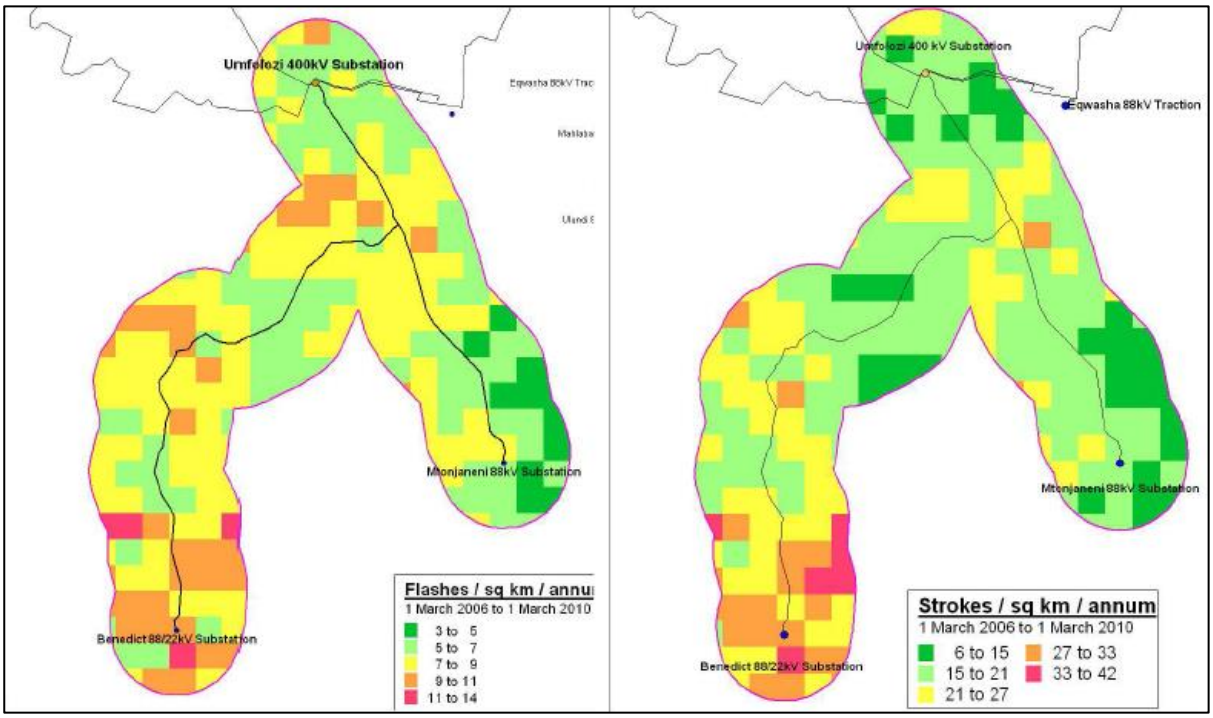


**Figure 2.6-1: Image on the left is a flash density map of an 88 kV overhead line for the period March 2006 to March 2010. The image on the right is a stroke density map of the same asset over the same period.**

From Figure 2.6-1 it can be seen that a lightning flash is made up of multiple strokes. In this example it is approximately a factor of 3 from the flash density map to stroke density map. This is an important map in determining the lightning risk profile of an asset. When doing simulations one can use accurate lightning density information to calculate expected performance of an asset. This type of analysis does not provide specific lightning details but merely a density map.

### 2.6.2 SMALL AREA EXPOSURE ANALYSIS

The Small Area Exposure Analysis provides information on individual lightning strokes over a selected period. The information provided is the number of lightning strokes on an asset, within a buffer region, the current magnitude (kA) for each strike, the polarity of the stroke and the date and time of the stroke.

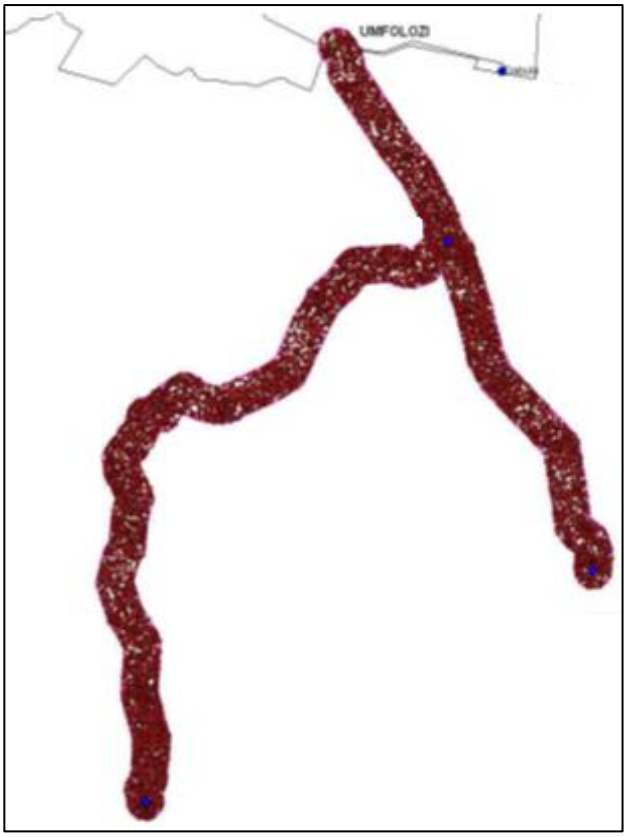


**Figure 2.6-2: Small Area Exposure Analysis of an 88kV overhead line for the period March 2006 to March 2010**

Each lightning stroke, Figure 2.6-2, is represented as a red dot. A buffer region of 1 km around the asset is chosen to cater for inaccuracies in the lightning detection network. Each red dot has a subset of information i.e. date and time, GPS coordinates, magnitude of stroke and polarity of stroke. This analysis is important in determining the current magnitude (kA) exposure of an asset. In determining line performance the current can be plotted as statistical distributions to determine the percentage of strikes that may result in exceedance of line insulation and cause insulator back flashover. In Eskom KZN the analysis conducted on various assets have revealed that in high flash density areas the resultant flash (multiple strokes down same lightning channel within 400 ms) current magnitude far exceed the line insulation. This is of particular concern on 88 kV networks due to the lower BIL (450 kV) of insulators.

### 2.6.3 RELIABILITY ANALYSIS

The reliability analysis is usually done after a line trip. To determine if lightning was the cause of the trip a reliability analysis is done. First the trip time of the line breaker must be known. This time together with the line asset is entered into FALLS and all lightning closest to this time is plotted on the line. When doing the analysis it is best practice to use a buffer of 60 s either side of the breaker trip time. This is to

account for time discrepancies from incorrect breaker remote terminal unit (RTU) stamping or lightning detection network time inaccuracies. The returned results are seen in Figure 2.6-3.

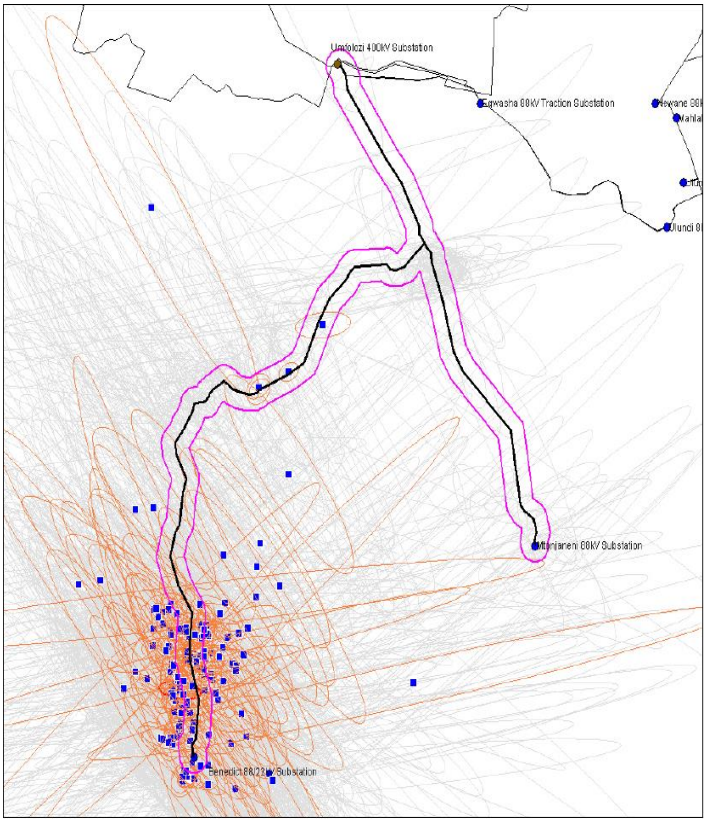


**Figure 2.6-3: Reliability analysis of selected asset**

All lightning strokes around the entered time and buffer time are displayed as blue dots. By selecting the dot closest to trip time one can determine the tower location and current magnitude of the stroke that caused the line trip. The tower footing resistance can then be tested and subsequent remedial measures implemented. During this analysis it is important to note that a flash will compromise of multiple strokes within a 400 ms window. If the strokes travel down the same lightning channel they usually terminate at the same point and thus the resultant summation of stroke current within the flash can be significant such that the tower voltage exceeds the flashover strength on the line insulator.

## 2.7 THE LIGHTNING FLASHOVER PROCESS

The interaction of lightning on high voltage overhead lines and its response can be described by the following three mechanisms [15]:

1. Induced overvoltages: When lightning strikes near power lines it induces voltages on the phase conductors. These voltages do not exceed 300 kV [15] hence they do not pose a risk of insulator

flashover on 88 kV and 132 kV networks. For 88 kV insulators used in Eskom the basic insulation level is 450 kV and for 132 kV insulators it is 550 kV.

2. Earthwire shielding failure: Overhead shielded networks are designed for lightning to strike and distribute along the shieldwires and dissipate through the tower earthing. The shieldwire protects the phase conductors against direct lightning strikes. When shielding failure occurs, lightning strikes the phase conductor directly. If the lightning current magnitude is high enough, the subsequent voltage rise may result in insulator flashover

3. Backflashover: This occurs when lightning current strikes the shieldwire and dissipates down the tower. The earthing impedance of the tower determines the voltage rise of the tower. On a high impedance tower the subsequent voltage rise from a high current magnitude strike may cause a flashover from the tower, across the insulator, to the phase conductor. This is called a backflashover.

This research focussed on the backflashover mechanism and improving line performance by reducing backflashovers.

As stated induced flashovers are not a concern on 88 kV and 132 kV structures. Shielding failures rarely occur in practice and if prevalent will point to a design issue rather than an earthing issue. There are industry methods to determine shielding failure based on calculations.

## 2.8 LINE INSULATION

The dielectric strength of an overhead tower line insulation under lightning conditions is determined by the shortest distance required from a live conductor (phase conductor) to earth ground (tower cross arm, insulator hardware connected to tower). Under lightning conditions this is typically the distance across an insulator. This distance varies on the phase voltage as a higher phase voltage will require a longer length insulator. To determine the dielectric strength, under lightning conditions, voltage impulses at different voltage levels are applied across the insulation to determine the probability of flashover. These tests can be described by a Gaussian distribution [16].

The Critical Flashover Voltage (CFO) of an insulator is the maximum steepness of an impulse wave that causes flashovers on 50% of the number of applied impulses.

Basic Insulation Level (BIL) is the electrical strength of insulation expressed in terms of the maximum steepness of a standard lightning impulse that causes flashovers on 10% of the number of applied impulses.

BIL can be calculated as follows:

$$\boldsymbol{BIL = (1 - 1.28c)CFO} \tag{2.8-1}$$

Where:

*c* is the normalized standard deviation.

## 2.9 OCCURRENCE OF BACKFLASHOVER

Backflashovers are the dominant cause in lightning related line trips. Backflashovers are dependent on several factors. These include tower footing earth impedance, soil ionisation of local electrode, coupling between the shieldwire and phase conductor, distribution of current along the shieldwire and down the structure.

An 88 kV tower was modelled in TFlash, shown in Figure 2.9-1. In this model a lightning impulse, CIGRE waveform, was injected down a tower. The voltage rise can be described with a simplified model which consists of an inductor, representing the tower impedance, with a series resistor that represents the earth resistance. The tower voltage can be determined as [17]:

$$\boldsymbol{V(t) = L\frac{dI(t)}{dt} + RI(t)} \tag{2.9-1}$$

From Equation 2.9-1 it can be seen that the maximum steepness (kA/μs) of the lightning current waveform will result in the highest voltage build up across the tower. Thus the highest voltage build up across the resistor will occur at peak current level (kA). This translates to the first 2 μs of a CIGRE waveform as being highest probability for insulator backflashover.

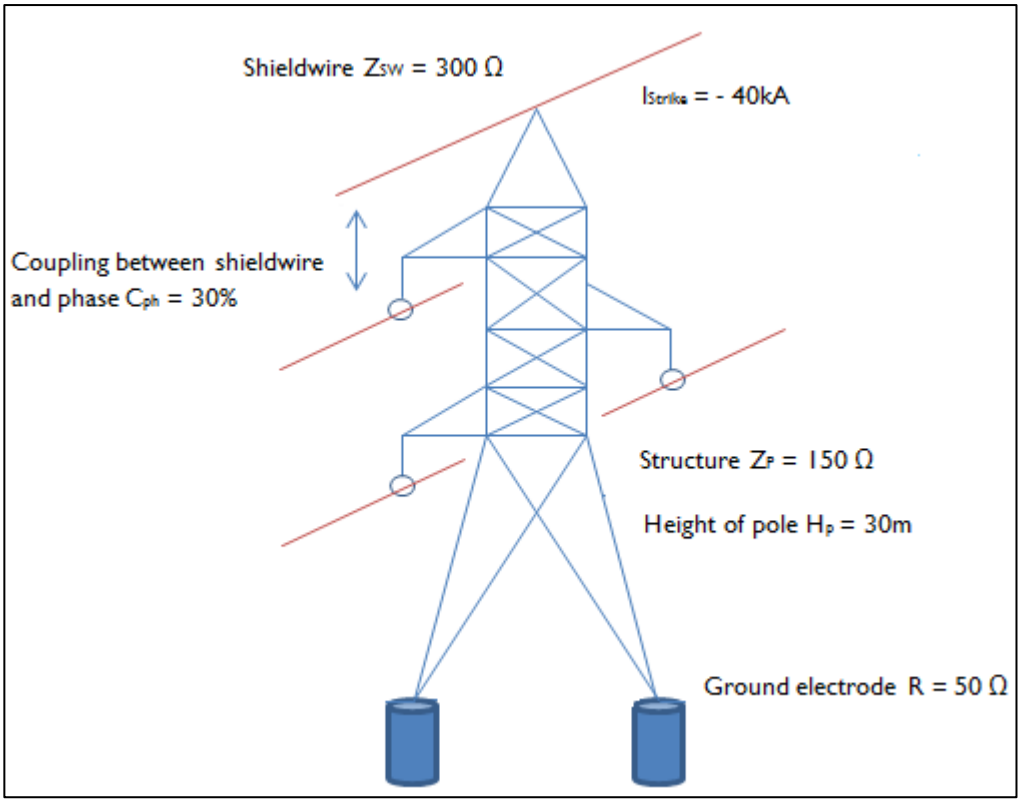


**Figure 2.9-1: Example for calculating the voltages generated during a lightning strike to a transmission line.**

Equation 2.9-1 is a simplified explanation of the tower response for a lightning strike. A more detailed explanation would consider the surge impedance of the shieldwire and tower, the coupling between the phase conductor and shieldwire and the refection wave from the earth electrode.

Using the same parameter as in Figure 2.9-1 the current and voltage travelling waves can be illustrated by the approach illustrated below [18].

- The lightning current divides between the shieldwire and tower based on their impedances. The shieldwire impedance is given as 300 Ω and the tower is 150 Ω [7]. Accordingly 50% of the current will travel down the tower with the remainder, 25% in each side, on the shieldwire.

$$I'_P = \frac{Z_{SW}}{Z_{SW} + 2Z_P} \times I_{Strike} \quad (2.9\text{-}2)$$

- The current surge will travel down to the tower base. The time it takes to reach the base is dependent on the height of the tower. The propagation speed of a lightning wave for a conductor in air is 300 m/µs. In this example a tower height of 30 m will result in the current surge taking 0.1 µs to reach the base. Part of the current will be transmitted to the earth electrode and part will be reflected back up the tower.

*Transmitted part:*

$$\boldsymbol{I_g = \frac{2Z_P}{Z_P + R_g} \times I'_P} \quad (2.9\text{-}3)$$

*Reflected part:*

$$\boldsymbol{I''_P = \frac{R_g - Z_p}{Z_P - R_g} \times I'_P} \quad (2.9\text{-}4)$$

- The reflected part will reach the top of the tower after 0.2 μs (after the initial strike). The net current at the tower top is the sum of the incident and reflected currents. Note that the resistance of the earth electrode is important for the reflected waveform.

- The voltage at tower top is calculated by

$$\boldsymbol{V_T = I_P \times Z_P} \quad (2.9\text{-}5)$$

- The coupling between the shieldwire and phase conductor is approximated to 30% i.e. the induced voltage from the shieldwire onto the phase conductor is 30%. The lightning surge currents that travel on the shieldwire are coupled onto the phase conductors thus raising the conductor voltage. Depending on the spacing between the phase conductors and shieldwire this coupling coefficient can be between 15% - 35% ($C_{ph}$). That is the voltage on the phase conductor can be between 15% - 35% of the voltage on the tower top and with the same waveform.

- The voltage across the insulator can be calculated as follows:

$$\boldsymbol{V_i = V_T \times (C_{ph} - 1)} \quad (2.9\text{-}6)$$

## 2.10 EARTH ELECTRODE RESPONSE

### 2.10.1 EARTH ELECTRODE RESISTANCE

Equations 2.9-2 - 2.9-5 show the importance of the earth electrode resistance on the reflected current wave. The earth electrode resistance is the most important factor in reducing line backflashovers.

When the earth electrode resistance is lower than the structure surge impedance the reflected current wave from the tower base will be negative. This will result in partial cancellation of the incident wave which will lead to a lower tower top voltage. This highlights the importance of the earth electrode in reducing the voltage across the insulator. This is further illustrated in Figure 2.10-1 which shows the tower top voltage for varying earth resistance. The impact of the earth resistance was simulated in TFlash.

The voltage rise on a tower was simulated using a -30 kA lightning strike for a range of tower footing resistance 5, 10, 20, 40 and 60 Ω. It can be seen that once the tower footing resistance is increased the tower voltage increases thus the risk of tower back flashover increases. Accordingly the earth electrode resistance has a profound effect on reducing the voltage across the insulator. It must be noted that the maximum voltage rise on the tower is determined in the first 2 μs of the lightning impulse which corresponds to the maximum steepness [16].

For an 88 kV overhead line with a standard 88 kV insulator BIL (Basic Insulation Level) of 450 kV a tower with poor earth resistance (greater than 50 Ω) will result in a high number of backflashovers during lightning flashes. This effect is most significant on 88 kV lines due to the lower insulation BIL of 450 kV. As the line voltage increase, greater insulation levels, this effect reduces.

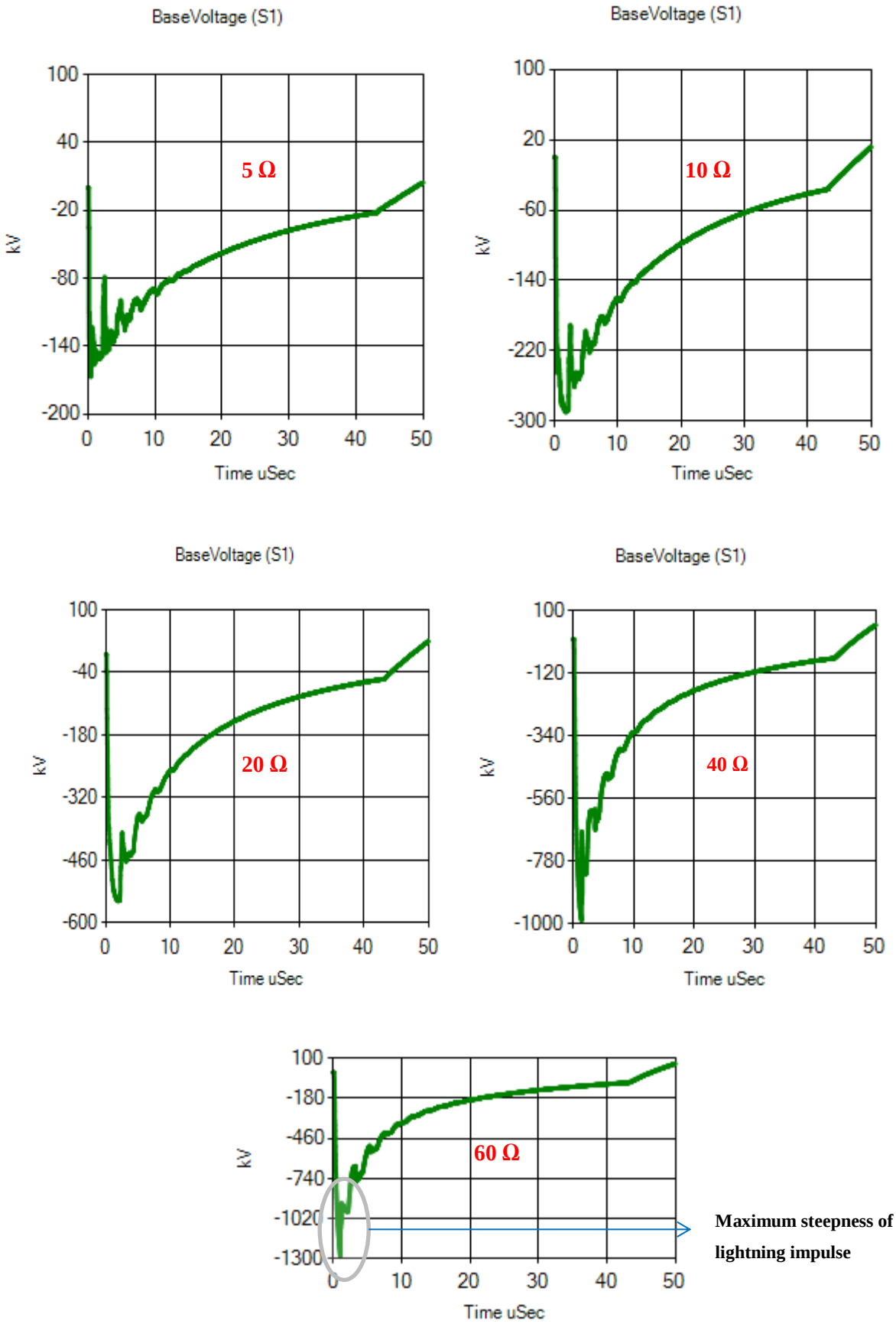


**Figure 2.10-1: Effect of the earth electrode resistance on the tower top voltage of the struck tower calculated using TFlash for varying resistances.**

### 2.10.2 RESPONSE OF TOWER FOOTING

The backflashover performance of a line is highly geared towards the tower footing resistance of the line. Power utility earthing standards states that the tower footing resistance on steel lattice towers is achieved through the concrete foundation and its contact to the surrounding earth. The earth electrode resistance can be thought of as constant for low frequency power system conditions (50 Hz). However for a lightning impulse the electrode response is very nonlinear. This dynamic behaviour of the earth electrode for a lightning impulse is difficult to calculate. Also the impact of soil ionisation needs to be considered.

A greater soil ionisation increases the lightning dissipation (kA) in the ground through breakdown of the soil and reduces the tower footing resistance. This reduces the voltage rise on the tower which reduces the risk of tower backflashover [19].

The Eskom standard for earthing of steel lattice towers is provided through the concrete foundations [2]. The concrete surrounds the tower foot rebar and is thus electrically connected to the tower leg. There is no external connection from the concrete to the surrounding material.

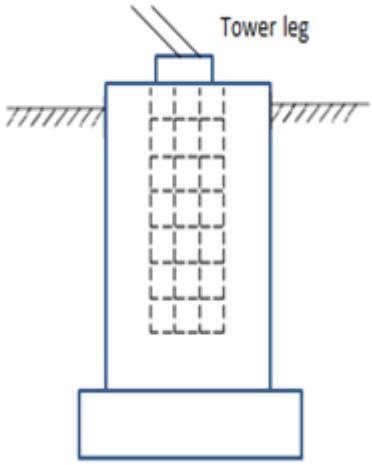


**Figure 2.10-2: Concrete foundation encasing tower leg, via steel rebar, as per Eskom Standard [2]**

The moisture content in the concrete, after some settling time, will reach equilibrium with the moisture in the soil surrounding it. This means the steel rebar can be viewed as been in direct electrical contact with the surrounding soil thus ignoring the concrete around it. During a lightning impulse, the high magnitude current may break down the soil and cause ionisation. However for concrete this is not the case as the concrete inhibits the formation of streamers. Thus when modelling a concrete foundation is must be treated as a constant resistance [20].

### 2.10.3 EARTH ROD RESISTANCE AND IONISATION

The resistance of an earth rod needs to be covered as it is one of the methods used to reduce tower footing resistance. For low frequency conditions, steady state with no soil ionisation, a vertical rod driven into the earth can be determined by Equation 2.10-1 [21]:

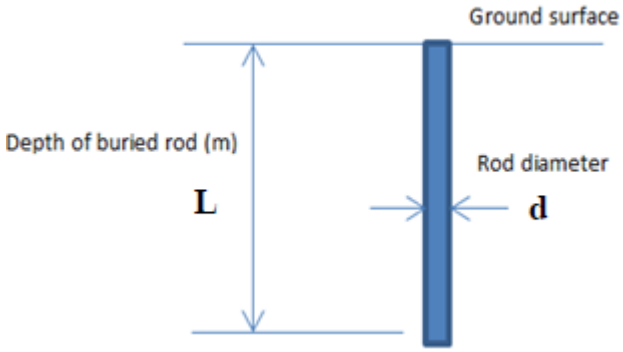


**Figure 2.10-3: Dimensions for a single vertical earth rod.**

$$\boldsymbol{R_0 = \frac{p}{2\pi L}\left[log\left(\frac{8L}{d}\right) - 1\right]} \tag{2.10-1}$$

Where:

$R_0$ = low frequency, low current resistance in Ω

$\rho$ = earth resistivity in Ω.m

$L$ = rod length in m

$d$ = rod diameter in m

The resistance $R_0$ is the resistance in a uniform infinite earth. This equation is used for low frequencies, low current conditions. It does not take account into lightning impulse currents, soil ionisation and variations in different soil layers. Hence this equation is not always applicable for dynamic situations.

For a lightning impulse on a vertical rod, the dynamic resistance of the earth rod will be less than its low frequency measurement. The voltage built up on the rod may be greater than the dielectric strength of the surrounding soil. This may lead to soil ionisation that consists of electrical streamers that has the effect of increasing the electrode surface area.

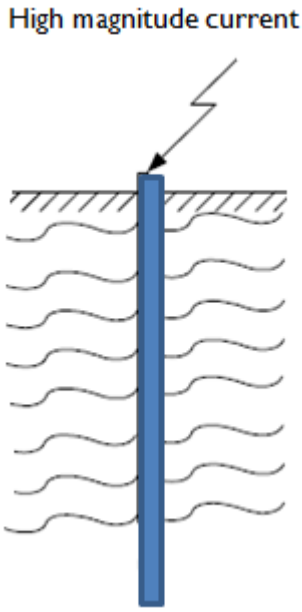


**Figure 2.10-4: Dielectric breakdown of soil around rod electrodes.**

It can be seen from Figure 2.10-4 that soil ionisation increases the electrical surface area (diameter) of the rod. From Equation 2.10-1 this will lead to a decrease in the rod resistance. Placing more rods in the ground will increase the soil ionisation and will reduce the rod resistance. This is an important concept in reducing the tower voltage and voltage across the insulator during a lightning strike.

EPRI conducted a study comparing the dynamic resistance for various earthing material shapes [22]. The study compared the reduction in dynamic resistance, for a lightning current surge, between a rectangular bar and round earth rod. It concluded that there is no difference in dynamic resistance for both geometries. The study concluded that variations in material geometries have little influence in the reduction of dynamic resistance for a lightning current surge.

A model was developed in TFlash to simulate the effect of soil ionisation on reducing tower footing resistance. A tower footing resistance of 50 Ω was used in all scenarios and varying current magnitudes, 1 kA, 10 kA, 15 kA, 20 kA and 30 kA, was applied. A concrete foundation with an externally connected counterpoise (5 m) and terminated with a 1.5 m vertical earth rod was used. The results are shown in Figure 2.10-5. An increase in current magnitude increased soil ionisation and thus reduced the tower footing resistance. Note, TFlash cannot model the frequency dependent behaviour of the earth electrode system hence the reduction in earth resistance, in the simulation, is localised to soil ionisation.

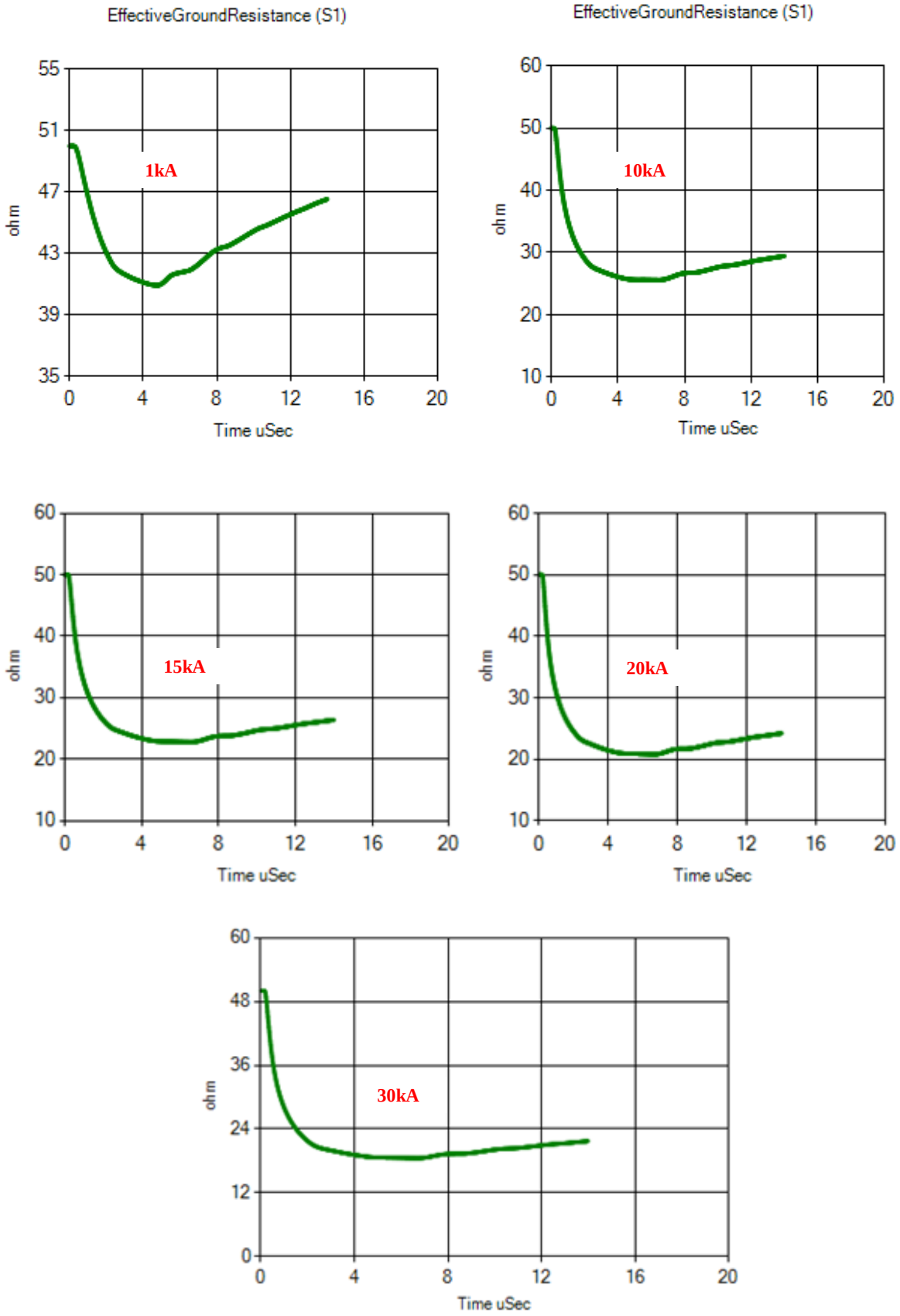


**Figure 2.10-5: Soil Ionization for varying current magnitudes**

## 2.10.4 CIGRÉ DYNAMIC RESISTANCE MODEL

There are various models for the dynamic resistance of earth rods. These models will be reviewed and a suitable model will be chosen. Actual electrical experiments on earth electrodes are difficult due to the limitations of the impulse generators being able to force to high frequency and magnitude currents into the earth electrode to correctly emulate the performance of an earth electrode.

The CIGRE model uses an earth rod that is modelled as a conducting hemisphere [23].

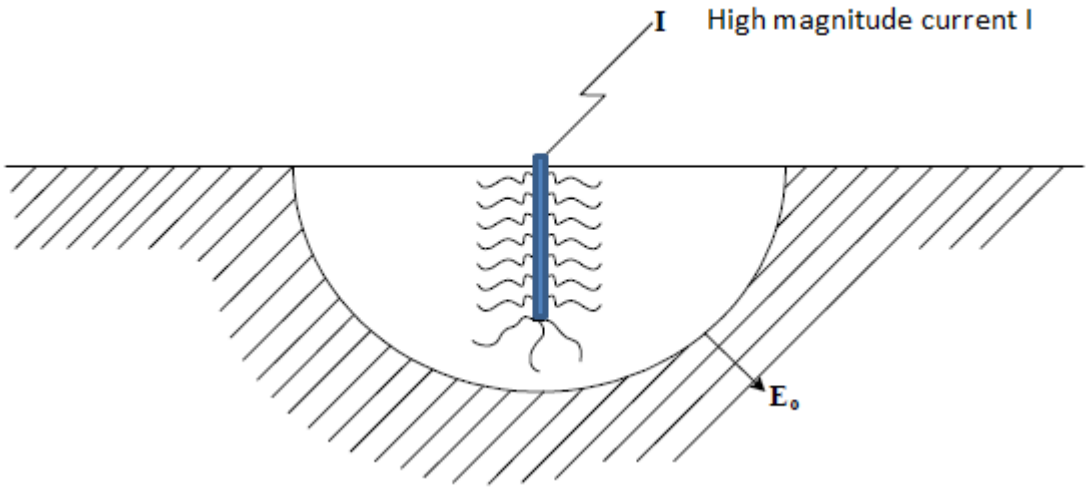


**Figure 2.10-6: Replacing an earth rod with a conducting hemisphere.**

In this model the hemispherical surface is approximated from the fact that the rods emit streamers and the resulting soil ionisation form a shape that represents a hemisphere.

One can also represent the dynamic resistance of a concrete foundation using an earth rod from the CIGRE model. This is derived as follows:

From Figure 2.10-1 the low frequency low current earth rod resistance $R_O$ is calculated as:

$$\boldsymbol{R_O = \frac{p}{2\pi r}} \tag{2.10-2}$$

Where $R_O$ = resistance in Ω

$p$ = soil resistivity in Ω.m

$r$ = sphere radius in m

The CIGRE Weck equation [23] replaces an earth rod with a foundation of low resistance:

$$I_O = \frac{PE_O}{2\pi R_O^2} \quad (2.10\text{-}3)$$

The high frequency dynamic resistance of the foundation can be represented by a spherical electrode as follows:

$$R = \frac{R_O}{\sqrt{\frac{I}{I_O}}} \quad (2.10\text{-}4)$$

Where $R$ = dynamic resistance in Ω

$R_O$ = low frequency, low current resistance in Ω

$I$ = instantaneous foundation current in kA

$I_O$ = a critical current when ionization starts in kA

## 2.11 WIDE BAND FREQUENCY NATURE OF ELECTRODE IN SIMULATION MODELS

The impedance of the earthing system is dependent on the frequency response of electrodes and the characteristic of the soil. The available transient programs have no way to account for the wide band frequency response of electrodes for a lightning impulse. The present time domain electromagnetic tools such as TFlash, ATP-EMTP and EMTP-RV are used to simulate line lightning backflashover performance. In these programs the frequency dependent behaviour of the tower footing system is not considered and the system is treated as a fixed resistor or lumped RLC circuit with static assumptions [24].

Modelling the high frequency behaviour of electrodes require electromagnetic field calculations. However these calculations are difficult to integrate into line transient programs. There has been recent progress in integrating electromagnetic field calculations into transient programs. However the shortcoming with this approach is that electromagnetic field solver must be reapplied whenever a new simulation is done [25], [26]. This becomes time consuming when changing line parameters in the simulation frequently.

A new method was proposed by Holdyk et al. [27]. In this method the field solver is run, for a variety of earthing systems at different frequencies, and then stored in a look up array. The stored results are then uploaded to the transient program for use. This eliminates the need to rerun the field solver when changing parameters in the line simulator program. The conclusion from this paper shows that the wide

band frequency modelling of tower electrodes (producing a tower voltage) is greater than 11 – 19% from that of traditional resistance models evaluated at power system frequency. However the proposed approach does not take into account the effect of soil ionisation at high frequency that reduces tower impedance. The effect of soil ionisation is significant as seen in Figure 2.10-5 and cannot be overlooked in the simulation.

A method proposed by Alemi et al. [28] uses a earthing system admittance matrix over a wide frequency range that is obtained from using the method of moments solution to Maxwell's equations. A pole residue model is then obtained which feeds into a transient program. The study modelled a 132 kV line earthing system for the following 3 conditions:

- Static model as per traditional transient programs.
- Wide band frequency model but assuming constant soil parameters i.e. no soil ionisation.
- Wide band frequency model assuming frequency dependent soil parameters i.e. the effect of soil ionisation.

The studies concluded that point 2 and 3 reduced the overall tower footing earthing impedance and the back flashover rate.

The above methods are computer simulated models. There have been numerous practical experiments conducted to measure the frequency response behaviour of an earthing system including horizontal and vertical earthing.

Ullah et al. [29] conducted practical experiments on a buried horizontal counterpoise to determine the frequency response and the voltage and current measurements at different points along the electrode for an applied lightning impulse. A current impulse with a magnitude of 5.4 A was applied with a waveform of 5.8/16 μs. The counterpoise length was 88.5 m, with a cross sectional area of 0.2 $cm^2$ buried at 30 cm. The experiment conducted that majority of current injected was dissipated near or around the injection point and the current waveform dampened when measuring towards the end of the electrode.

A similar study conducted by Choi et al. [30] on a 50 m length horizontal electrode, 3 mm in diameter buried in 0.5 m. The length of the 40 m electrode was divided into four 10 m sections. At one end of the electrode an earth enhancing, carbon, material mixed with the soil was used to create a low resistivity soil type. Another section along the electrode used a high soil resistivity soil type. Different Impulse currents with rise-times of 4 μs and 39 μs were injected to the horizontal electrode. It was observed for the fast impulse rise time the earthing impedance was inductive and the slow rise time displayed a resistive behaviour. The experiment conducted that majority of current injected was dissipated near or around the injection point and the current waveform dampened when measuring towards the end of the electrode.

# CHAPTER 3 LIGHTNING PERFORMANCE OF LINE

To identify a line that has poor lightning performance:

- The number of trips for a line must be quantified. This is easily obtainable from a network data base.
- Normalise the number of trips to number of faults per 100 km (Faults/100 km).

There are international benchmarks on an acceptable Faults/100km. When determining this number, factors such as customer base served, alternate line supply and load capacity must also be taken into account when prioritising improvement on lines. The number used in Eskom for 88 kV and 132 kV lines is 10 Faults per 100 km.

For the total fault count, auto reclosers (ARCs) and permanent faults must be added. The difference between the two is simply based on the fault location. In this study, poor performing lines as a result of lightning are identified as follows:

- Make use of FALLS to determine if lightning is the root cause of trips.
- If available look at the construction documents to obtain results of tower footing resistance prior to stringing of shieldwire.
- If there are no tower footing resistance values available, site testing would have to be done to obtain values. A suitable high frequency meter must be used.
- Load tower footing results, structure parameters, line flash density into a suitable transient program to determine line performance.

Use a line transient program to simulate various mitigation scenarios such as additional earthing, line surge arresters or increasing line insulation level to reduce backflashovers. The practicality and economic cost of each solution must be considered.

## 3.1 CASE STUDY OF AN 88 KV OVERHEAD LINE

This research has focussed on a line that experienced a high interruption rate from lightning backflashovers.

The research aims to simulate the line problem, provide various solutions and put forward results from the implementation of a chosen solution. A simulation model, using a transient program, was developed to account for the wide band nature of the lightning impulse problem. The model provides voltage and current profiles at the tower and across the insulator for an applied lightning current surge. It also simulates the response of different electrode configurations during a lightning current surge. This determined the electrode configuration chosen.

The line model was developed using EPRI's Transmission Line Workstation software which makes use of TFlash.

## 3.2 BACKGROUND

The simulated line is 48.3 km long and supplies three substations. The line is strung with WOLF ACSR phase conductors and steel shieldwires. The line comprises a mix of 88 kV composite and 7 or 8 glass disc strings.

The line spans across 173 towers on the main line with two Tee-off's at Tower 57 and 104 respectively. The first tee-off consists of four structures and the second tee consists of 17 towers and is 3.64 km long. The total customer base of this line is 8259 with an installed MVA base of 50 MVA.

### 3.2.1 FAULT HISTORY

The line traverses a high lightning corridor, Figure 3.2-1 and Figure 3.2-2, and it experiences a high number of lightning related trips. Table 3-1 shows all faults, lockouts and ARCs, on the line for the period 2010 – 2015. The line experienced 182 faults in this period with 93% of these faults due to lightning. There is no differentiation between the type of fault for an ARC and lockout on an HV network. The line experiences an average of 54 Faults/100 km per year which is above accepted rate of 10 Faults/100 km.

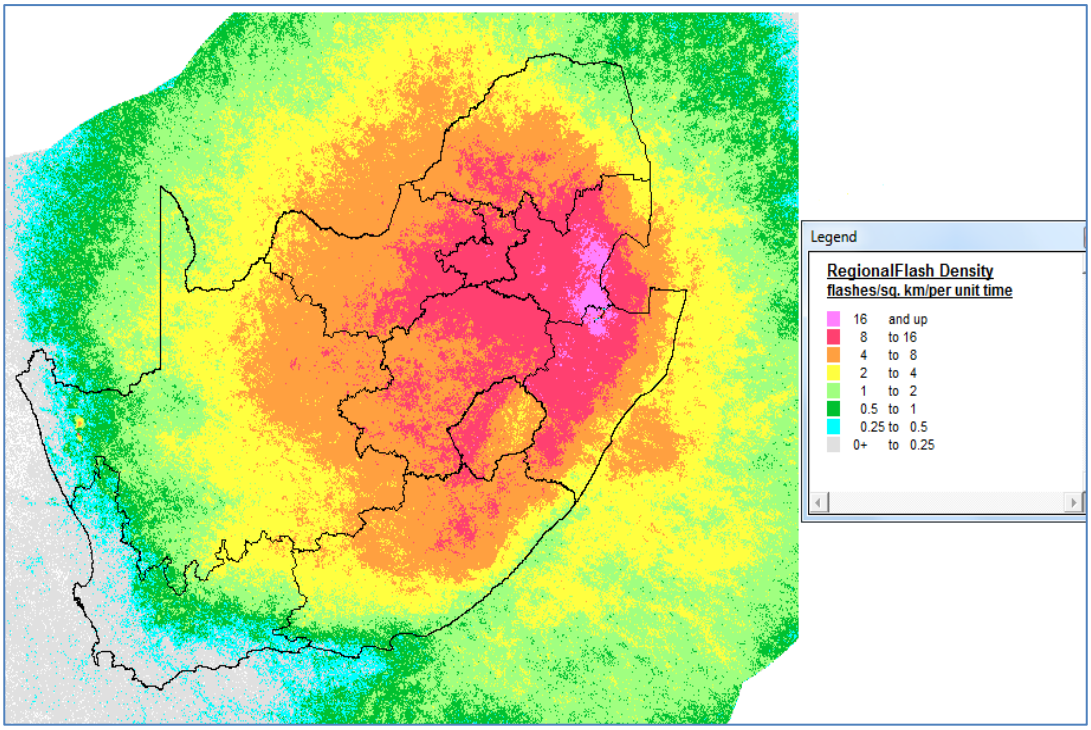


**Figure 3.2-1: Eight year (2007 – 2014) Flash Density Map across South Africa – Highest flash density in Mpumalanga and Northern KwaZulu-Natal**

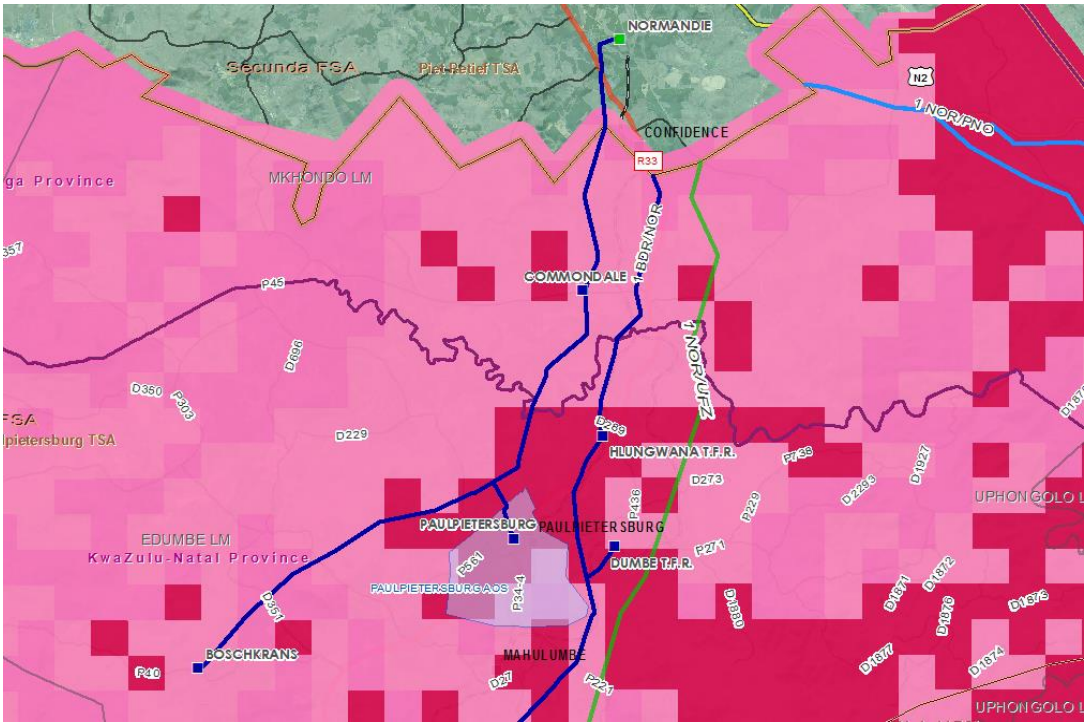


**Figure 3.2-2: Flash Density Map of selected line – The line traverses the highest lightning corridor in KZN**

**Table 3-1: Line lightning performance – Total number of lightning trips and F/100 km**

| Year | Total number of trips | Lightning caused trips | F/100 km |
|---|---|---|---|
| **2010** | 24 | 22 | 42 |
| **2011** | 22 | 21 | 40 |
| **2012** | 50 | 46 | 88 |
| **2013** | 33 | 31 | 60 |
| **2014** | 29 | 27 | 52 |
| **2015** | 24 | 22 | 42 |

## 3.3 APPROACH TO IMPROVING LINE PERFORMANCE

Once lightning is confirmed as been the source of trips the mechanism responsible must be identified. It can either be from induced flashovers, earthwire shieldwire failure or backflashovers.

Induced back flashovers can be eliminated as the cause of flashovers. Induced back flashovers do not exceed 300 kV, given the line insulation strength for an 88 kV line is 450kV the line will not experience lightning induced back flashovers.

Direct strikes to the phase conductor, shielding failure, can be eliminated once the line is patrolled and shieldwire locations confirmed as per design. The allowed movement of shieldwires during winds are within design limits such that coverage over the phase conductors is maintained.

The problem can then be narrowed down to insulator back flashovers as being the cause of line trips. To improve line lightning performance and reduce insulator back flashovers the following approaches can be taken:

- Reduce tower footing resistance
- Increase line insulation i.e. longer length insulator
- Add additional shieldwire
- Add line surge arresters

Firstly before exploring the above options the line needs to be modelled and a base case file setup. Once set the options above can be added in turn and its potential benefit examined. Creating a model of the entire line can be a tedious task and require input parameters for each tower. To make this process easier it is recommended that a segment of line be used in the model. The section of line to be used must be the

most frequently affected with highest earthing resistance and flash density. Usually all these factors correlate with each other.

## 3.4 DEVELOPING THE MODEL

### 3.4.1 TFLASH SIMULATION MODEL

The EPRI TFlash is an electromagnetic transient program used to determine line lightning performance and backflashover rates of power lines. TFlash can be used to calculate where lightning will terminate on the line and whether it will cause a flashover or backflashover. It can calculate line performance and its resilience to induced flashovers (not a concern on 88 kV and above lines), shielding failure resulting in flashovers and tower insulator back flashovers. The program helps during the line design stages and for improving existing line performance [16]. It assists in finding an optimal cost effective solution in improving line performance. It accounts for the surge impedance of different tower types as well as the reflections from the ground electrode to tower top for different tower heights and reflections from adjacent towers. It also accounts for corona by adjusting line capacitance [31]. The user specifies the required CFO which is used in determining insulator flashover. It uses the leader progression model to determine whether insulation will flashover [32]. TFlash allows the user to select different impulse waveshapes.

For steady state conditions TFlash considers the tower footing resistance to be constant. However when lightning current travels on the electrode, the tower footing resistance may reduce as a result of soil ionisation. This is due to the current magnitude causing electrical breakdown of the soil around the earth electrode. To cater for the change in resistance when lightning current travels on the electrode TFlash calculates the electric field in the soil around the earth electrode. If the current is high enough it may result in soil ionisation. TFlash takes this into account by increasing the size of the electrode thus reducing resistance.

TFlash allows the user to select different earthing electrodes. These include:

- Concrete foundation – this is modelled as a linear resistor connected to the tower. For this type of foundation the effect of soil ionisation is not considered.
- Driven earth rods are modelled as nonlinear resistances. This is done to take into the effects of soil ionisation.
- For horizontal counterpoise electrodes, a combination of travelling waves along the electrode and nonlinear resistances are used.

- TFlash can also simulate a combination of concrete foundation with a counterpoise or rod.

A concrete foundation in TFlash will display constant resistance and does not change with frequency and current magnitude. For the other type of electrodes, an increase in frequency and current magnitude reduces overall tower footing resistance.

### 3.4.2 EARTH RESISTANCE TESTING AND EQUIPMENT

In order to ensure accurate line modelling of the towers it is essential that the correct tower footing resistances are used. This is the most important feature when simulating line resistance. The earth resistance value is used by TFlash to calculate voltage rise at tower top, voltage rise on phase conductor and voltage across the insulator. The voltage rise can be described with a simplified model which consist of an inductor, represents the tower, and with a series resistor that represents the earth system. The tower voltage can be determined as:

$$\boldsymbol{V(t) = L\frac{dI(t)}{dt} + RI(t)} \tag{3.4-1}$$

Conventional earth resistance measuring instruments operate at low frequencies (between 100 to 150 Hz). They provide the tower voltage of the resistive component i.e. at the power system frequency.

For a lightning impulse the highest voltage occurs at the maximum steepness (kA/μs) of the waveform. The EPRI Zed-Meter is an instrument that measures the earthing impedance of overhead towers. For a lightning impulse down a tower the impedance of tower becomes the dominant factor in determining the voltage rise across the tower [33].

The Zed meter was developed by EPRI to provide an accurate tool for utilities to determine tower footing impedance of overhead lines. With this meter there is no need to disconnect the shieldwire to isolate the tower under test. The Zed meter injects a lightning like current into the tower base. A potential tower rise is then measured at the tower base. Once the effects of the tower reflections have taken place the meter computes the tower footing impedance.

Ideally during line construction the tower footing resistance is done before the shield wire is connected with a low frequency Megger instrument. However even with the shieldwire disconnected this meter cannot produce the required current impulse steepness required to determine the tower footing impedance component of Equation 3.4-1. To determine the inductive component the EPRI Zed meter must be used.

The ABB HW2A high frequency meter uses a fixed frequency of 26 kHz however a CIGRE working group [34] recommended that 150 kHz is a better choice.

### 3.4.3 FIELD TESTING

For the 88 kV line in the used in the case study, all towers tested were done using the EPRI Zed meter. It was important before conducting any analysis to first understand the resistance profile of the line. Testing is not a simple process and can quickly lead to frustration from the tester. It is important to cover the following pre plan activities before testing;

- Access to towers – contact local field staff for assistance
- Obtain previous tower soil resistivity measurements if available
- Plan ahead with weather forecasts – testing cannot be done during lightning conditions
- Ensure spare components are available during testing – this will avoid down time
- For every tower tested make a note of its soil type, surroundings and elevations.

### 3.4.4 ANALYSING THE RESULTS

The results obtained showed that the line suffered from poor tower footing resistance. From the 165 towers tested, 44 were above 20 Ω. The towers with poor tower footing resistance correlated to locations of flashed insulators. Also during testing the surroundings provided a gauge on the potential tower test result based on soil type.

The tower footing results were then entered into EPRI's TLW software. A section of line with the highest fault occurrences, from FALLS and noted flashed insulators, and poor tower footing resistance will be modelled.

### 3.4.5 DEVELOPING THE MODEL

Before creating the line model the following parameters need to be known:

- Structure height – the structure height affects the time taken for a lightning impulse to travel down the tower. A taller structure will have a greater voltage at the tower top because of the greater travel required to setup the reflection wave.
- Structure type - determines the distance of the phase conductor to shieldwire and the subsequent coupling.

- Number of shieldwires on the structure
- Line insulation – details of the insulator type and the electrical clearance values i.e. dry arc distance.
- Ground flash density to determine the number of lightning strikes to the power line.

Developing a model of the entire line can be a tedious task and require input parameters for each tower. To make this process easier it is recommended that a segment of line be used in the model. The section of line to be used must be the most frequently affected with highest earthing resistance and flash density. Usually all these factors correlate with each other.

For this case study T22 – T41 was chosen for the simulation. This section had the highest number of flashed insulators and the highest measured tower footing resistance on the line. For this case study T22 – T41 will be referred to as T1 –T20 in the simulation. The line model catered for tower elevations. The measured tower footing resistances used in the simulation are given in Figure 3.4-1. The configuration data for the line is given in Table 3-2:

**Table 3-2: Parameters entered into TFlash**

| Parameter | Value | Tower Type |
|---|---|---|
| Lightning GFD | 45 strokes/km$^2$/year | 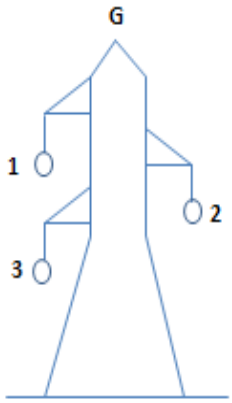  |
| System voltage | 88 kV | |
| Phase conductor | ACSR Wolf Conductor | |
| Shield wire | 19/3mm steel | |
| Insulators | 88 kV composite with a CFO of 450 kV | |
| Span length | 200 m | |
| Line length | 3800 m | |
| Number of structures | 20 | |
| Earth electrode | Concrete foundation with actual measured resistance used | |
| Soil resistivity | Variable and calculated from earth electrode resistance | |

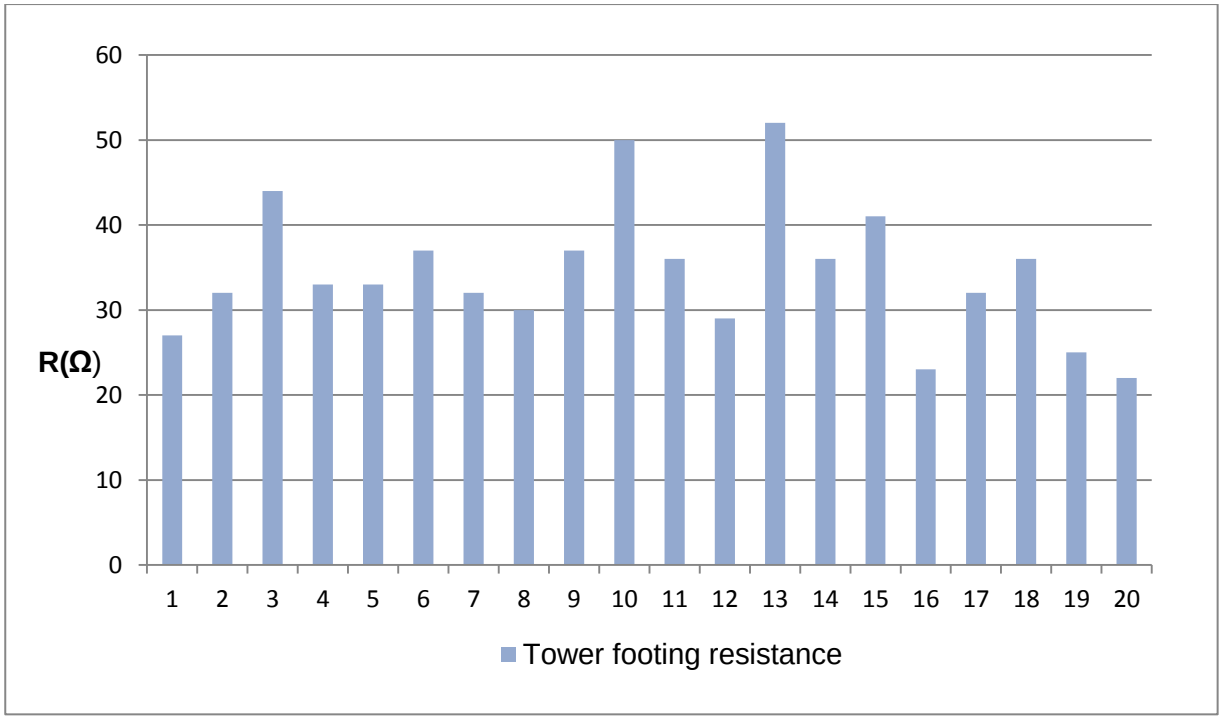


**Figure 3.4-1: Measured tower footing resistances for the 88kV line from T22 –T41**

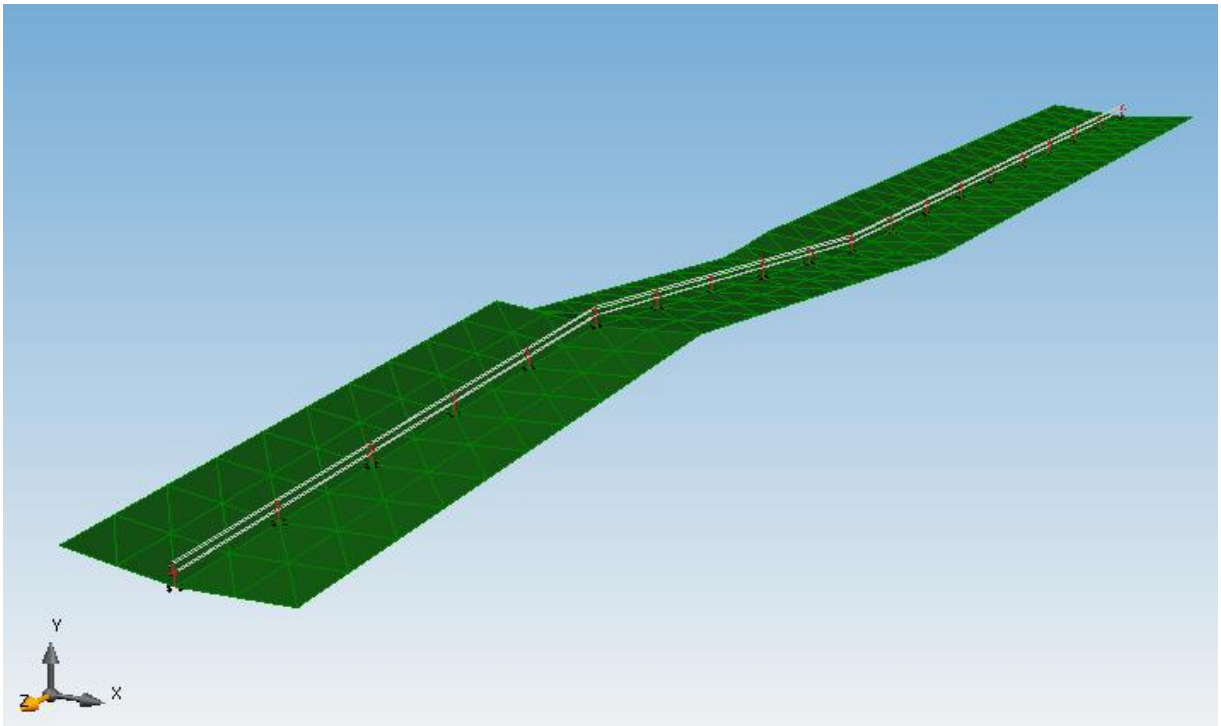

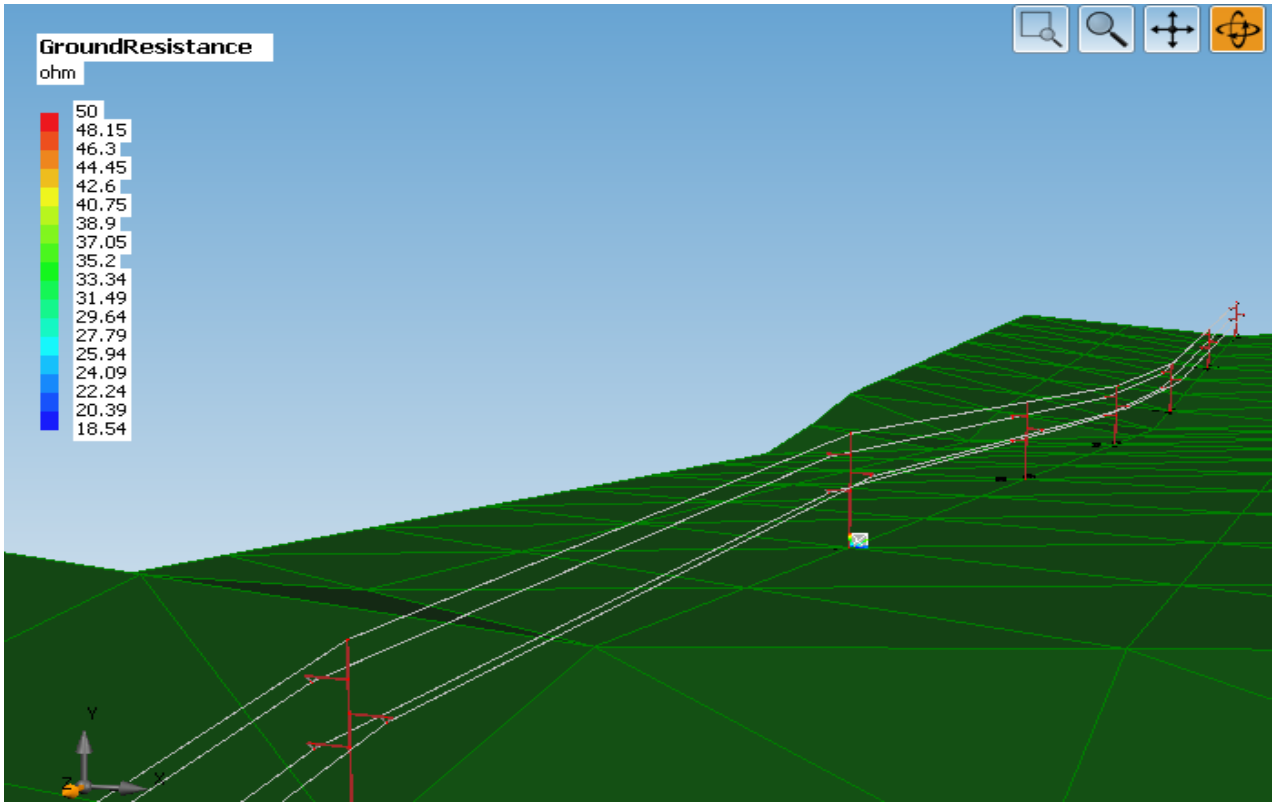


**Figure 3.4-2: 3D line view of model developed in TFlash showing structure selection, hardware and terrain**

## 3.5 SIMULATED PERFORMANCE

The following parameters were entered into the line model;

- Using FALLS data a stroke flash density of 45 strokes/km$^2$/year
- The magnitude of surge current ranged from -10 kA to -250 kA. Positive strokes are greater in magnitude than negative strokes however they compromise less than 3% of total strikes hence it is not considered in this study [3].
- A CIGRE waveshape with a rise time of 2 µs, tail time of 20 µs and a total time of 50 µs.
- Concrete foundation as the earthing electrode and its dimensions. The measured tower footing resistance must be entered. TFlash models the concrete foundation as a non-ionising earth electrode.
- Earth resistivity of 1000 Ω.m.

### 3.5.1 BASE PERFORMANCE CALCULATION

The performance summary as calculated by TFlash is as follows:

**Table 3-3: Simulated results for line section T1-T20 from TFlash**

| | | Expected Range |
|---|---|---|
| Direct Strikes Per Year | 38 | 17 to 73 |
| Back Flashovers | 22 | 7.2 to 30.1 |
| Phase Strike/Shielding Failure Flashovers | 0 | 2.8 to 12.3 |
| Flashovers From Nearby Strikes | 0 | 0.0 |
| Total Flashovers | 22 | 9.9 to 42.6 |

The simulated results in Table 3-3 show that a line section of approximately 4 km had up to 22 flashovers for the year. This was not taking into account other sections of line with poor tower footing resistance. The calculation shows that all flashovers were caused by backflashovers which were a result of high tower footing resistance. This highlights the importance of having accurate tower footing resistance measurements. Cleary improving performance in this section of line would reduce the overall line outage rate.

To better understand the backflashover mechanism the following two scenarios were simulated in TFlash:

Scenario 1: Consider a -20 kA lightning impulse, CIGRE waveform, striking the shieldwire at T10 (with a measured tower footing resistance of 50 Ω), the simulated transient behaviour and its voltage and current distribution along the line is as follows:

Result: Flashover on Tower 10 phase C @ -20.0 kA at 2.02 μs

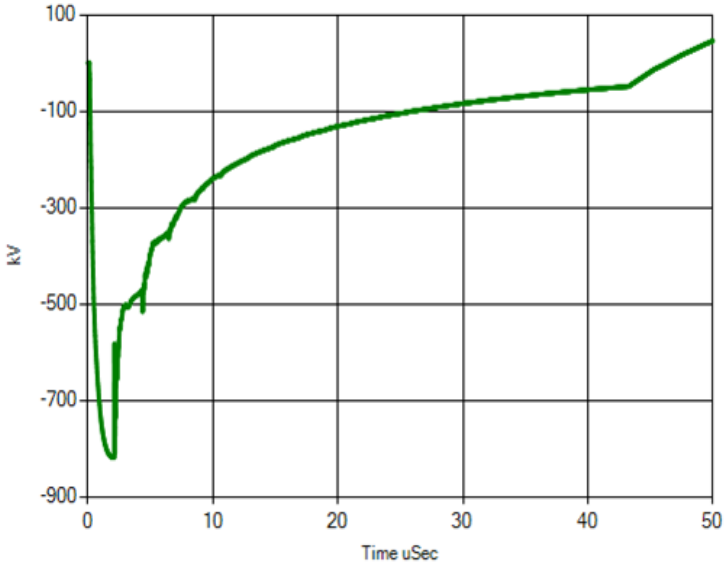


**Figure 3.5-1: Tower Base voltage**

The voltage rise on T10 is shown in Figure 3.5-1. The high tower voltage is caused by the high tower footing resistance. The maximum voltage occurs during the first 2 μs of the lightning impulse since this is the maximum steepness of the waveform.

Figure 3.5-2 shows the conductor voltage on phase A, and the subsequent insulator voltage. The negative voltage on the conductor is from coupling from the shieldwire to Phase conductor. The A phase will experience the greatest coupling since it is closest to the shieldwire. The voltage across the insulator is calculated by subtracting the conductor voltage from the tower voltage. The travelling wave reflections from adjacent towers also help reduce the tower voltage on the incident tower. The propagation speed of a lightning wave for a conductor in air is 300 m/μs. If we assume the span length to be 300 m then the total travel time (to and back) is 2 μs.

Figure 3.5-3 shows a similar pattern on the B phase. The coupling effect between the shieldwire and phase conductor is less than the A phase and thus a lower voltage on the phase conductor is produced. However the coupling is still significant such that there is no flashover across the insulator.

Figure 3.5-4 shows the conductor voltage on the C phase and voltage across the insulator. The coupling effect between the shieldwire and phase conductor is much less than the other two phases and as such the voltage across the insulator reaches a high level for a backflashover. For a flashover in TFlash the insulator becomes a short circuit and the voltage goes to zero.

Phase A:

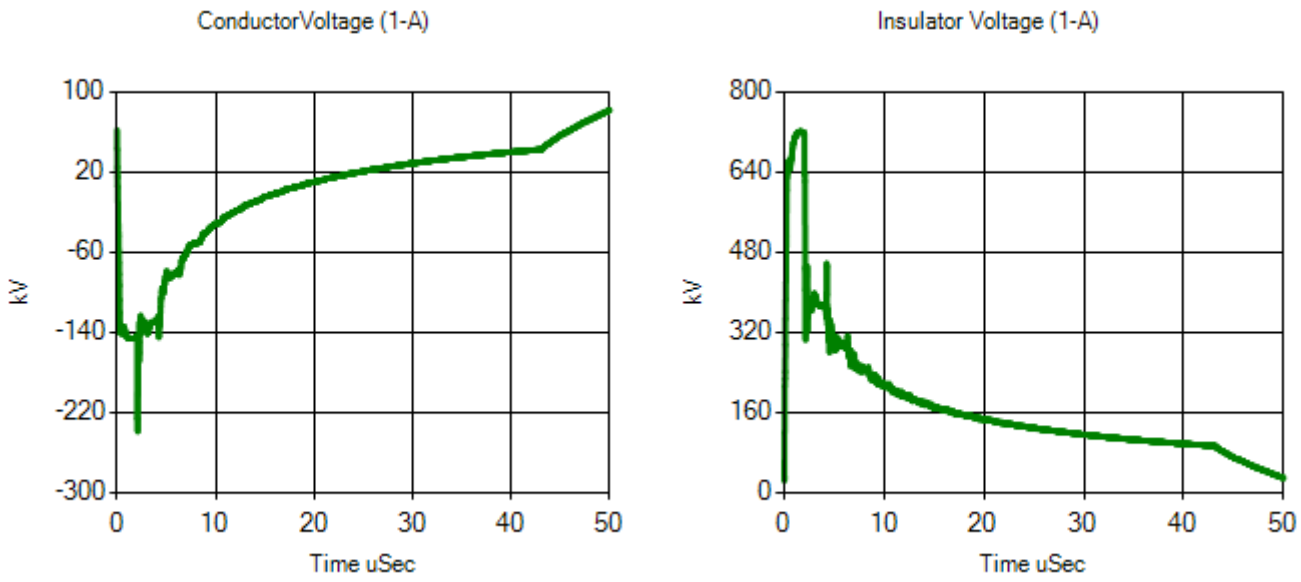


**Figure 3.5-2: Left: Phase conductor voltage from shieldwire coupling. Right: Voltage profile across insulator.**

Phase B:

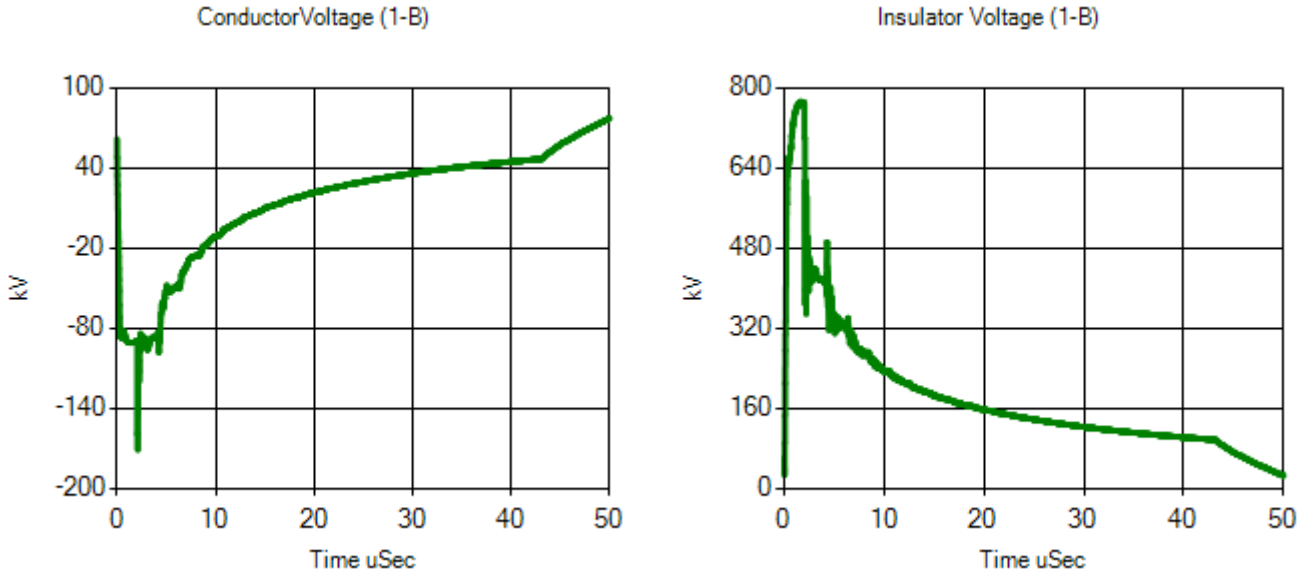


**Figure 3.5-3: Left: Phase conductor voltage from shieldwire coupling. Right: Voltage profile across insulator.**

Phase C:

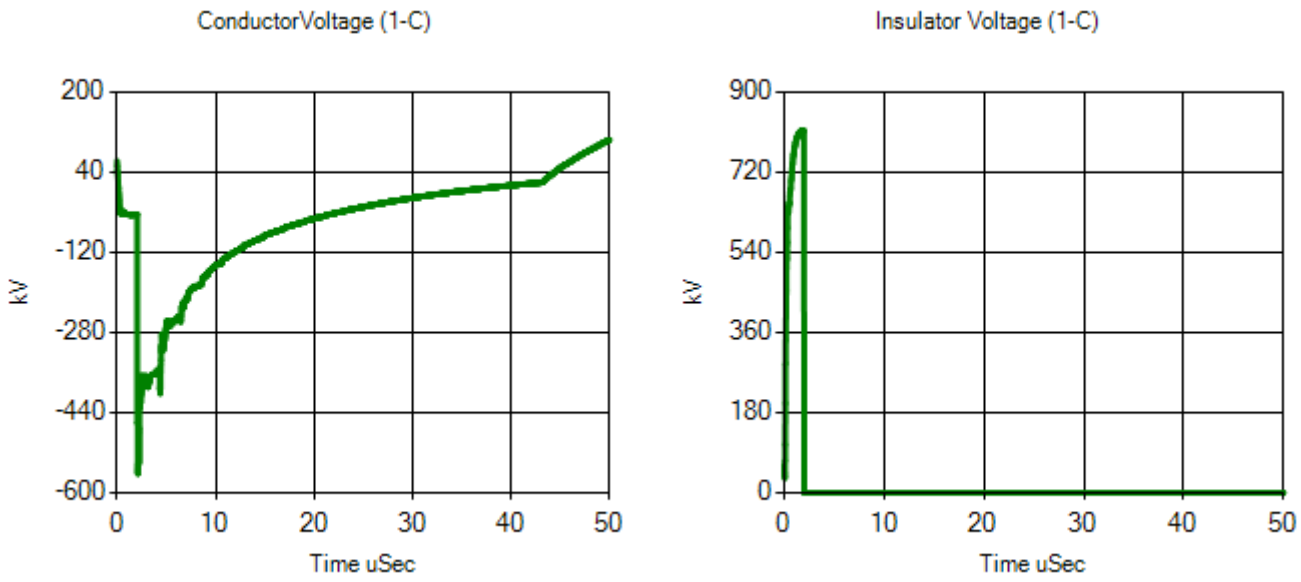


**Figure 3.5-4: Image on left: Phase conductor voltage from shieldwire coupling. Image on Right: Voltage profile across insulator.**

Scenario 2: Consider a -50 kA lightning impulse, CIGRE waveform, striking the shieldwire at T10 (with a measured tower footing resistance of 50 Ω), the simulated transient behaviour and its voltage and current distribution along the line is as follows:

Result:

Flashover on Tower 10 circuit 1 phase A @ -50.0kA at 0.58usec

Flashover on Tower 10 circuit 1 phase B @-50.0kA at 0.60usec

Flashover on Tower 10 circuit 1 phase C @ -50.0kA at 0.64usec

Flashover on Tower 9 circuit 1 phase A @ -50.0kA at 2.42usec

Flashover on Tower 11 circuit 1 phase A @ -50.0kA at 2.42usec

Flashover on Tower 9 circuit 1 phase B @ -50.0kA at 2.50usec

Flashover on Tower 11 circuit 1 phase B @ -50.0kA at 2.50usec

Flashover on Tower 8 circuit 1 phase A @ -50.0kA at 3.50usec

Flashover on Tower 12 circuit 1 phase A @ -50.0kA at 3.50usec

Flashover on Tower 8 circuit 1 phase B @ -50.0kA at 3.54usec

Flashover on Tower 12 circuit 1 phase B @ -50.0kA at 3.54usec

Flashover on Tower 8 circuit 1 phase C @ -50.0kA at 3.58usec

Flashover on Tower 12 circuit 1 phase C @ -50.0kA at 3.58usec

For this simulation Tower 10 experienced flashovers on all three phases due to the high magnitude lightning strike and high tower footing resistance. The tower voltage rise on Tower 10, phase A conductor voltage and voltage across the insulator is shown in Figure 3.5-5. It can be seen that the highest voltage occurs at the maximum steepness (kA/μs) of the current surge waveform.

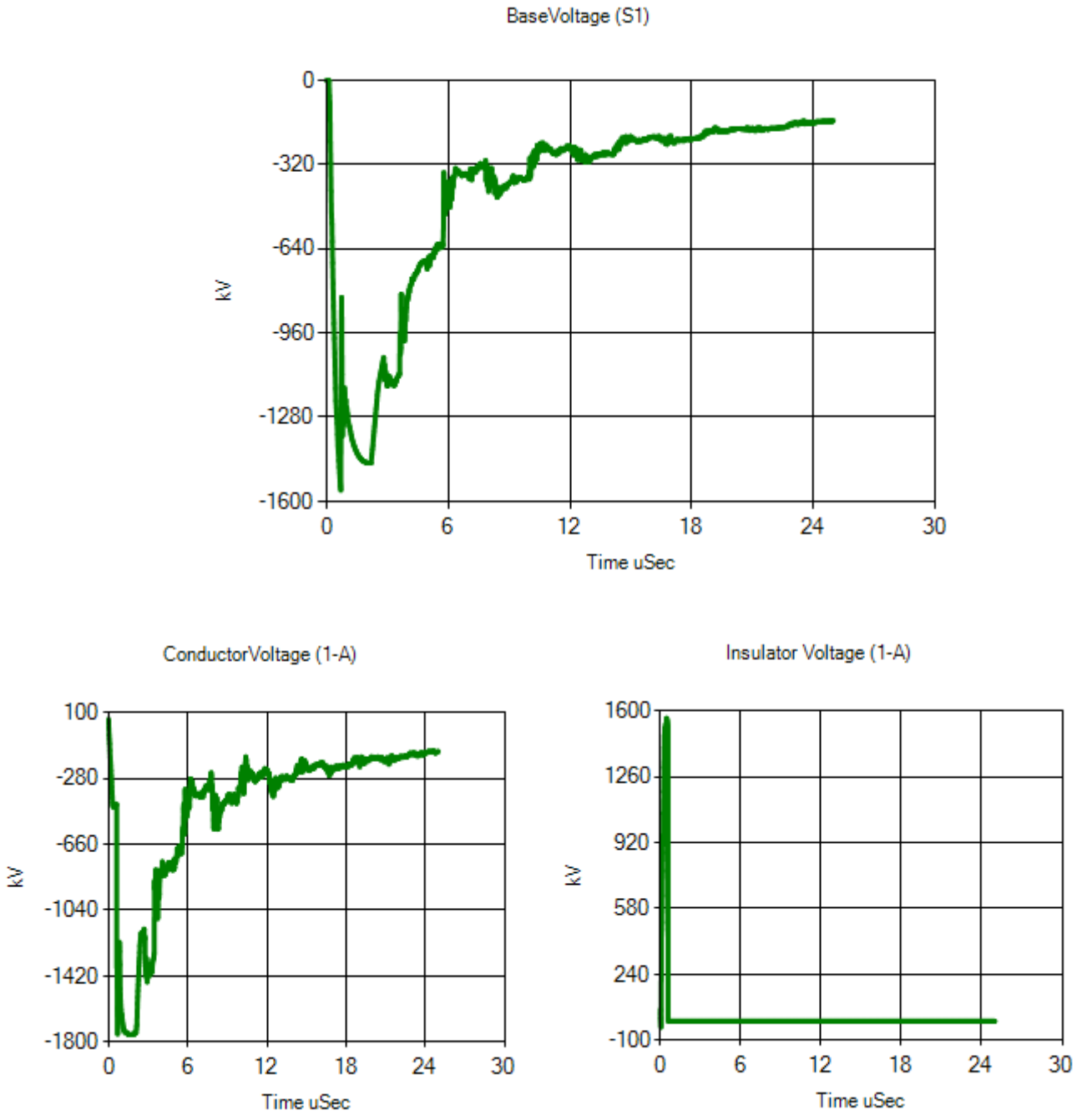


**Figure 3.5-5: Voltage profiles for the A Phase on T10. Similar waveforms are observed on the other two phases.**

Flashovers at adjacent Towers:

The backflashovers at T10 on all three phases injects current on the phase conductors which travels to the neighbouring towers. The resultant voltage from Equation 3.5-1, if high enough can cause flashovers on the neighbouring towers. This is observed in Figure 3.5-6 which shows the flashover at T8 on the A phase.

$$\boldsymbol{V = L\frac{di}{dt}} \tag{3.5-1}$$

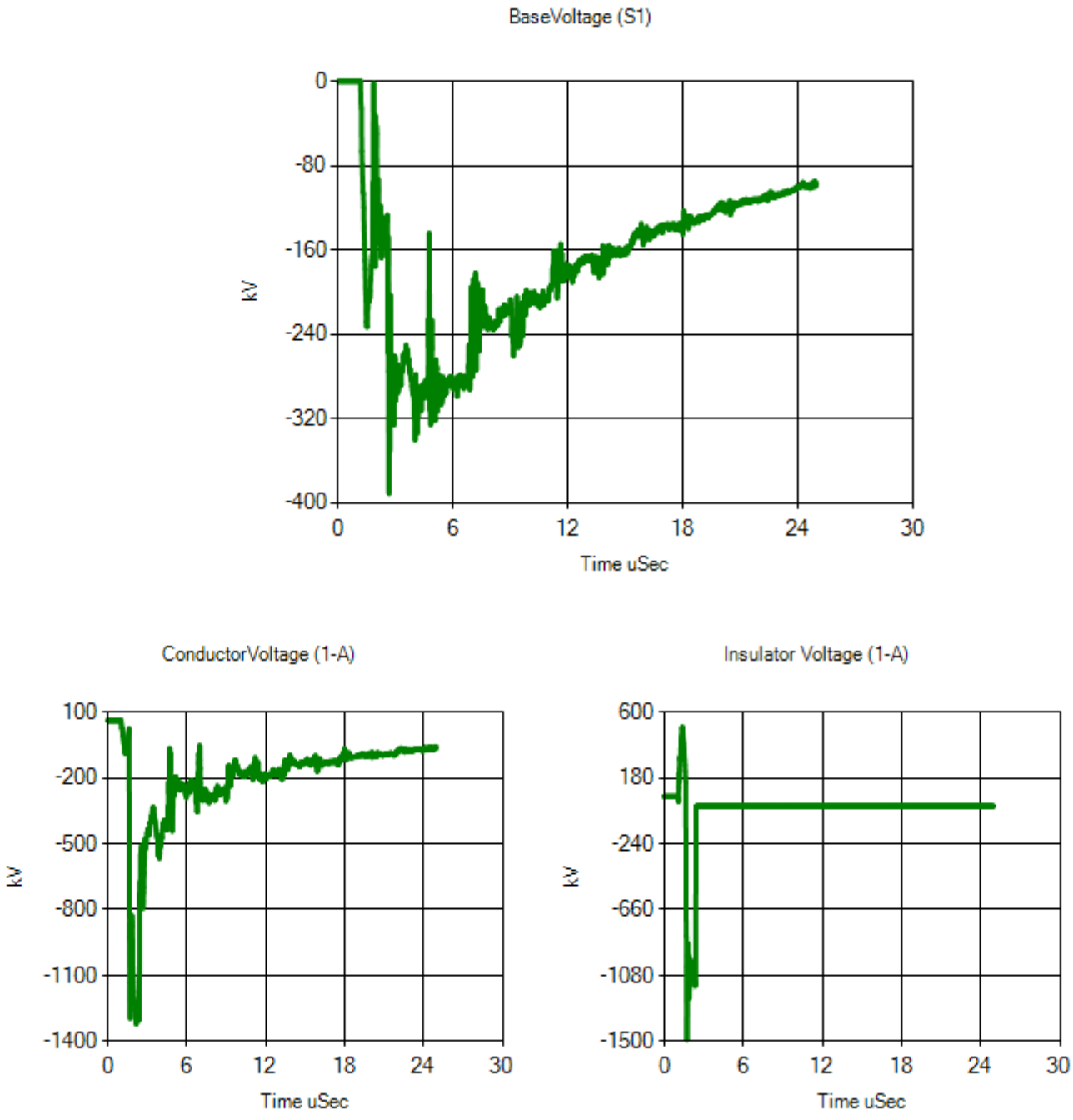


**Figure 3.5-6: Phase voltage on the A phase of T8 showing the voltage rise from a flashover on T10**

## 3.6 IMPROVING LINE PERFORMANCE

Improving line performance by reducing tower backflashovers can be done in the following ways [35]:

- Increase line insulation level
- Install line surge arresters
- Reduce tower footing resistance

### 3.6.1 INCREASE LINE INSULATION LEVEL

Increasing line insulator length can be achieved by installing an insulator with a longer dry arc distance. For example on an 88 kV line a 132 kV insulator can be installed to increase the BIL from 450 kV to 550 kV. When increasing insulator length, clearance to the tower or phase below, on a suspension structure, must be maintained. Also the mixing of insulators, 88 kV and 132 kV, on a line can cause confusion among field staff when changing out flashed insulators. Using the same line section and parameters, the insulation level is increased to 550 kV and the simulation results are as follows:

The total number backflashovers have reduced from 22 to 19. This is not surprising considering the high tower footing resistance in this line section. If the towers in this section had a lower tower footing resistance, less than 25 Ω, then increasing the line insulation level to reduce backflashovers would have a more significant impact.

### 3.6.2 INSTALL LINE SURGE ARRESTER

Installing line surge arresters can be a costly exercise depending on the extent of line section that requires it. Also the application of surge arresters is important. The surge arrester is applied between the phase conductor and tower. Its function is to limit line voltage by conducting current and absorbing energy to prevent insulator flashover. Studies have shown that the optimal placement of arresters must be on all 3 phases on towers with high tower footing resistance and must also be installed on the nearest drain towers (towers with low footing resistance).

An Optimizer feature in EPRI's TLW software allows for the placement of surge arresters and its simulated impact on line performance. For this case study it showed that by placing surge arresters on every tower, all 3 phases, the line back flashovers would be eliminated. However this would come at a

significant cost. The cost for an 88 kV line surge arrester was approximately R80 000 at the time of the study. To eliminate backflashovers on 20 towers, all 3 phases, would cost:

R 80 000 per tower × 20 towers × 3 phases = R 4.8 million

There would also the added cost of replacing surge arresters when they do fail. Thus this option was not preferred due to the high material cost and future maintenance costs.

### 3.6.3 REDUCE TOWER FOOTING RESISTANCE

The most practical and cost effective solution to reduce line backflashovers is to reduce tower footing resistance. The cost of additional earthing is far cheaper than installing line surge arresters.

# CHAPTER 4 ELECTRODE MODELLING, DESIGN AND INSTALLATION

Before simulating line performance improvement, by installing additional earthing, a suitable electrode must be designed. The design aspects of an earthing electrode are as follows:

- Dimensions and cost of electrode - the surrounding terrain must be considered when designing a solution. Sometimes valleys or servitude make it impractical to install longer electrodes for example. The total electrode cost would increase as electrode dimensions increase.
- Cost of installation – installation cannot be done manually and would require excavation machinery. Longer electrodes would increase excavation time and thus installation costs.
- Theft – the material selection must cater for theft areas i.e. copper cannot be used due to its high economic appeal. The chosen material must be a theft deterrent while ensuring good electrical, mechanical and corrosive properties

While the resistance of the earth electrode is the most critical component, it is also important to consider the frequency response of the earth electrode due to the rise times of the lightning strike (di/dt) as well as the reflection times of the travelling waves on the electrodes.

There are various electrode materials and configurations that can be used for high frequency applications to reduce earth impedance. These include horizontal counterpoises, parallel electrodes and vertical rods. To determine the performance of each configuration a suitable high frequency electrode model was developed.

A rise time of 2 μs was considered in the simulation and as such the frequency response of electrodes up 10 MHz was considered, where the region of interest was around 500 kHz.

## 4.1 SINGLE EARTH ELECTRODES

At low frequencies the earth impedance of the electrode is represented by a resistor (examples of finite element models of the earth resistance are found in Appendix B). For high frequencies the earth impedance is represented by a RLC circuit [36], as shown in Figure 4.1-1.

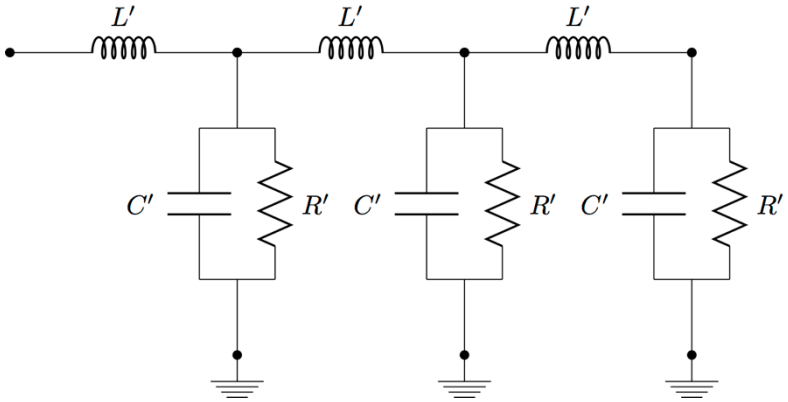


**Figure 4.1-1: High frequency lumped RLC circuit with multiple conductor segments**

For a buried single vertical rod the resistance, inductance and capacitance are given by [36]:

$$R = 1/G = \frac{\rho}{2\pi l}A; \qquad L = \frac{\mu_0 l}{2\pi}A; \qquad C = \frac{2\pi\varepsilon l}{A}$$

$$A = ln\frac{4l}{a} - 1 \tag{4.1-1}$$

Where $l$ and $a$ are the length and radius of the rod respectively.

The earth electrode can further be viewed as a transmission line with an open circuit at the lower end [36].

$$Z(\omega) = Z_0 coth(\gamma l) \tag{4.1-2}$$

Where the characteristic impedance ($Z_0$) and the propagation constant ($\gamma$) are given by:

$$Z_0 = \sqrt{j\omega L/(G + j\omega C)} \tag{4.1-3}$$

$$\gamma = \sqrt{j\omega L(G + j\omega C)} \tag{4.1-4}$$

Implementing Equation 4.1-2 in MATLAB the earth impedance for a 1.5 m vertical rod with a 16 mm diameter was calculated for different earth resistivities and the results are shown in Figure 4.1-2. A relative permittivity of 10 was used for the soil.

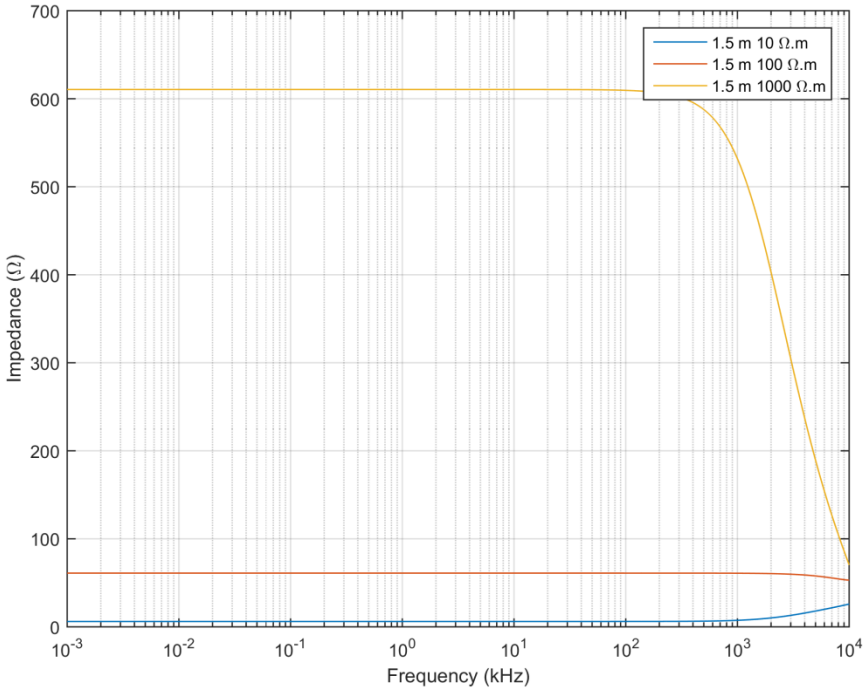


**Figure 4.1-2: Frequency response of 1.5 m vertical earth rod**

In Figure 4.1-2, for soil a resistivity of 10 Ω.m and 100 Ω.m the earth impedance remains fairly constant for increasing frequencies thus exhibiting a resistive behaviour. For the 10 Ω.m there is an inductive increase in the impedance, but it was at higher frequency than the region of interest. For a soil resistivity of 1000 Ω.m the earth impedance for frequencies below 300 kHz is extremely high. However for frequencies above 300 kHz the earth impedance reduces drastically. This is because the electrode displays a greater capacitive behaviour at these frequencies.

Figure 4.1-3 shows the frequency response for different lengths of earth rods for a soil resistivity of 1000 Ω.m. The 1.5 m and 3 m electrodes decreased in impedance at around 500 kHz whilst the 10 m electrode increased in impedance. The 10 m electrode acted as inductive earth impedance due to its greater length. This highlights the importance of shorter electrodes on reducing earth impedance. From the result multiple shorter vertical electrodes were proposed to avoid a high impedance around the frequency of interest.

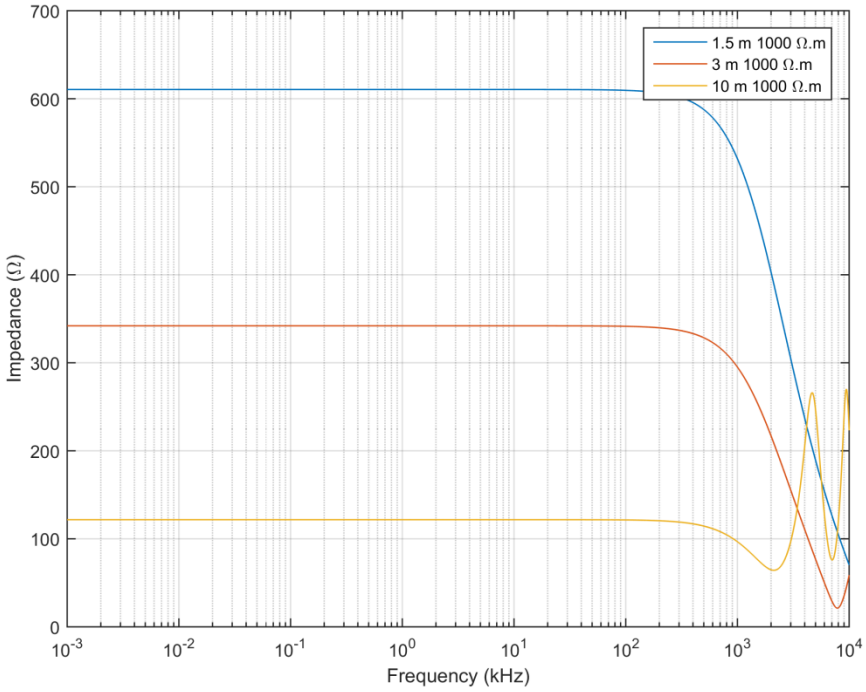


**Figure 4.1-3: Frequency response of vertical earth rods with different lengths**

For a buried horizontal wire the resistance, inductance and capacitance are given by [36]:

$$R = 1/G = \frac{\rho}{\pi l}A; \qquad L = \frac{\mu_0 l}{2\pi}A; \qquad C = \frac{2\pi\varepsilon l}{A}$$

$$A = ln\frac{2l}{\sqrt{2ad}} - 1 \tag{4.1-5}$$

Where $l$, $a$ and $d$ are the length, radius and buried depth of the wire respectively.

Equation 4.1-5 was applied to determine the earth impedance of a horizontal counterpoise over a range of frequencies. Figure 4.1-4 shows the impulse impedance for different horizontal conductor lengths, 25 mm × 3 mm flat bar, for an earth resistivity of 1000 Ω.m. The simulation showed that longer electrodes at higher frequency display inductive behaviour and thus greater impedance at high frequencies. The shorter 10m electrode at 500 kHz reduces in impedance then becomes inductive at higher frequencies. From the result longer electrodes appeared to offer little benefit and multiple shorter horizontal electrodes were proposed to avoid a high impedance around the frequency of interest.

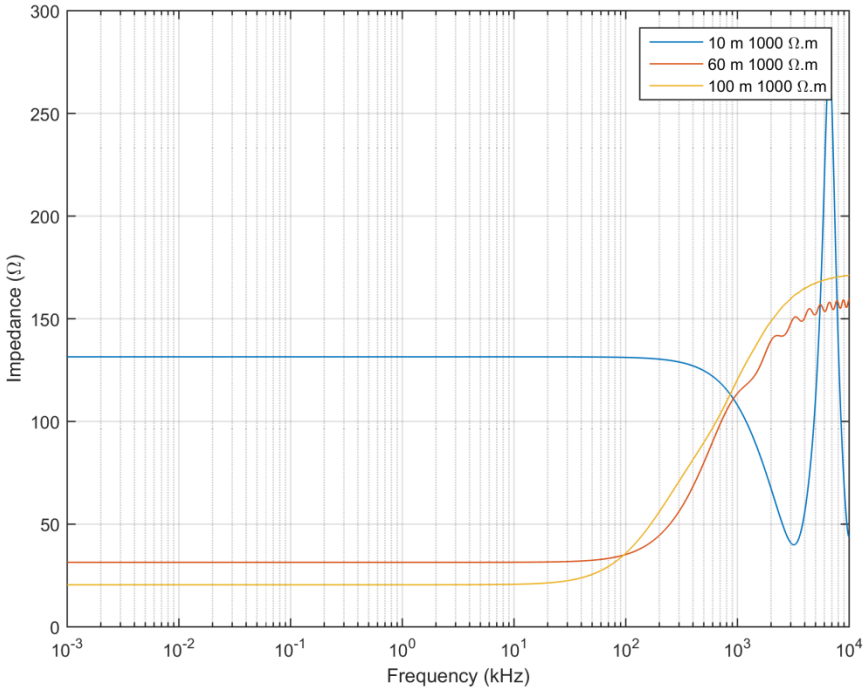


**Figure 4.1-4: Frequency response of horizontal conductor for different lengths**

## 4.2 MULTIPLE EARTH ELECTRODES

The coupling between the electrodes was not considered in the above section and the impedance and configuration of multiple parallel (or partially parallel) conductors needed to be investigated. The impedance consists of the earth resistance, capacitance and the inductance. Of the parameters the inductance was important for the distribution of the current in the conductors. To determine the inductance, the method of partial self and mutual inductances was used [37].

### 4.2.1 PARTIAL INDUCTANCE

Inductance is defined as the constant of proportionality between current and the magnetic field it produces.

$$\phi = LI \tag{4.2-1}$$

To produce a magnetic flux $\phi$ there must be a flow of current in a current loop. In the case of earth electrodes, there is no return loop hence the concept of partial inductance is useful. Partial inductance allows the loop, electrode, to be broken into multiple segments [37].

Each conductor segment will have a partial self-inductance based on their conductor dimensions. The distance between conductors will contribute a partial mutual inductance. The total partial inductance is then a sum of the partial self-inductance plus the partial mutual inductance.

### 4.2.2 PARTIAL SELF-INDUCTANCE

The partial inductance for a length of wire is given by:

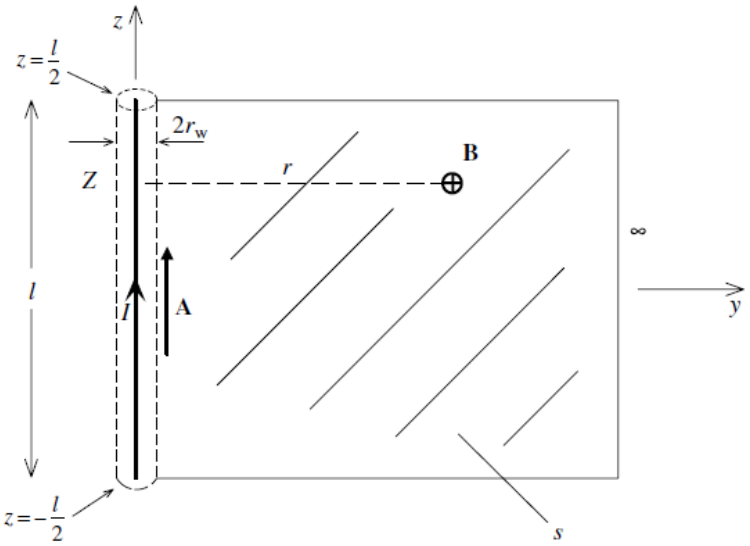


**Figure 4.2-1: Determination of partial self-inductance of a current carrying conductor taken from [37]**

The formulas used to derive the partial self-inductance of a current carrying conductor are complex and long. The final formula approximates to:

$$\boldsymbol{L_P \cong 2 \times 10^{-7} l \left( \ln \frac{2l}{r_w} - 1 \right)} \qquad \boldsymbol{l \gg r_w} \tag{4.2-2}$$

Where;

$l$ = length of the conductor in m

$r_w$ = wire radius in m

### 4.2.3 PARTIAL MUTUAL INDUCTANCE OF PARALLEL STRAIGHT CONDUCTORS

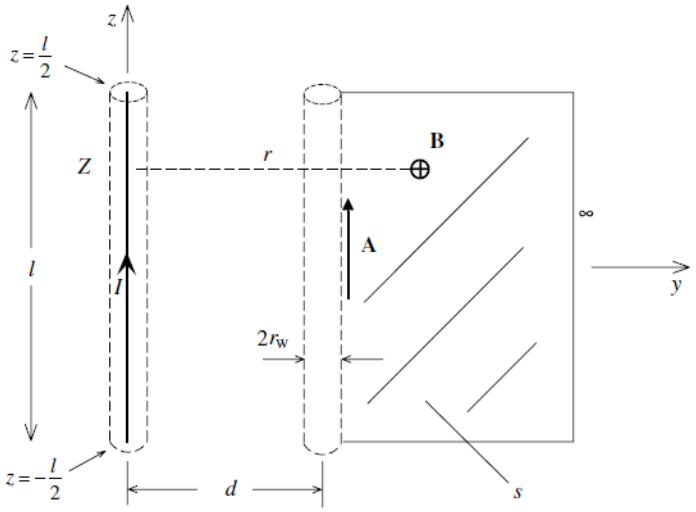


**Figure 4.2-2: Determination of partial mutual inductance between parallel conductors taken from [37]**

The mutual inductance between two parallel conductors is calculated from the following formula:

$$\boldsymbol{M_P \cong \frac{\mu_0}{2\pi} l \left(\ln \frac{2l}{d} - 1\right)} \qquad \boldsymbol{l \gg d} \tag{4.2-3}$$

Where;

$l$ = length of the conductor in m

$d$ = distance between conductors in m

### 4.2.4 PARTIAL MUTUAL INDUCTANCE OF ANGLED STRAIGHT CONDUCTORS

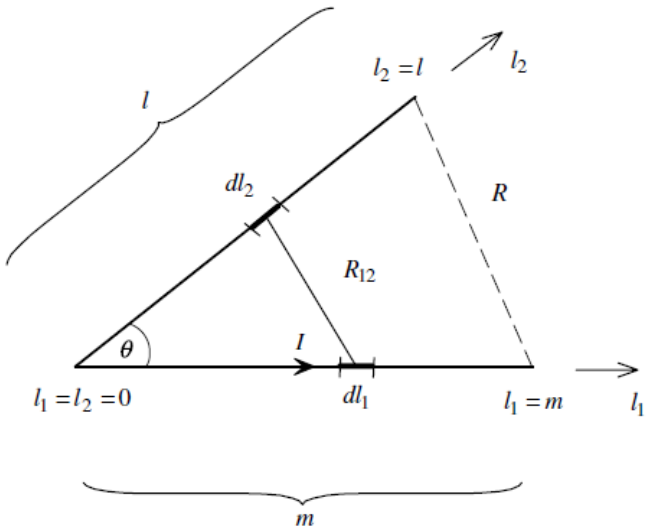


**Figure 4.2-3: Determination of partial mutual inductance between angled conductors where *l* = *m* taken from [37]**

The mutual partial inductance between angled conductors is given by:

$$\boldsymbol{M_P = \frac{\mu_0}{4\pi} cos\theta \left(2l \ln \frac{R+2l}{R}\right)} \quad (4.2\text{-}4)$$

### 4.2.5 INDUCTANCE OF EARTH ELECTRODE

A model was developed to calculate the partial self-inductance and partial mutual inductance of parallel and angled (the crow's foot) horizontal conductor earth electrodes, Figure 4.2-4. The model provided logical understanding of the conductor inductance and how the conductors may influence each other.

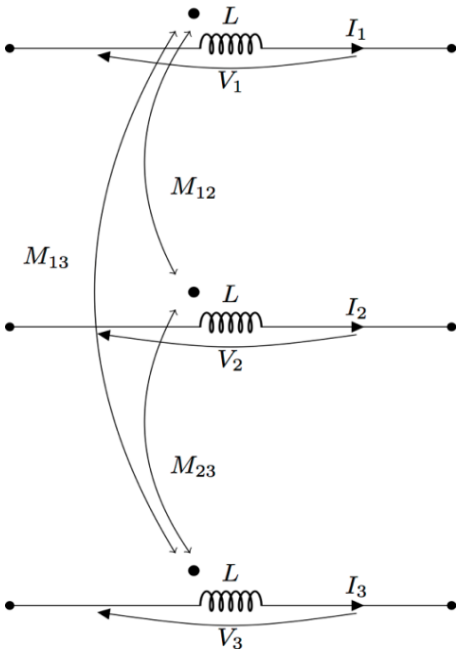


**Figure 4.2-4: Model of partial self-inductance and partial mutual inductance of electrode**

To solve for the total inductance, inductance of each conductor segment and mutual inductance between conductors, we have to create a matrix and solve for $V = IZ$

Ignoring resistance; $$\boldsymbol{[V] = [X_S][I] + [X_M][I]} \quad (4.2\text{-}5)$$

Where $X_S$ is the partial self-inductance and $X_M$ is the partial mutual inductance

$$\begin{bmatrix} V_1 \\ V_2 \\ V_3 \end{bmatrix} = \begin{bmatrix} X_s & 0 & 0 \\ 0 & X_s & 0 \\ 0 & 0 & X_s \end{bmatrix} . \begin{bmatrix} I_1 \\ I_2 \\ I_3 \end{bmatrix} + \begin{bmatrix} 0 & X_{12} & X_{13} \\ X_{12} & 0 & X_{23} \\ X_{13} & X_{23} & 0 \end{bmatrix} . \begin{bmatrix} I_1 \\ I_2 \\ I_3 \end{bmatrix}$$

In a crow's foot configuration, to calculate the current division, the electrode is connected at a point therefore $V_1 = V_2 = V_3 = V = 1$.

The total inductance of the electrode can be calculated by;

$$\boldsymbol{Z = \frac{V}{I_{Total}}}; \qquad \text{Where } \boldsymbol{I_{Total} = I_1 + I_2 + I_3} \tag{4.2-6}$$

Equation 4.2-3 and 4.2-4 was used to compare the performance of parallel straight conductors and angled conductors. The results were plotted, using MATLAB, and it shows that angled conductors have a lower inductance than parallel conductors and as the angle between conductors increase, the inductance decreases. This is because of a lower partial mutual inductance between conductors. (i.e. the magnetic field couples less as the angle increases, where the maximum coupling occurs when conductors are parallel to each other and the minimum when the conductors are perpendicular to each other.)

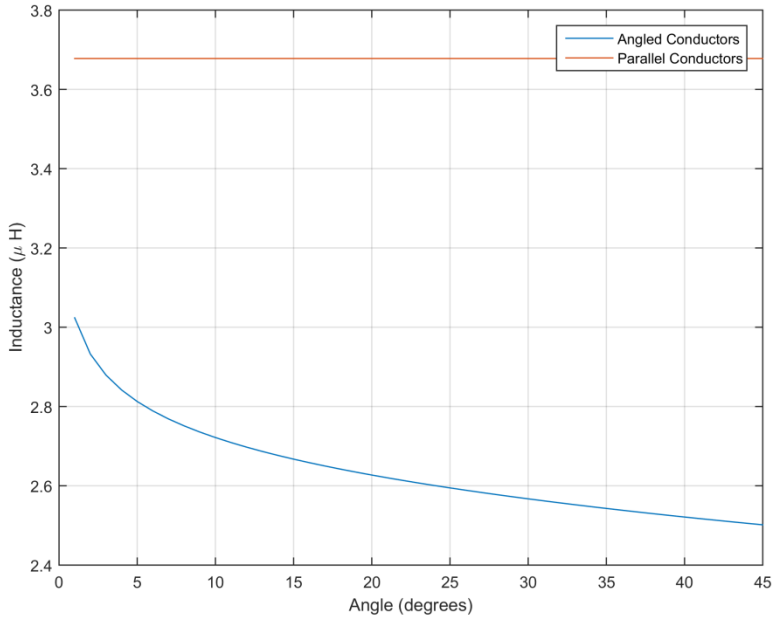


**Figure 4.2-5: Inductance of parallel straight conductors and angled straight conductors**

## 4.2.6 EARTH ELECTRODE IMPEDANCE

The impedance for the multiple earth electrodes for a range of frequencies was calculated using the transmission line approach presented earlier. Figure 4.2-6 compares the frequency response of three parallel vertical rods, three parallel horizontal conductors and a crow's foot consisting of three parallel conductors. An earth resistivity of 1000 Ω.m was used.

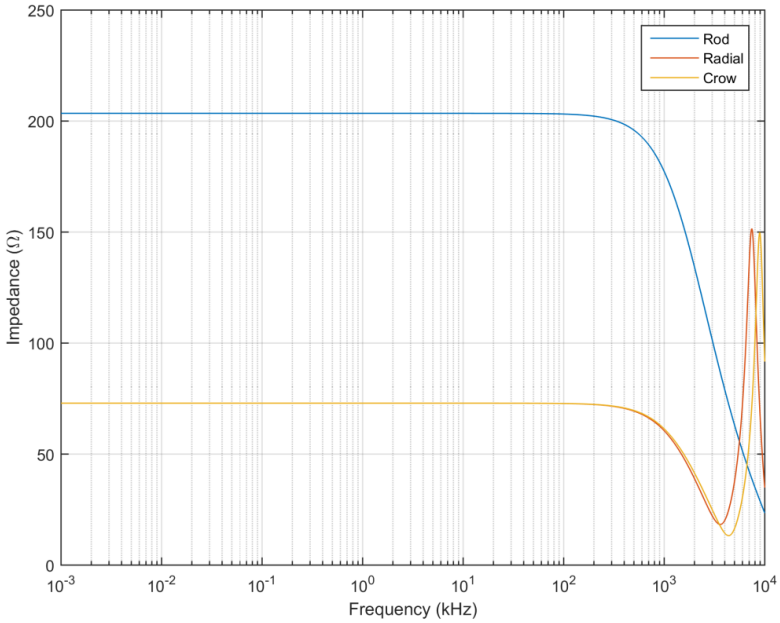


**Figure 4.2-6: Frequency response of different electrode configurations**

For frequencies below 400 kHz all electrode configurations display resistive behaviour. At frequencies above 400 kHz the vertical rod decreases in impedance however the net impedance is still significant. The horizontal conductor and crow's foot configuration both reduce in impedance at frequencies between 500 kHz – 3000 kHz then increase once the frequency exceeds 3000 kHz.

The simulations show that the crow's foot configuration provides the best earth impedance reduction at high frequencies. Shorter parallel conductors outperform longer conductors due to its inductive behaviour.

## 4.3 EARTH ELECTRODE MATERIALS

The earth electrode materials are important. Generally copper is considered the best conductor. However due to theft, steel conductors are used. The performance of the earth electrode made of copper and copper clad steel under lightning current conditions was investigated.

At higher frequencies the current density is the highest on the surface of the conductor. The skin depth is known as the depth into the conductor for where the majority of current flows. The equation for skin depth is given by:

$$\delta = \sqrt{\frac{2\rho}{2\pi f \mu}}$$

Where:

The skin depth for copper and steel is illustrated in Figure 4.3-1, where the conductivity of copper and steel were 5.8 x $10^7$ and 2.0 x $10^7$ respectively, and the relative permeability of copper and steel were 1 and 1000 respectively. It is seen that the skin depth for copper is much lower than that of steel.

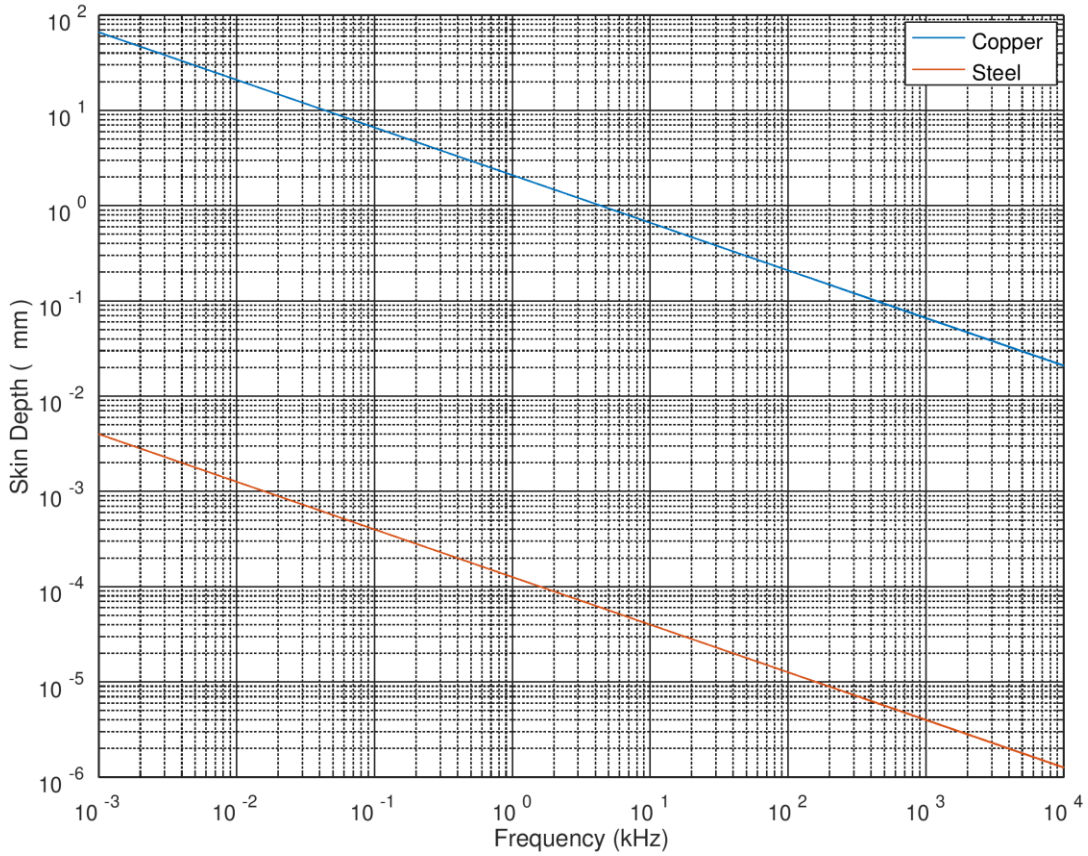


**Figure 4.3-1: Skin depth for different electrode materials**

Finite Element Method Magnetics (FEMM) was used to further illustrate the performance of copper electrodes and copper clad steel electrodes [38]. In the electrode design it was used to model the current density around the electrode and the interaction of magnetic fields between parallel current carrying conductors. The material used in the simulation was Copper-Clad Steel (CCS). It is a material that is used widely on MV applications for transformer earthing.

In the proceeding simulations CCS with a conductor diameter of 7 mm was used, with 0.2 mm copper on the outer surface and the remaining material set to steel. The conductivity used for copper was 5.8 x $10^7$ S/m and 20 x $10^6$ S/m for steel. A permeability of 1000 was used for the steel and the length of the conductor was set to 10 m. The current was set to 1 A flowing through the electrode.

The image in Figure 4.3-2 shows the distribution of current in the conductor and on the conductor surface. A magnetic flow problem was used to determine the current density at a frequency of 50 kHz. The results showed the current density is highest on the surface of the conductor with 99% of the current

distribution on the outer copper layer whilst the remaining current is in the steel core. This was due to skin effect which causes the high frequency field or magnetic flux density to be confined to the surface of the conductor. Table 4-1 displays the results for different materials and frequencies where further examples of skin effect are shown in Appendix B.

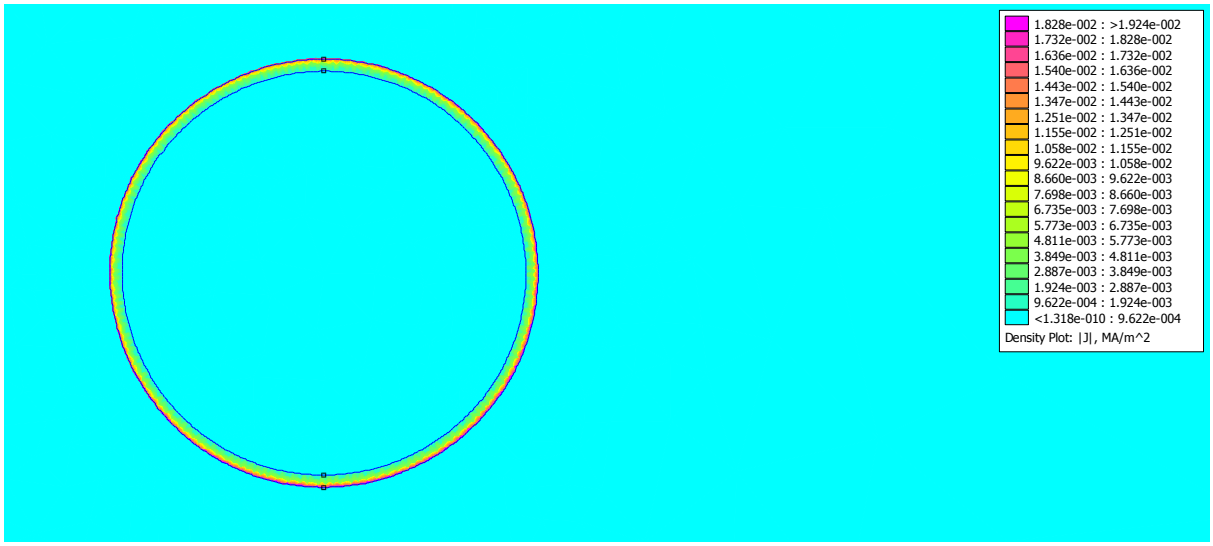


**Figure 4.3-2: Current density around CCS conductor at 50 kHz**

**Table 4-1: Current distribution comparison between Copper and CCS conductors**

| **Frequency** | **Percentage current in outer 0.2 mm of the conductor** | |
|---|---|---|
| | **Cu** | **CCS** |
| **1 Hz** | 11 % | 77 % |
| **50 Hz** | 24 % | 96 % |
| **50 kHz** | 96 % | 99 % |

## 4.4 SIMULATED LINE PERFORMANCE WITH ADDITIONAL EARTHING

The simulations done using the high frequency electrode model and the concept of partial inductance have shown that shorter parallel horizontal conductors, with vertical earth rods at the end, are the optimal solution to reduce earth impedance. FEMM was then used to model the electromagnetic behaviour of the electrode. The model showed that using parallel conductors that are adequately spaced perform better than a single conductor.

The propagation speed of a lightning wave for a conductor in air is 300 m/µs [39]. If we assume the span length to be 300 m then the total travel time (to and back) is 2 µs. The propagation speed of a lightning wave for a conductor buried in ground is 100 m/µs. This is important when selecting electrode length.

The maximum tower voltage occurs on maximum steepness of the lightning waveform which is within the first 2 μs. The reflection from the far end of a radial counterpoise must reach the tower before 2 μs for it to reduce the steepness of the voltage across the insulator. If we assume a radial counterpoise length of 100 m, the reflected wave form the counterpoise will reach the tower in 2 μs which is at the end point of maximum steepness in the lightning waveform. Any counterpoise beyond 100 m in length will be ineffective as the reflection wave will not act on the maximum steepness of the lightning waveform. Clearly for an electrode to be effective it must act in the 2 μs time frame. This then calls for a design with shorter conductors to reduce tower voltage rise during the initial lightning impulse.

TFlash further validated electrode selection by showing the impact of different earth electrode configurations on tower voltage rise during a lighting impulse. The dimensions and configurations of the simulated electrodes were as a result of conclusions in Chapters 4.1 and 4.2. The following electrode configurations were used;

- A single 60 m horizontal conductor terminated with a 1.5 m vertical rod.
- Crow's foot (parallel 10 m horizontal conductors) terminated with 1.5 m vertical rods on each conductor.

A tower was simulated in TFlash with the following parameters:

- Tower footing resistance of 50 Ω in concrete foundation
- Earth resistivity of 1000 Ω.m
- Insulator BIL of 450 kV
- Lightning strike magnitude of -30 kA

The base case tower voltage rise was calculated. The tower voltage rise from both electrode configurations was then calculated. The results for the two electrode configurations are shown below;

**Case 1**: 60 m horizontal conductor terminated with a 1.5 m vertical rod and installed on two tower legs.

The image on the left of Figure 4.4-1 shows the tower voltage rise for the base case concrete foundation. The image on the right of Figure 4.4-1 shows the reduction in tower voltage rise with the installation of two 60m electrodes. The reduction in voltage rise is achieved by a reduction on the effective tower footing resistance as seen in Figure 4.4-2.

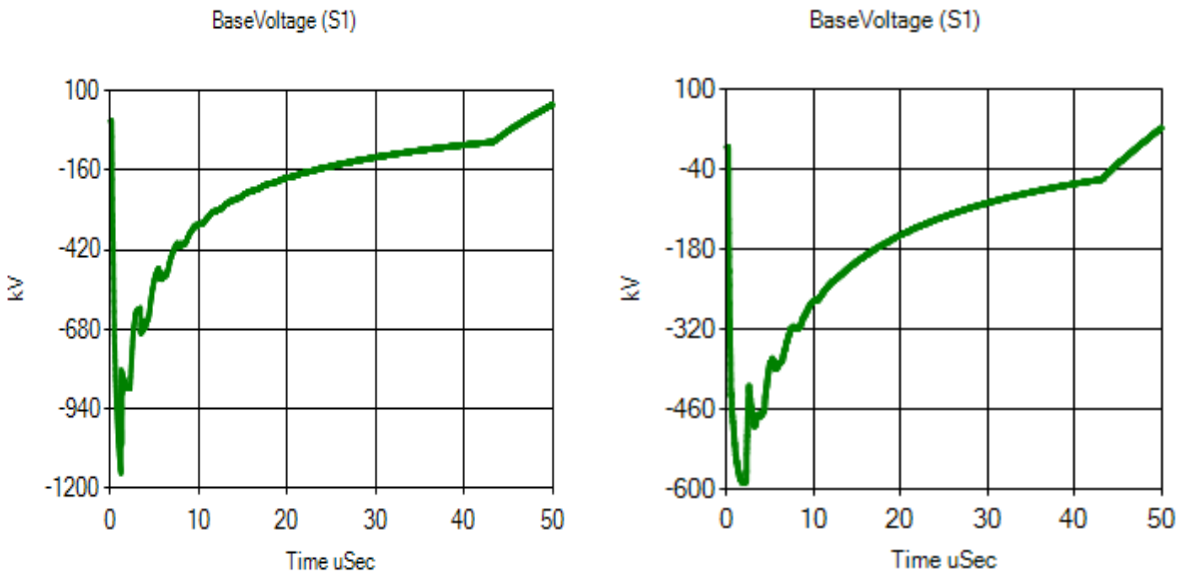


**Figure 4.4-1: Tower voltage rise, Left: Concrete foundation. Right: 60 m electrodes on two tower legs.**

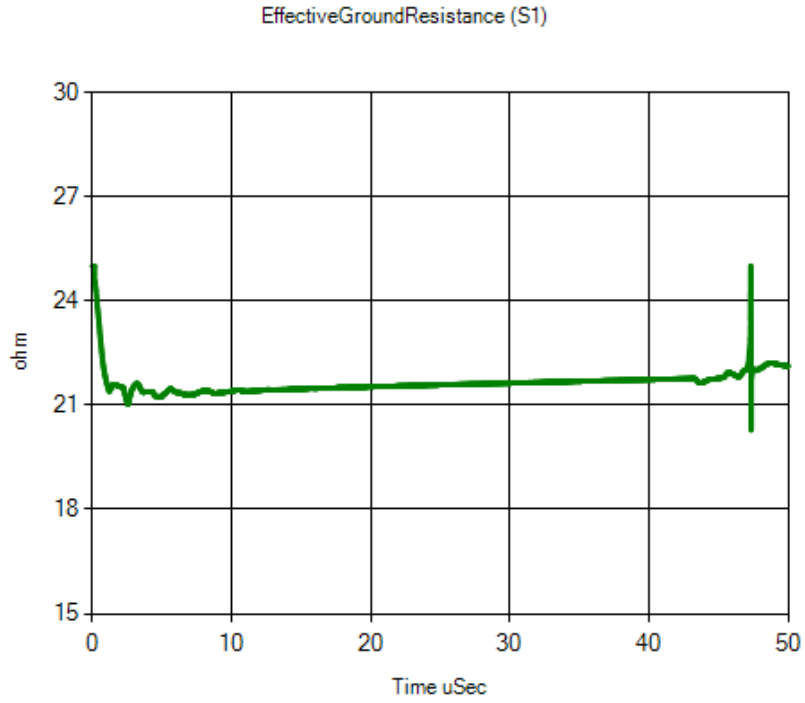


**Figure 4.4-2: Reduction in tower footing resistance by installing 60 m electrodes on two tower legs.**

**Case 2**: Crow's foot (parallel 10 m horizontal conductors) terminated with 1.5 m vertical rods and installed on two opposite tower legs.

The image on the left of Figure 4.4-3 shows the tower voltage rise for the base case concrete foundation. The image on the right of Figure 4.4-3 shows the reduction in tower voltage rise with the installation of

shorter parallel electrodes. The reduction in voltage rise is achieved by a reduction on the effective tower footing resistance as seen in Figure 4.4-4.

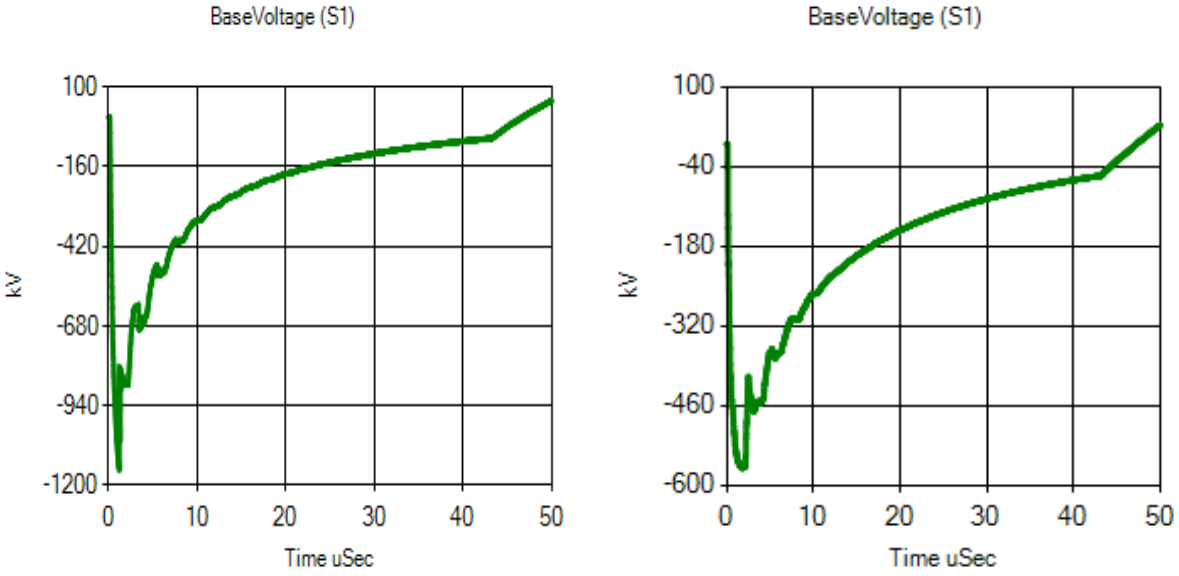


**Figure 4.4-3: Tower voltage rise, Left: Concrete foundation. Right: Crow's foot on two opposite tower legs.**

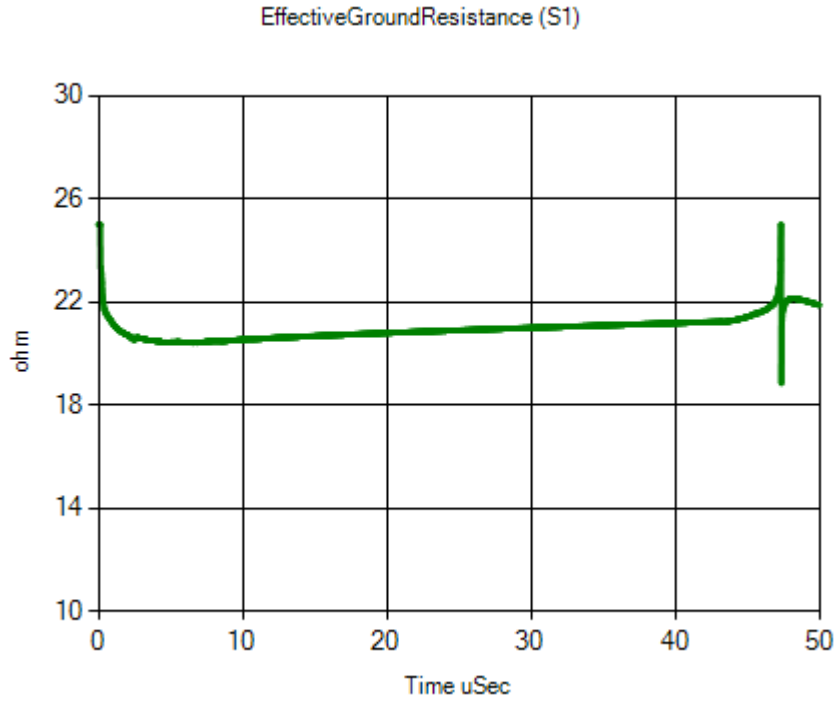


**Figure 4.4-4: Reduction in tower footing resistance by installing crow's foot on two opposite tower legs.**

The above electrode configurations were then used in TFlash to model the twenty towers used in the case study line (Chapter 3) with additional earthing. The line performance was simulated for both electrode configurations and its improvement from the base case performance is calculated. Both earth electrode

configurations reduced backflashovers in the study from 22 to 2, improving line performance by 91%. The simulated improvement in tower footing resistance for both electrode configurations is shown in Figure 4.4-5.

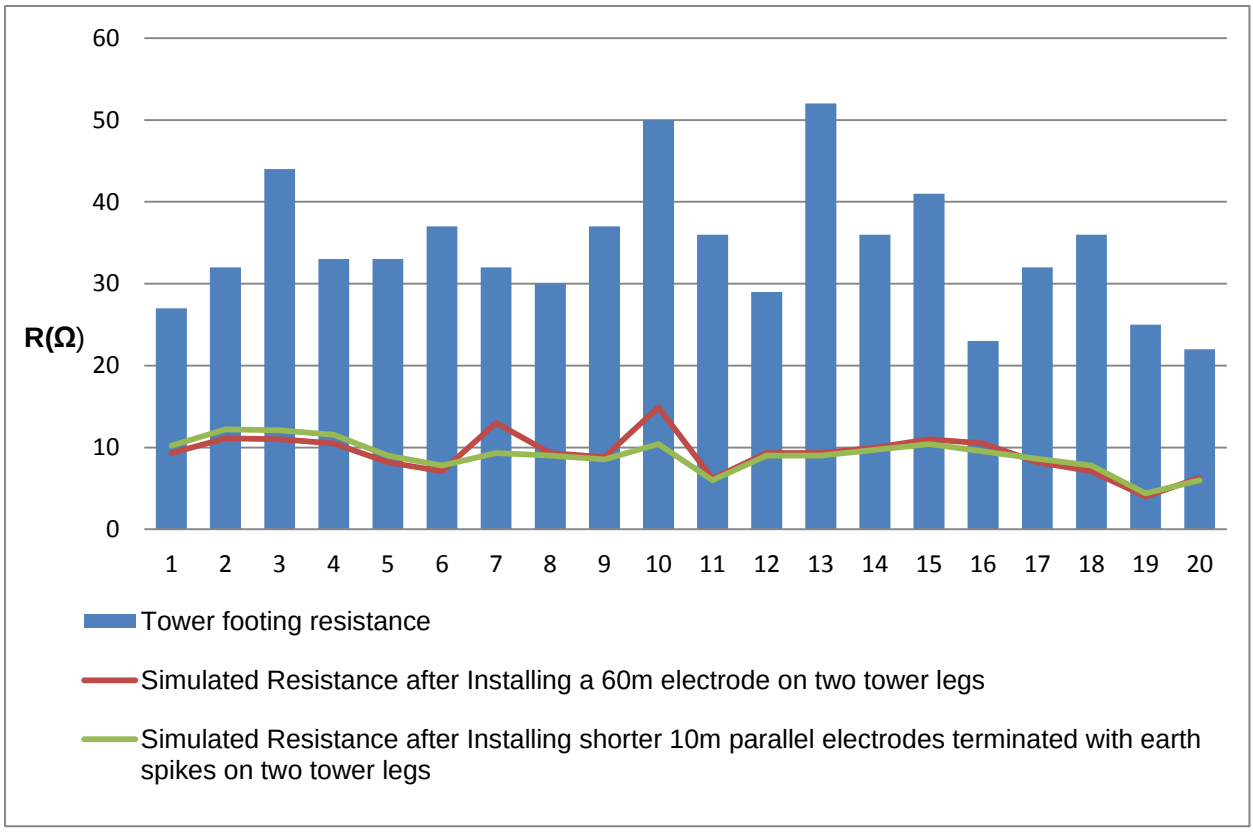


**Figure 4.4-5: Simulated tower footing resistance improvement for both earth electrode configurations**

The results show shorter parallel electrodes achieve a similar reduction in tower footing resistance than a single conductor. It is effective in reducing the tower voltage rise in the first 2μs of the lightning impulse. It also has the added advantage of lower material and installation costs.

## 4.5 ELECTRODE DESIGN

An electrode was designed with dimensions shown in Figure 4.5-1. The preceding sections clearly showed the performance benefit of using shorter parallel electrodes as opposed to other earth electrode configurations.

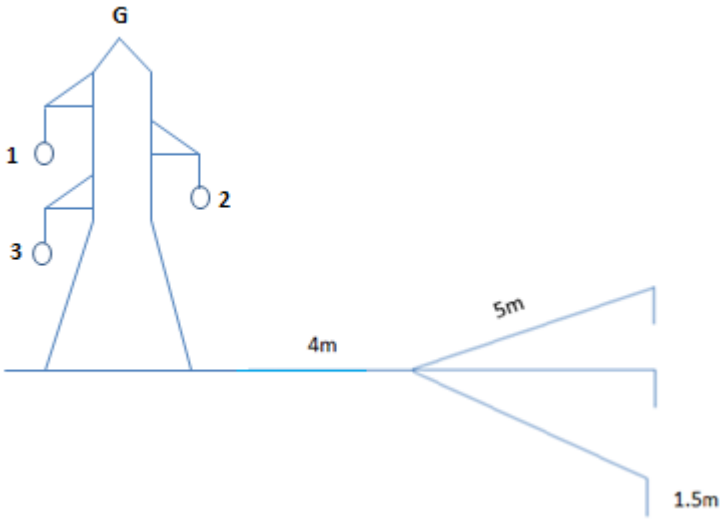


**Figure 4.5-1: Earth electrode deign**

It is a crow's foot configuration terminated with vertical earth rods at the end. The dimensions for the earthing design are as follows:

- Three leg crows foot earth. Each leg is to be 5 m in length and connected to a central node that's exothermic welded to a 4 m length tail. The end of each leg is to be exothermic welded to a copper plated steel core earth rod (1.5 m 16 mm diameter rod). The copper spike termination increases the surface area for soil ionisation and reduces impedance. The 16 mm diameter rod is a standard available item and is adequately sized due to skin effect at high frequencies.
- The 4 m length tail must be terminated with a galvanised steel lug to bolt onto an M16 mm diameter pylon leg. The termination must be an exothermic joint. Ensuring that all welds are pre done ensures quality and welded joints provide better continuity than clamps. The exothermic welds provide excellent electrical continuity and mechanical rigidity. The conductor used must be tarnished on the visible section above ground that connects to the tower.
- Exothermic connections are recommended due to its high mechanical integrity, no corrosion at interface between materials and no maintenance requirements.

The use of a copper electrode is seen as high risk due to its theft and economic appeal therefore it cannot be used. The Eskom standard recommends mild steel straps (25 mm × 3 mm flat bar). However steel is prone to corrosion when buried and particularly at the transition from air to ground. The added protective bitumen layer does not provide sufficient protection in moist soil conditions and degrades after a period of 5 years.

With the above taken into account it was decided to use Copper-Clad Steel (CCS). It is a bimetallic conductor that is manufactured by a mechanical bonding process that produces metallurgical bond

between a solid oxygen-free copper layer and a steel core [40]. It is a solution that was available to Eskom as a theft deterrent material on MV transformer installations that are prone to downwire earth lead theft. The material fulfils the following criteria:

- High electrical ampacity
- Corrosion resistance
- Mechanically robust
- Theft deterrent solution due to low scrap value – difficult to separate material due to bonding process.

A standard and easily available CCS size was chosen. As shown previously the diameter of the conductor does not have to be large since at high frequency, 99% of the current flow is on the outer surface. The CCS used is a 40% IACS conductivity product [40]. The specifications are available in Table 4-2.

**Table 4-2: CCS comparison to copper equivalent**

| | Number of strands | Overall diameter, mm | Fusing rating for 1 s at 1084 ˚C, kA | Fusing rating for 3 s at 1084 ˚C, kA | Nominal DC resistance at 20 ˚C, Ω/km | Minimum break load, kN |
|---|---|---|---|---|---|---|
| CCS stranded conductor equivalent to 16mm$^2$ copper | 7 | 6.55 | 4.95 | 2.86 | 1.693 | 6.31 |
| CCS rod equivalent to 50mm$^2$ copper | 1 | 8.54 | 10.82 | 6.25 | 0.768 | 15.48 |

For the electrode CCS stranded conductor (16 mm$^2$ copper equivalent) was chosen. The reason for choosing a stranded conductor over a solid rod is that the stranded conductor is easier to handle, transport and install. The solid rod requires specialised equipment to shape and bend which becomes a costly and time consuming exercise.

The final electrode product is shown in Figure 4.5-2. The design is lightweight, easy to transport and easy to install. All exowelded connections are pre done by the manufacturer thus eliminating human error during the installation process. The stranded material makes handling and manoeuvring of the electrode easy without the need for specialised equipment.

**Figure 4.5-2: Built up earth electrode**

## 4.6 TOWER FOOTING RESISTANCE IMPROVEMENT

Using the dimensions and equations presented previously the impedance of this electrode at low frequencies for a range of soil resistivities is shown in Figure 4.6-1, where for a soil resistivity of 1000 Ω.m, the resistance was 50 Ω. Installing two electrodes on a tower would reduce this to 25 Ω and considering the tower foundations further reduced the resistance.

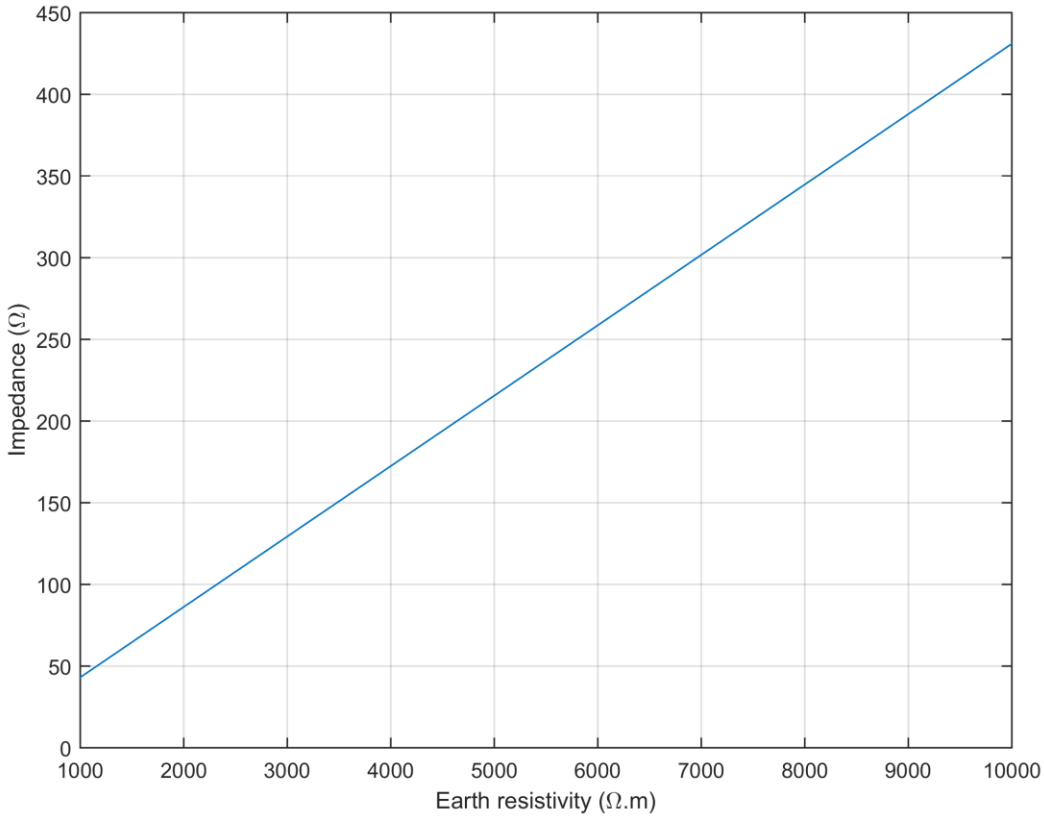


**Figure 4.6-1: Earth electrode resistivity against earth resistivity**

Earth electrodes were installed on all twenty towers used in the case study. Two earth electrodes were installed per tower (on opposite legs). This reduces tower footing resistance and adds redundancy in the event of a single electrode becoming disconnected.

The total material cost for correcting twenty towers was (at the time of the dissertation):

R 1800 per electrode × 2 electrode per tower × 20 towers = R72 000

The electrode was installed at a depth of 0.5 m and bolted onto a tower leg as low as possible. A sticker was also wrapped on the visible tail indicating that the material does not have scrap value to deter thieves.


**Figure 4.6-2: Installation pictures of the additional earthing**

## 4.7 PERFORMANCE OF THE LINE

After installing additional earthing on twenty towers, the tower footing resistances were measured. The results are displayed in Figure 4.7-1. It can be seen that all towers were below 20 Ω and there is good correlation to the simulated improvement.

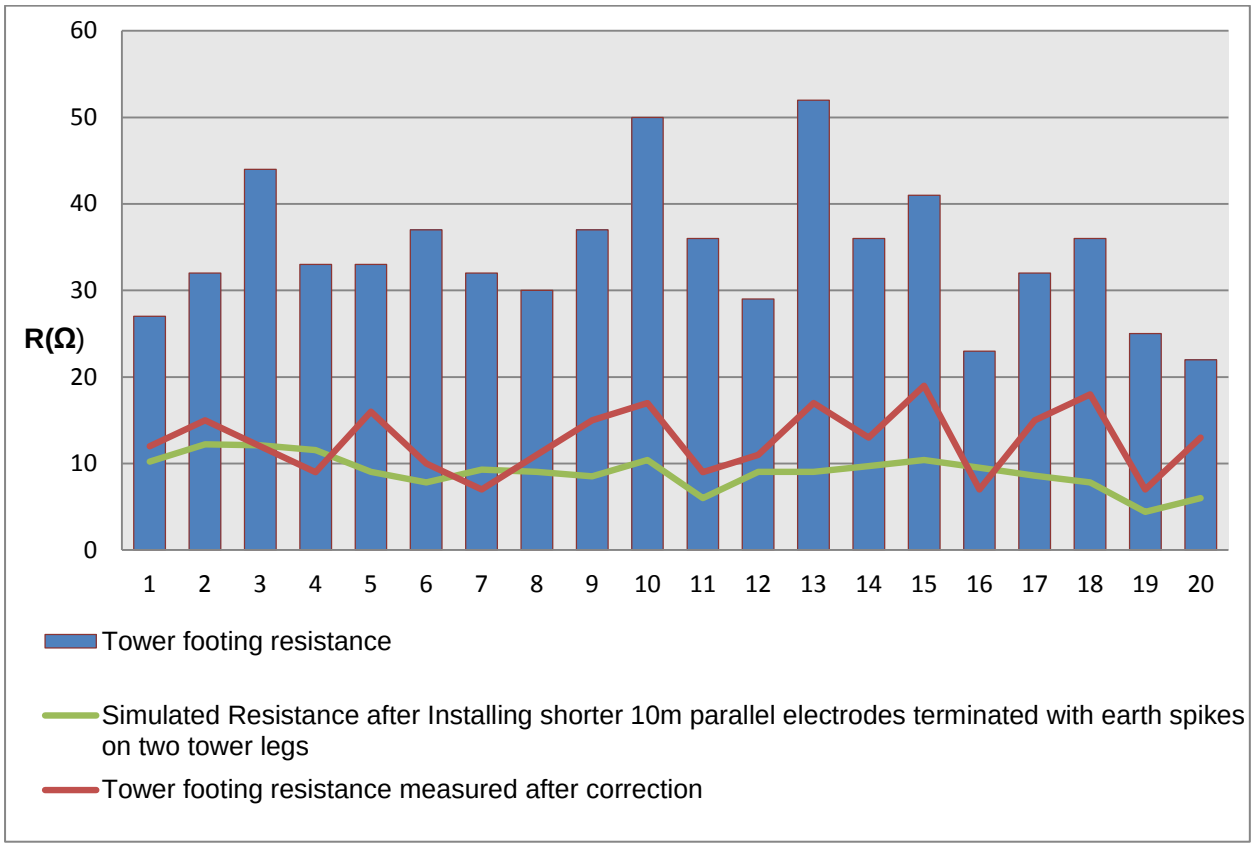


**Figure 4.7-1: Installation pictures of the additional earthing**

Although the results from TFlash are good approximations there would always be variances between the simulated results and measured results after correction due to the following variables:

- Soil resistivity
- Effect of soil ionisation around electrode in reducing tower footing resistance
- High frequency behaviour of electrode system
- Structure height
- Distance to adjacent towers
- Inductance in measuring equipment leads and cables etc.

The improvement in tower footing resistance reduced line backflashovers from 22 to 2 (91% improvement) in the simulated line section. The option of correcting earthing (R78 000) versus line surge arresters (R4.8 million) makes additional earthing the preferred solution. It also has the benefit of being maintenance free once installed. By correcting towers only in this line section it is expected that overall line performance would improve by 65% or more. The benefit of using shorter parallel electrodes was demonstrated during its initial response, within 2 μs, to a lightning impulse by reducing tower voltage rise and preventing insulator backflashovers.

The simulations done all indicated that shorter parallel electrodes outperform other electrode configurations in reducing tower footing resistance. The final electrode design is cost effective, practical and easy to install. The material selection acts as a theft deterrent and provides longevity against corrosion.

A total of 45 towers were corrected on the line used in this study in 2015. Prior to corrections the line averaged 54 lightning related trips per annum. After corrections the number of lightning related trips dropped to 12 (78% reduction) in 2016 and 9 (83% reduction) in 2017. The lightning exposure from 2010 – 2017 remained consistent thus the improvement in line performance is directly attributed to the reduction in tower footing resistance.

# CHAPTER 5 CONCLUSION AND RECOMMENDATIONS

This research highlights the importance of tower footing resistance on tower voltage rise during a lightning impulse. A lower resistance will lower the tower voltage rise thus reducing the risk of backflashovers. A section of line was modelled in an electromagnetic transient simulation program and its base case lightning performance calculated. The results showed the preferred method to improve line lightning performance was to reduce tower footing resistance.

The improvements in tower footing resistance from shorter parallel electrodes outperform other electrode configurations. This is shown with a high frequency electrode model, partial inductance electrode calculation and a FEMM electrode simulation. This is important as shorter electrodes require less material and installation costs compared to traditional longer electrodes. An electrode design was proposed and then installed on an 88 kV line. The measured tower footing resistance after installation of electrodes showed the simulated improvement correlated with the actual measured improvement.

Currently, line transient programs cannot account for the wide band frequency response of the ground electrode. Future work should entail incorporating a high frequency ground electrode model into a line transient program like TFlash. A soil model must also be developed. This will create an accurate assessment of soil ionisation for different soil types surrounding the electrode. The ultimate solution is to incorporate all three aspects into one model i.e. the line transient model, the high frequency ground electrode model and a soil model.

This electrode design is currently being used by Eskom KZN. It is a complete solution with only excavation work required to install it. Once installed the electrode is maintenance free. The material selection caters for theft while maintaining electrical and mechanical integrity. It is envisioned that this electrode design be incorporated into the national standard for high voltage tower earthing covering system voltages from 66 kV to 765 kV.

# REFERENCES


[1] EPRI, EPRI AC Transmission Line Reference Book—200 kV and Above, Palo Alto, CA: EPRI, 2005.

[2] ESKOM, "Distribution Standard Part 6: Sub-Transmission Lines Section 6: Earthing of Sub-Transmission Line Structures," ESKOM, 2002.

[3] EPRI, "Handbook for Improving Overhead Transmission Line Lightning Performance," EPRI, Palo Alto, CA, 2004. 1002019.

[4] IEEE, "Guide for Improving the Lightning Performance of Transmission Lines," IEEE, 1243/1997.

[5] D. Kosc and P. S. Hamer, "Grounding Practices—A System-Wide Systematic Approach," *IEEE Transactions on Industry Applications,* vol. 39, no. 5, October 2003..

[6] EPRI, "Guide for Transmission Line Grounding: A Roadmap for Design Testing and Remediation: Part I—Theory Book," EPRI, Palo Alto, CA, 2008. 1013900.

[7] EPRI, "The Lightning Flash and Its Parameters," in *Overhead Transmission Line Lightning and Grounding Reference Book*, Palo Alto, CA, EPRI, 2013, p. 35.

[8] EPRI, "Chapter 6: Lightning and Grounding," in *EPRI AC Transmission Line Reference Book—200 kV and Above*, Palo Alto, CA, EPRI, December 2005, p. 362.

[9] IEEE, "IEEE Standard 4. IEEE Guide for High Voltage testing," IEEE, Piscataway, N.J., 2000.

[10] CIGRE, "Guide to Procedures for Estimating the Lightning Performance of Transmission Lines," in *Working Group 01 (Lightning) of Study Committee 33 (Overvoltages and Insulation Co-ordination),* Paris, 1991.

[11] M. A. Uman, "The Lightning Flash," in *Academia Press*, San Diego, 1987.

[12] R. B. Anderson and A. J. Eriksson, "Lightning Parameters for Engineering Application," *Electra,* vol. 69, pp. 65-102, 1980.

[13] A. J. Eriksson, "The Incidence of Lightning Strikes to Power Lines," *IEEE Transactions on Power Delivery,* vol. 2, no. 3, p. 859–870, July 1987.

[14] M. Gijben , "The lightning climatology of South Africa," *S Afr J Sci,* vol. 108, no. 3, 2012.

[15] EPRI, "Chapter 6," in *Overhead Transmission Line Lightning and Grounding Reference Book*, Palo

Alto, California, EPRI, 2013, pp. 270 - 272.

[16] EPRI, “An Approach for Using TFlash to Improve the Lightning Performance of Transmission Lines,” EPRI, Palo Alto, California, December 2009.

[17] EPRI, “An Approach for Using TFlash to Improve the Lightning Performance of Transmission Lines,” in *Chapter 2: LIGHTNING PERFORMANCE OF TRANSMISSION LINES*, Palo Alto, California, EPRI, December 2009, pp. 37-40.

[18] A. R. Hileman, “Insulation Coordination for Power Systems,” in *Marcel Decker*, New York, 1999.

[19] A. M. Mousa, “The Soil Ionization Gradient Associated With Discharge of High Currents Into Concentrated Electrodes,” *IEEE Trans. on Power Delivery,* vol. 9, no. 3, July 1994.

[20] B. Thapar, V. Gerez and A. Balakrishnan, “Ground Resistance of Concrete Encased Electrodes - Field Tests,” *Proceedings of the American Power Conference,* vol. 52, pp. 421-425, 1990.

[21] A. C. Liew and M. Darveniza, “Dynamic Model of Impulse Characteristics of Concentrated Earths,” *Proceedings of the IEE,* vol. 121, no. 2, Feb. 1974..

[22] EPRI, “Tower Grounding and Soil Ionization Report,” EPRI, Palo Alto, CA, 2002. 1001908.

[23] K. H. Weck, “The Current Dependence of Tower Footing Resistance,” CIGRÉ 33-88 (WG01), 14IWD, 1988 and 33-89 (WG 01), 7IWD, 1989.

[24] IEC, “Insulation co-ordination—Part 4: Computational guide to insulation coordination and modelling of electrical networks,” TR 60071-4, Jun. 2004.

[25] M. Heimbach and L. D. Grcev, “Grounding system analysis in transients programs applying electromagnetic field approach,” *IEEE Trans. Power Del,* Vols. 12, no. 1, p. 186–193, Jan. 1997.

[26] K. Sheshyekani, M. Akbari, B. Tabei and R. Kazemi, “Wideband modeling of large grounding systems to interface with electromagnetic transient solvers,” *IEEE Trans. Power Del,* Vols. 29, no. 4, p. 1868–1876, Aug. 2014.

[27] A. Holdyk and B. Gustavsen, “Inclusion of Field-Solver-Based Tower Footing Grounding Models in Electromagnetic Transient Programs,” *IEEE,* vol. 51, no. 6, NOVEMBER/DECEMBER 2015.

[28] M. . R. Alemi and K. Sheshyekani, “Wide-Band Modeling of Tower-Footing Grounding Systems for the Evaluation of Lightning Performance of Transmission Lines,” *IEEE TRANSACTIONS ON ELECTROMAGNETIC COMPATIBILITY,* vol. 57, no. 6, pp. 1627 - 1637, DECEMBER 2015.

[29] M. Ahmeda, N. Ullah, N. Harid, H. Griffiths and A. Haddad, “Current and voltage distribution in a

horizontal earth electrode under impulse conditions," in *Proceedings of the 44th International Universities Power Engineering Conference*, Glasgow, UK, 2009.

[30] J. Choi, J. Kim, B. Lee and Y. Chung, "An analysis of conventional grounding impedance based on the impulsive current distribution of a counterpoise," in *Proceeding of 30th International Conference On Lightning Protection*, Cagliari, Italy, 2009.

[31] EPRI, EPRI Transmission Line Reference Book—345 kV and Above, Second Edition, Revised, Palo Alto, CA, 1987.

[32] CIGRE Working Group 33-01, "Guide to procedures for estimating the lightning performance of transmission lines," CIGRE Brochure 63, October 1991.

[33] EPRI, "EPRI Zed-Meter v3.0 Software Manual," EPRI, Palo Alto, California, November 2013.

[34] CIGRE, "Methods for measuring the earth resistance of transmission towers equipped with earth wires," CIGRE Brochure 275, June 2005.

[35] IEEE, "Guide for improving the lightning performance of electric power overhead distribution lines," IEEE Standard 1410, 2004.

[36] L. Grcev, "High-frequency grounding," in *Lightning Protection*, London, United Kingdom, The Institution of Engineering and Technology, 2010, pp. 536-559.

[37] P. R. Clayton, "The Concept of Partial Inductance," in *Inductance: Loop and Partial*, Hoboken, New Jersey, John Wiley & Sons, Inc., 2010, pp. 211-261.

[38] D. Meeker, "Finite Element Method Magnetics User's Manual," October 25, 2015.

[39] W. A. Chisholm, and W. Janischewskyj, "Lightning Surge Response of Ground Electrodes," *IEEE Trans on Power Delivery,* Vols. PWRD-4, no. 2, pp. 1329-1337, 1989.

[40] NRS 102:2014, "Theft deterrent earthing materials," SABS, 2014.

[41] Y. Baba and M. Ishii., "Numerical Electromagnetic Field Analysis on Lightning Surge Response of Tower with Shield Wire," *IEEE Transactions on Power Delivery,* vol. 15, no. 3, 2000.

# APPENDIX A: TOWER FOOTING RESISTANCE

**Table 0-1: Tower footing resistance before and after correction and values used in simulation**

| Tower number | Tower footing resistance | Number of Strikes per year | Simulated Resistance: 60m electrode on two tower legs | Simulated Resistance:10m parallel electrodes terminated with earth spikes on two tower legs | Tower footing resistance measured after correction | % Improvement |
|---|---|---|---|---|---|---|
| 22 | 27 | 40 | 9.3 | 10.2 | 12 | 55.56% |
| 23 | 32 | 40 | 11.1 | 12.2 | 15 | 53.13% |
| 24 | 44 | 40 | 11 | 12.1 | 12 | 72.73% |
| 25 | 33 | 40 | 10.5 | 11.6 | 9 | 72.73% |
| 26 | 33 | 40 | 8.2 | 9.0 | 16 | 51.52% |
| 27 | 37 | 40 | 7.1 | 7.8 | 10 | 72.97% |
| 28 | 32 | 40 | 13 | 9.3 | 7 | 78.13% |
| 29 | 30 | 40 | 9.3 | 9.0 | 11 | 63.33% |
| 30 | 37 | 40 | 8.8 | 8.5 | 15 | 59.46% |
| 31 | 50 | 40 | 14.9 | 10.4 | 17 | 66.00% |
| 32 | 36 | 40 | 6.2 | 6.0 | 9 | 75.00% |
| 33 | 29 | 40 | 9.3 | 9.0 | 11 | 62.07% |
| 34 | 52 | 40 | 9.3 | 9.0 | 17 | 67.31% |
| 35 | 36 | 40 | 10 | 9.7 | 13 | 63.89% |
| 36 | 41 | 40 | 11 | 10.4 | 19 | 53.66% |
| 37 | 23 | 40 | 10.5 | 9.5 | 7 | 69.57% |
| 38 | 32 | 40 | 8.2 | 8.6 | 15 | 53.13% |
| 39 | 36 | 40 | 7.1 | 7.8 | 18 | 50.00% |
| 40 | 25 | 40 | 4 | 4.4 | 7 | 72.00% |
| 41 | 22 | 40 | 6.3 | 6 | 13 | 40.91% |

# APPENDIX B: FEMM MODELS

## A.1 CURRENT DISTRIBUTION

The results below are from the FEMM model where the skin effect was assessed. The model compared a copper clad steel (CCS) to a pure copper conductor (Cu). The CCS conductor has a total diameter of 7 mm with a steel core of 6.8 mm and copper covering of 0.2 mm. The conductivities for the copper and steel were 58 x $10^6$ S/m and 20 x $10^6$ S/m respectively and the relative permeabilities were 1 and 1000 respectively. The conductor was located 1 m below the surface of the soil. The soil has a conductivity of 1000 Ω.m and a relative permeability of 1 the magnetic vector potential at the boundary was set to 0. The current was set to 1 A through the circuit and the frequency was altered to ascertain the effect of frequency on the distribution of the current in the conductor.

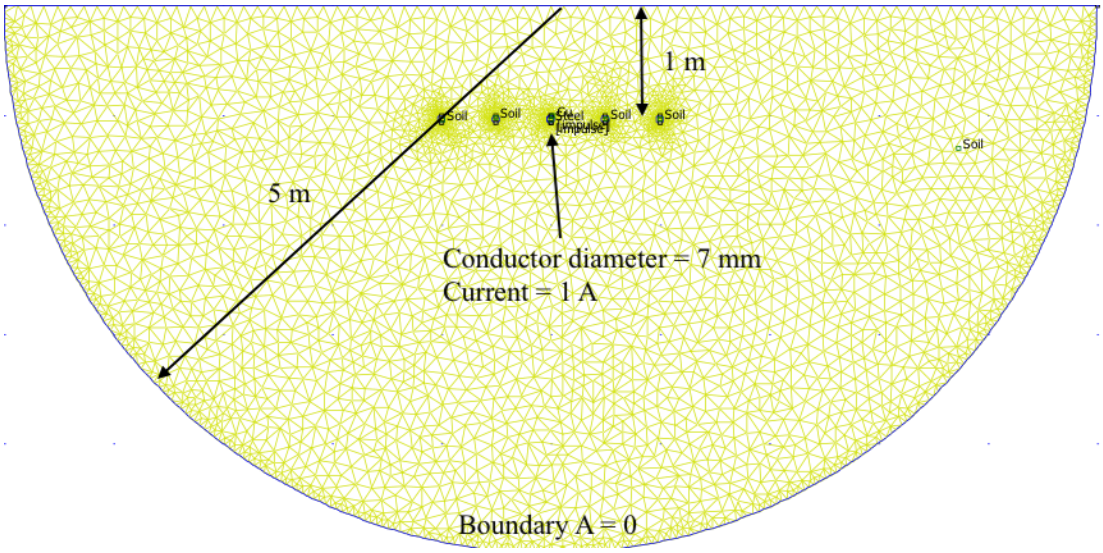


**Figure 0-1: Geometry with details and mesh**

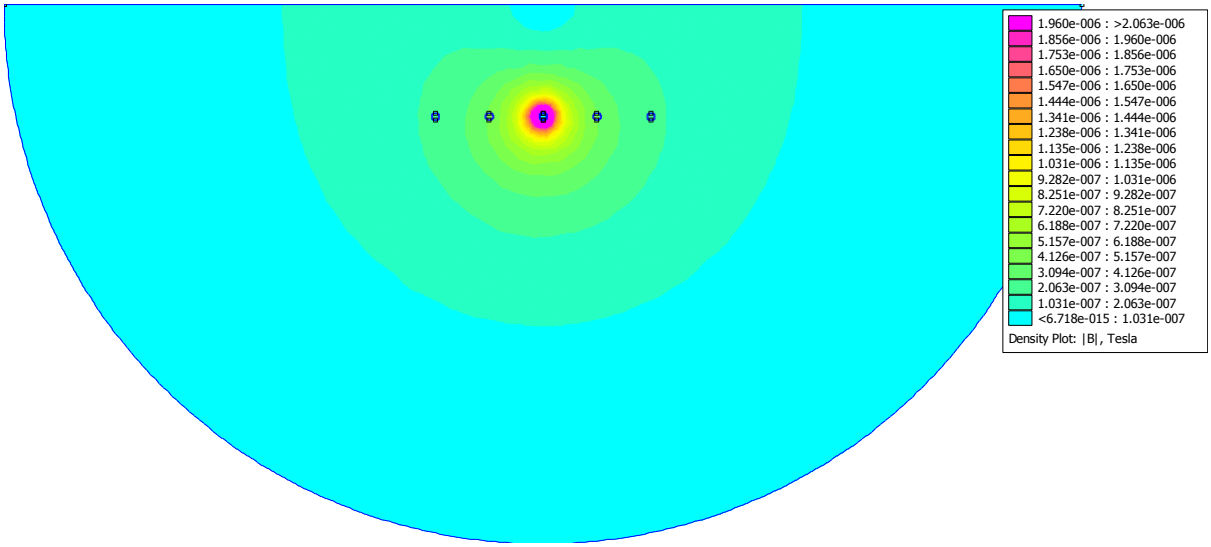


**Figure 0-2: Magnetic flux distribution around conductor**

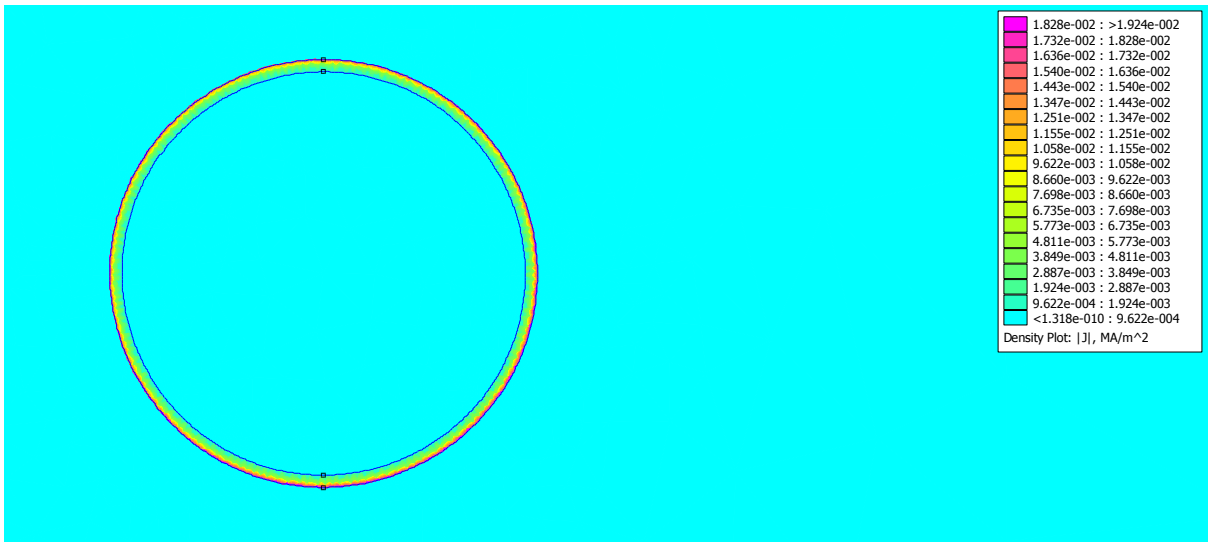


**Figure 0-3: CCS conductor at 50 kHz where 0.99 A was in copper layer and the remaining current was in steel**

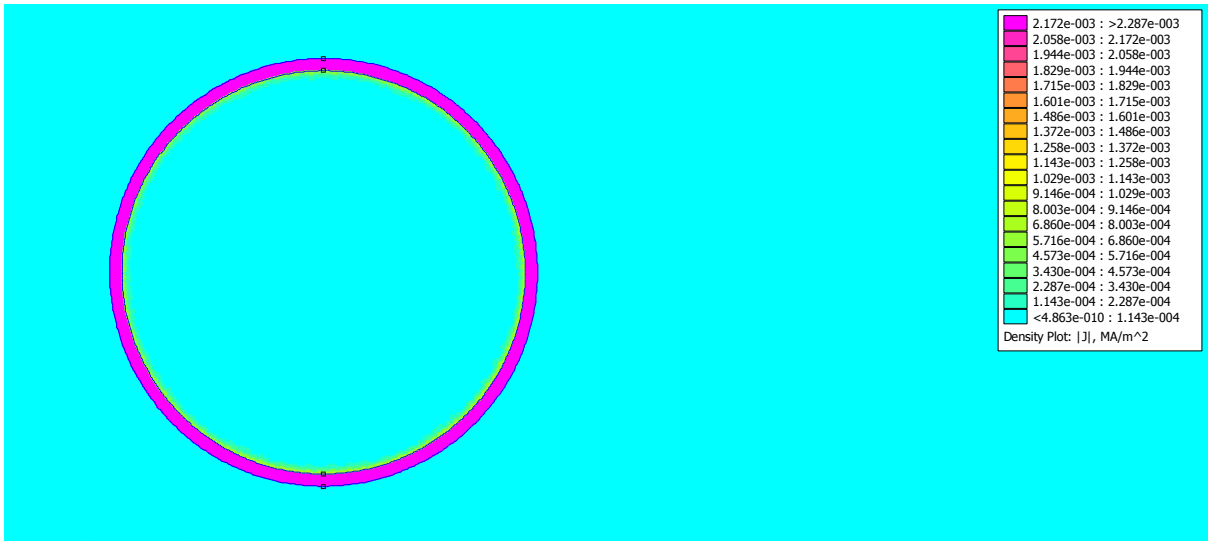


**Figure 0-4: CCS conductor at 50 Hz where 0.96 A was in copper layer and the remaining current was in steel**

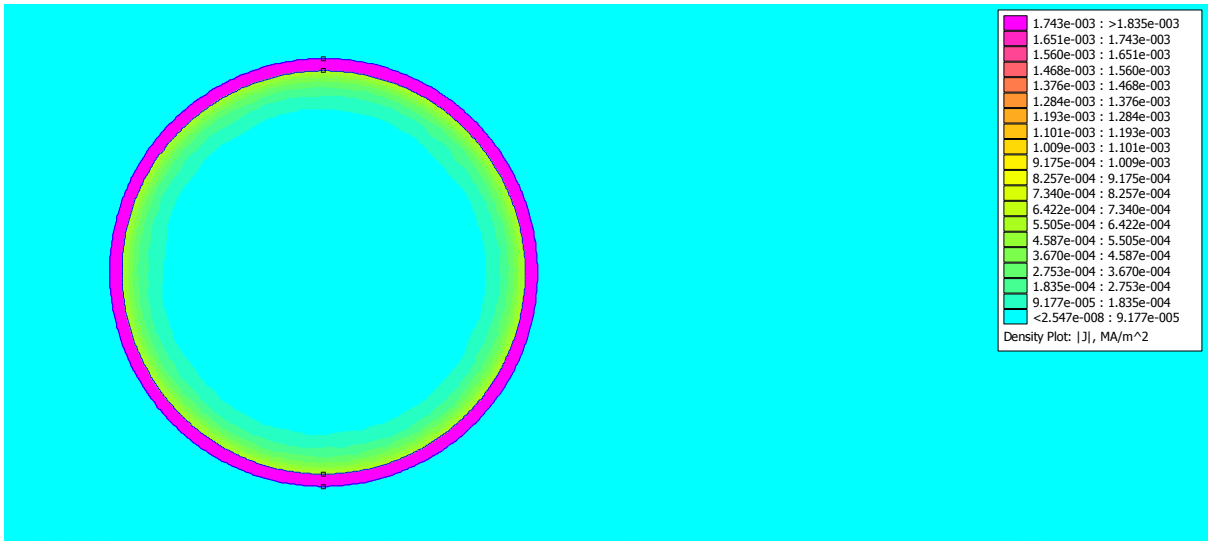


**Figure 0-5: CCS conductor at 1 Hz where 0.77 A was in the copper layer and the remaining current was in steel**

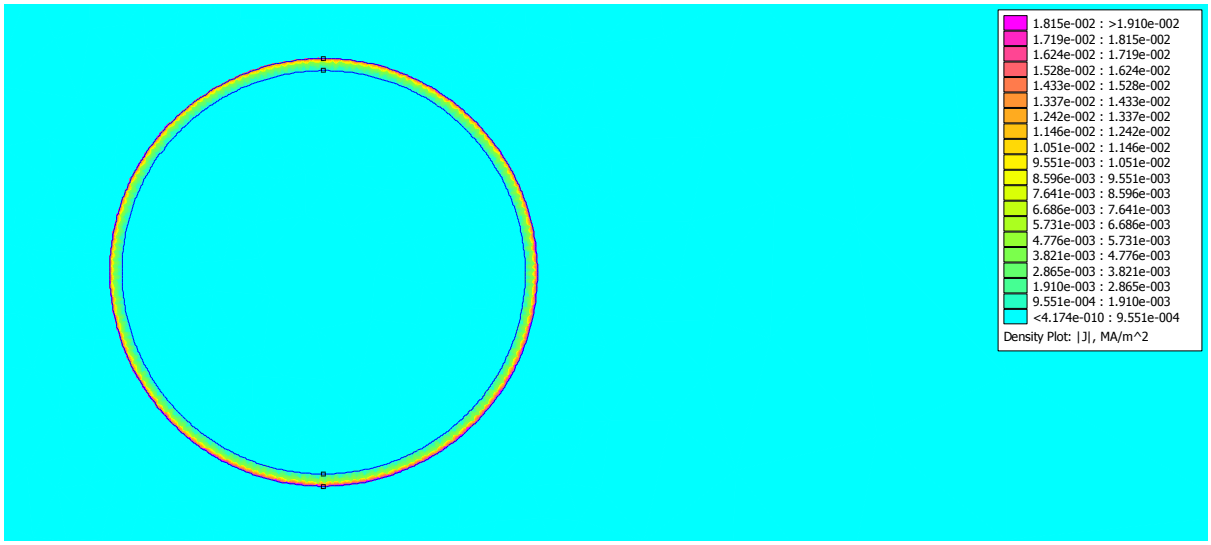


**Figure 0-6: Cu conductor at 50 kHz demonstrating current distribution in a conductor including skin effect**

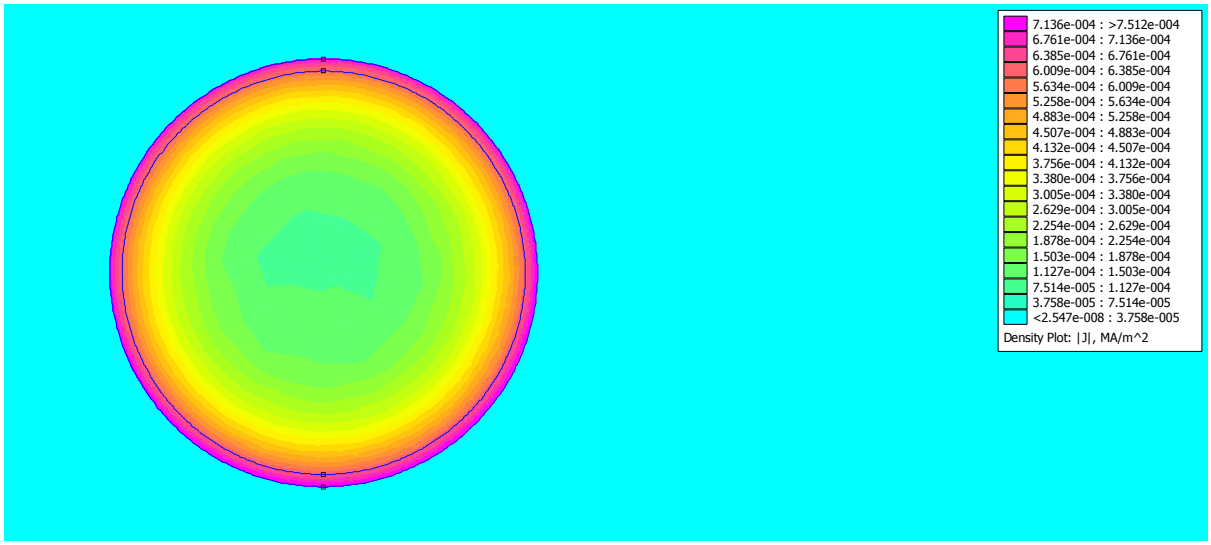


**Figure 0-7: Cu conductor at 50 Hz demonstrating current distribution in a conductor including skin effect**

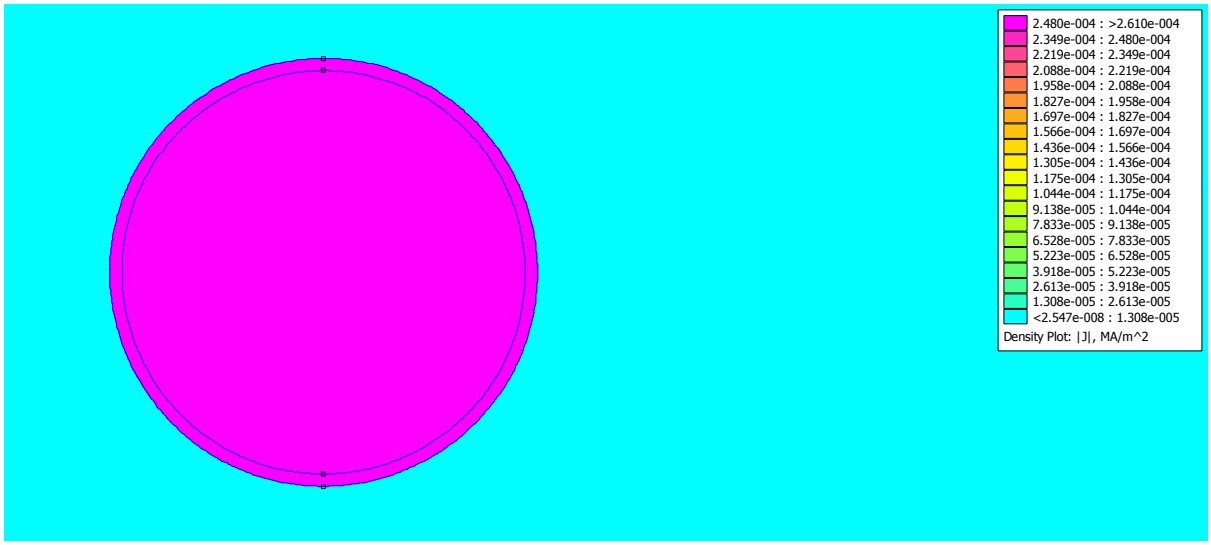


**Figure 0-8: Cu conductor at 1 Hz demonstrating current distribution in a conductor**

## A.2 EARTH ELECTRODE RESISTANCE

Figure 0-1 shows the voltage plot around a 1.5 m vertical rod with a soil resistivity of 1000 Ω.m. The density is greatest around the outer surface of the electrode and decreases as the distance from the electrode increases. If the voltage gradient around the electrode is high enough it may exceed the critical soil ionisation gradient depending on soil type. This may lead to soil ionisation which will reduce the overall earth impedance.

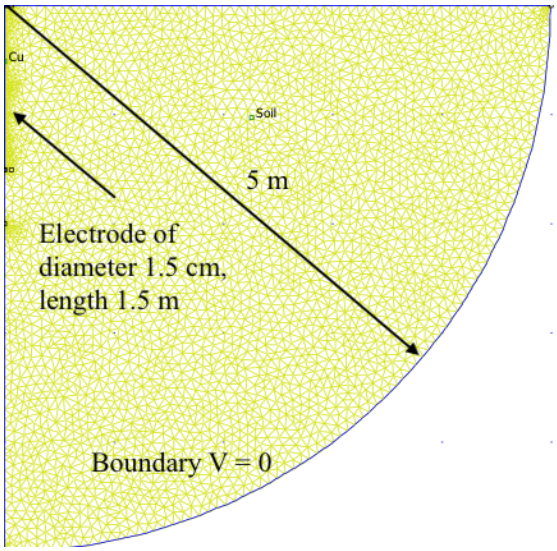


**Figure 0-1: Vertical rod**

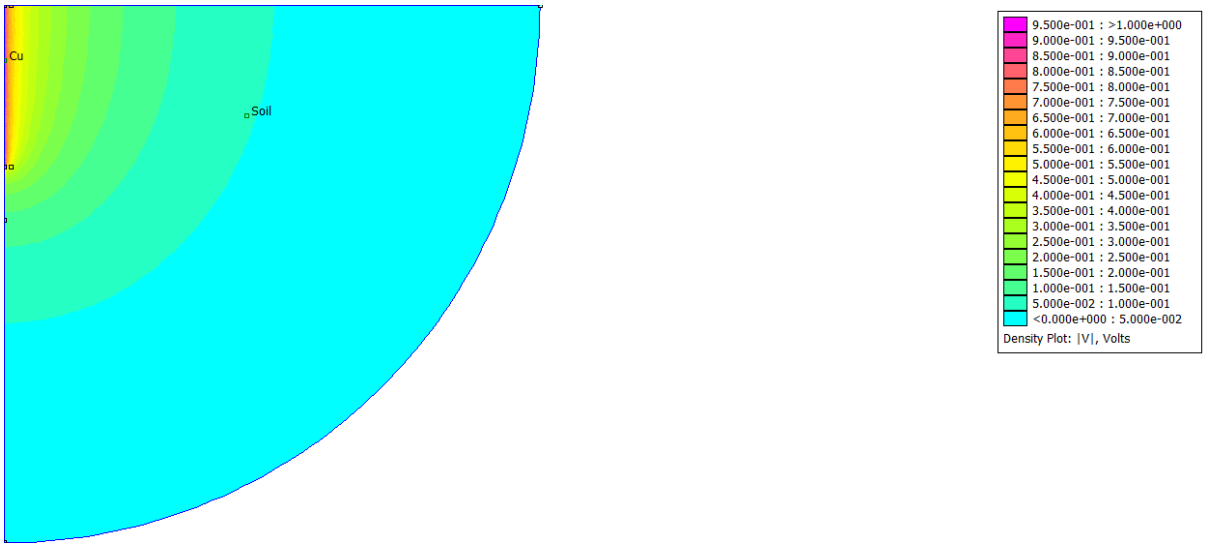


**Figure 0-2: Resistance of earth electrode is 588 Ω Ohms**

For a horizontal electrode configuration, the three 10 m horizontal conductors were simulated to show the interaction of parallel current carrying conductors and the effect of conductor spacing. The conductor voltage was set at 1V with a soil resistivity of 1000 Ω.m. The boundary was set at 0 V.

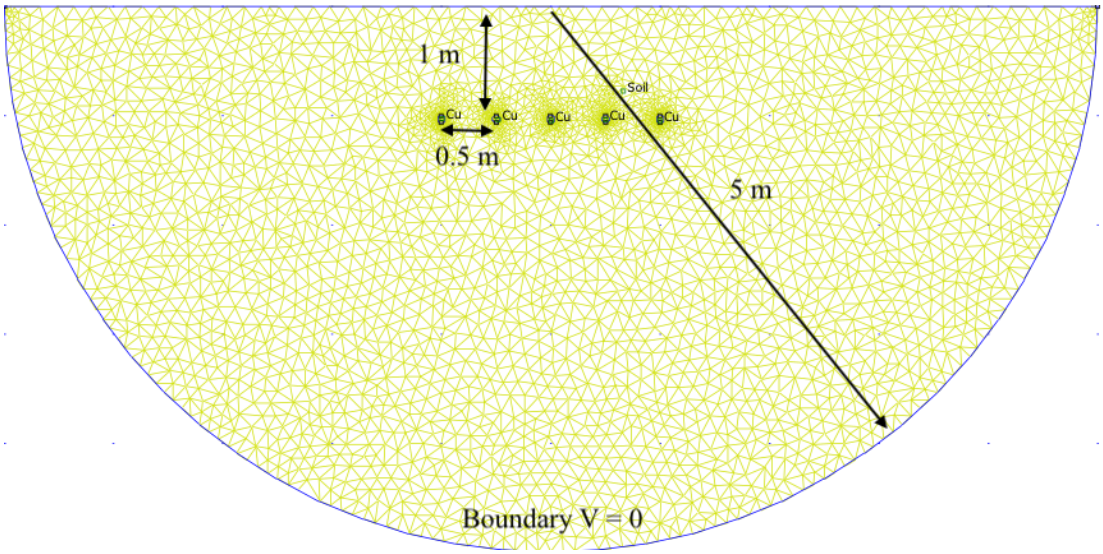


**Figure 0-3: Resistance of 5 parallel horizontal earth electrodes was 50 Ω**

A single 10 m horizontal conductor was simulated and its resistance was calculated. The total resistance calculated was 91 Ω. The steepest voltage gradient is observed around the conductor.

A simulation of three parallel horizontal conductors (each 10 m CCS conductor) was then done using the same circuit conditions. The spacing between conductors was varied and the results are shown in Table 0-1.

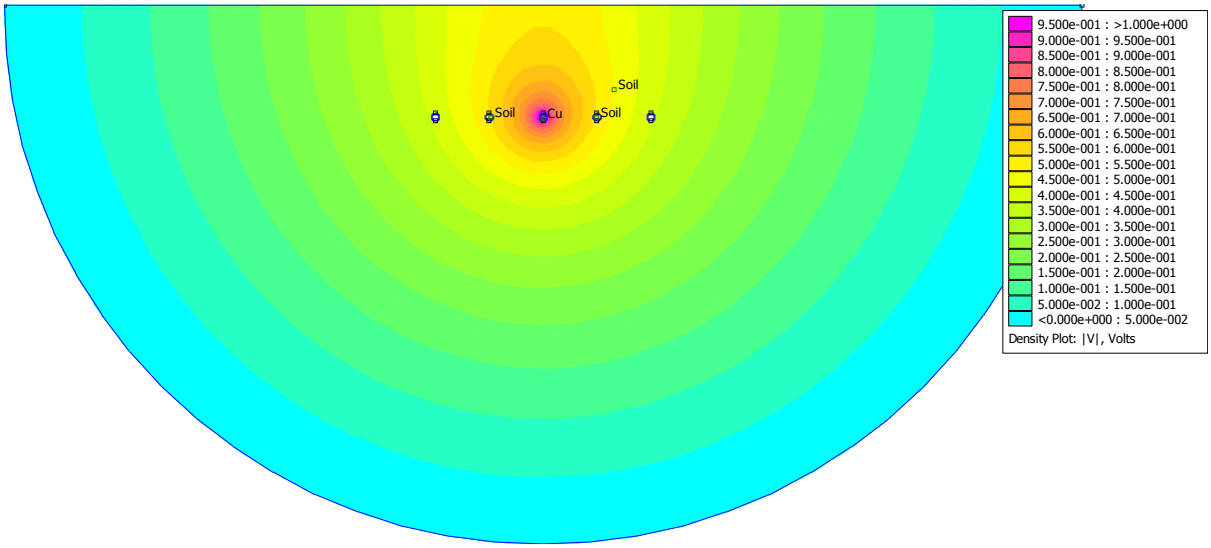


**Figure 0-4: Resistance of 1 horizontal earth electrode is 92 Ω**

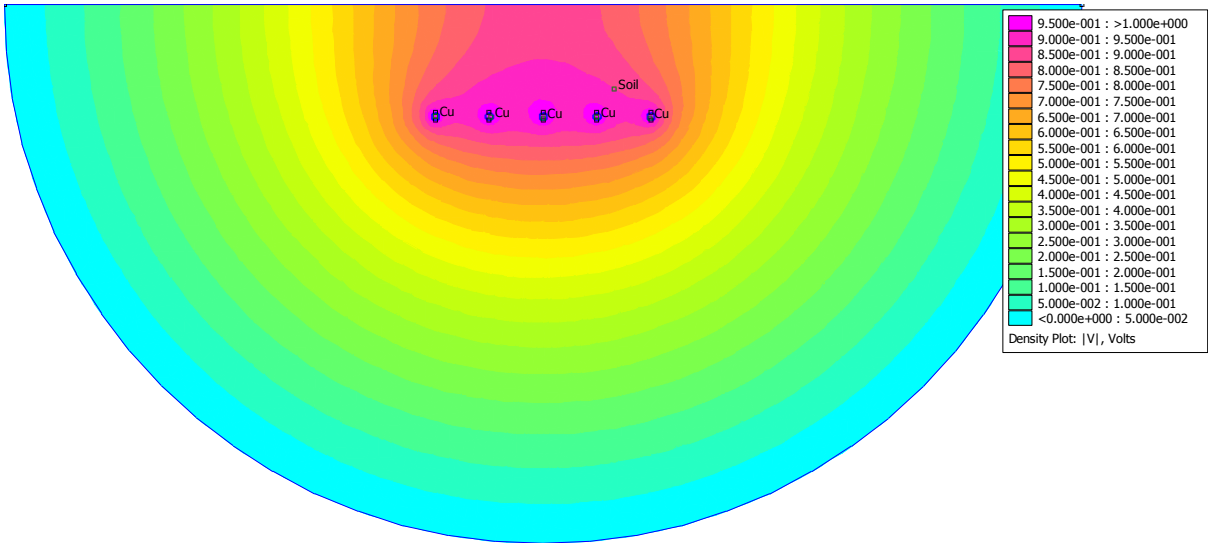


**Figure 0-5: Resistance of 5 parallel horizontal earth electrodes is 50 Ω**

**Table 0-1: Earth electrode resistance from FEMM**

| Electrode | Resistance (Ω) |
|---|---|
| 1 vertical rod | 320 |
| 1 horizontal conductor | 91 |
| 3 parallel horizontal conductors spaced 1 m apart | 53 |
| 3 parallel horizontal conductors spaced 0.5 m apart | 61 |
| 3 parallel horizontal conductors spaced 2 m apart | 41 |
| 5 parallel horizontal conductors spaced 0.5 m apart | 50 |

The total resistance reduced as the separation distance between conductors increased. The difference between 1 parallel conductor and multiple parallel conductors is evident as the total resistance decreased significantly. The difference between 3 and 5 conductors spaced between 0.5 m and 1 m apart had less of an impact in reducing the total resistance. For 3 independent parallel electrodes one would expect the resistance to be around 30 Ω, however this does not take into account the coupling between the conductors, the potential gradient appeared to be important in the total resistance and the electrodes that were further apart performed better. In the case presented, the optimum performance of the electrode could be achieved by fewer parallel conductors spaced further apart.

# APPENDIX C – MATLAB CODE

## C.1 EARTH.M

```
clear
rho = 1000;                         % Ohm.m
r = 0.007;                  % m

mu_0 = pi*4e-7;                     % H/m
eps_0 = 8.85e-12;

eps = 10;
mu = 1000;

f = 1:1e1:10e6;
w = 2*pi*f;



% Single electrode
l = 1.5;                            % m

Zw1 = rod(f,10,l,r,mu_0,eps*eps_0);
Zw2 = rod(f,100,l,r,mu_0,eps*eps_0);
Zw3 = rod(f,1000,l,r,mu_0,eps*eps_0);

Zr1 = rod(f,1000,l,r,mu_0,eps*eps_0);
Zr2 = rod(f,1000,3,r,mu_0,eps*eps_0);
Zr3 = rod(f,1000,10,r,mu_0,eps*eps_0);



%Plotting

figure(1),semilogx(f/1000,abs(Zw1),f/1000,abs(Zw2),f/1000,abs(Zw3)), grid on, xlabel('Frequency (kHz)'),ylabel('Impedance ({\Omega})'),legend('1.5 m 10 {\Omega}.m','1.5 m 100 {\Omega}.m','1.5 m 1000 {\Omega}.m'),print('rod1.png','-dpng','-r300')
```

```
figure(2),semilogx(f/1000,abs(Zr1),f/1000,abs(Zr2),f/1000,abs(Zr3)), grid on, xlabel('Frequency (kHz)'),ylabel('Impedance ({\Omega})'),legend('1.5 m 1000 {\Omega}.m','3 m 1000 {\Omega}.m','10 m 1000 {\Omega}.m'),print('rod2.png','-dpng','-r300')



% Radial

d = 1;

Zw1 = radial(f,10,10,r,d,mu_0,eps_0*eps);

Zw2 = radial(f,100,10,r,d,mu_0,eps_0*eps);

Zw3 = radial(f,1000,10,r,d,mu_0,eps_0*eps);

Zr1 = radial(f,1000,10,r,d,mu_0,eps_0*eps);

Zr2 = radial(f,1000,60,r,d,mu_0,eps_0*eps);

Zr3 = radial(f,1000,100,r,d,mu_0,eps_0*eps);

Zrod = rod(f,1000,l,r,mu_0,eps*eps_0)/3;

Zradial = par(f,1000,5,r,d,mu_0,eps_0*eps);

ang = 30;

Zcrow = crow(f,1000,5,r,d,ang,mu_0,eps_0*eps);

figure(4),semilogx(f/1000,abs(Zrod),f/1000,abs(Zradial),f/1000,abs(Zcrow)), grid on, xlabel('Frequency (kHz)'),ylabel('Impedance ({\Omega})'),legend('Rod','Radial','Crow'),print('compare.png','-dpng','-r300')

%Plotting

figure(5),semilogx(f/1000,abs(Zr1),f/1000,abs(Zr2),f/1000,abs(Zr3)), grid on, xlabel('Frequency (kHz)'),ylabel('Impedance ({\Omega})'),legend('10 m 1000 {\Omega}.m','60 m 1000 {\Omega}.m','100 m 1000 {\Omega}.m'),print('radial1.png','-dpng','-r300')

figure(6),semilogx(f/1000,abs(Zw1),f/1000,abs(Zw2),f/1000,abs(Zw3)), grid on, xlabel('Frequency (kHz)'),ylabel('Impedance ({\Omega})'),legend('10 m 10 {\Omega}.m','10 m 100 {\Omega}.m','10 m 1000 {\Omega}.m'),print('radial2.png','-dpng','-r300')

fi = 5000;

ang = 30;

rho = 1000:1000:10000;

Zrod = rod(fi,rho,l,r,mu_0,eps*eps_0)/3;

Zradial = radial(fi,rho,5,r,d,mu_0,eps_0*eps);
```

```
Zcrow = crow(fi,rho,5,r,d,ang,mu_0,eps_0*eps);

Ztotal = (1./Zradial+1./Zcrow+1./Zrod).^-1;


figure(9),plot(rho,abs(Ztotal)), grid on, xlabel('Earth resistivity (\Omega.m)'),ylabel('Impedance ({\Omega})'),print('total.png','-dpng','-r300')



% Skin effect for copper clad steel versus copper


sig_cu = 58e6;

sig_ccs = 20e6;


del_cu = sqrt(2./w/mu_0/sig_cu)*1000;

del_ccs = sqrt(2./w/mu/mu_0/sig_ccs)*1000;



figure(12),loglog(f/1000,del_cu,f/1000,del_ccs), grid on, xlabel('Frequency (kHz)'),ylabel('Skin Depth ({mm})'),legend('Copper','Steel'),print('skin.png','-dpng','-r300')

function [Z] = par(f,rho,l0,r,d,mu,eps)



w = 2*pi*f;


A2 = log(2*l0/sqrt(2*r*d))-1;


Rr = rho/pi/l0*A2/3

%Lr = l0*mu/2/pi*A2


% Inductance

s = 0.5;

Lp = self(l0,r);

M1 = muts(5,s);

M2 = muts(5,2*s);


x =  1;

R = 0;
```

```
Zs = [R+j*x*Lp 0 0;
   0 R+j*x*Lp 0;
   0 0 R+j*x*Lp];

Zm = j*x*[0 M1 M2;
   M1 0 M1;
   M2 M1 0];

Z = (Zs+Zm);

Z = Z^-1;

V = ones(3,1);

I = Z*V;

Zt = 1/sum(I);
Lr = imag(Zt)/x;

% Capacitance
Cr = 3*l0*pi*eps/A2;

Grp = 1/(Rr*l0);
Lrp = Lr/l0;
Crp = Cr/l0;

Zr = sqrt(i*w*Lrp./(Grp+i*w*Crp));
gr = sqrt(i*w*Lrp.*(Grp+i*w*Crp));

Z = Zr.*coth(gr*l0);

End

function [Z] = radial(f,rho,l0,r,d,mu,eps)
```

```
w = 2*pi*f;

A2 = log(2*l0/sqrt(2*r*d))-1;

Rr = rho/pi/l0*A2
Lr = l0*mu/2/pi*A2;
Cr = l0*pi*eps/A2;

Grp = 1./(Rr*l0);
Lrp = Lr/l0;
Crp = Cr/l0;

Zr = sqrt(i*w*Lrp./(Grp+i*w*Crp));
gr = sqrt(i*w*Lrp.*(Grp+i*w*Crp));

v = 1/sqrt(Lrp.*Crp);
v = v/1e6

Z = Zr.*coth(gr*l0);

End

function [Z] = crow(f,rho,l0,r,d,ang,mu,eps)


w = 2*pi*f;

A2 = log(2*l0/sqrt(2*r*d))-1;

Rr = rho/pi/l0*A2/3;
%Lr = l0*mu/2/pi*A2

% Inductance
Lp = self(l0,r);
```

```
M1 = muta(l0,ang);
M2 = muta(l0,2*ang);

x =  1;
R = 0;

Zs = [R+j*x*Lp 0 0;
   0 R+j*x*Lp 0;
   0 0 R+j*x*Lp];

Zm = j*x*[0 M1 M2;
   M1 0 M1;
   M2 M1 0];

Z = (Zs+Zm);

Z = Z^-1;

V = ones(3,1);
I = Z*V;
Zt = 1/sum(I);
Lr = imag(Zt)/x;

% Capacitance
Cr = 3*l0*pi*eps/A2;
Grp = 1./(Rr*l0);
Lrp = Lr/l0;
Crp = Cr/l0;

Zr = sqrt(i*w*Lrp./(Grp+i*w*Crp));
gr = sqrt(i*w*Lrp.*(Grp+i*w*Crp));

Z = Zr.*coth(gr*l0);

end
```

## C.2 INDUCTANCE.M

```
clear

rho = 100;              % Ohm.m
r = 0.007;              % m

mu_0 = pi*4e-7;                 % H/m
eps_0 = 8.85e-12;

eps = 10;
mu = 100*mu_0;

f = 1:1e3:50e6;
w = 2*pi*f;

%figure(1),semilogx(f/1000,abs(Zw1)), grid on, xlabel('Frequency (kHz)'),ylabel('Impedance ({\Omega})'),legend('1.5 m 10 {\Omega}.m','1.5 m 100 {\Omega}.m','1.5 m 1000 {\Omega}.m'),print('rod1.png','-dpng','-r300')



% Self partial inductance
d = 0.5;
Lin = mu/8/pi
Lp = self(5,r)
M1 = muts(5,d);
M2 = muts(5,2*d);
%M3 = muts(5,0.707);

w = 100e3;
R = 0;

Zs = [R+j*w*Lp 0 0;
   0 R+j*w*Lp 0;
   0 0 R+j*w*Lp];
```

```
Zm = j*w*[0 M1 M2;
   M1 0 M1;
   M2 M1 0];

Z = (Zs+Zm);

Z = Z^-1;

V = ones(3,1);

I = Z*V;
Zt = 1/sum(I)
Lt1 = imag(Zt)/w*ones(1,45);


% Impedance of a crows foot
Zt = 0;
Lt = 0;
for n = 1:45

theta = n*1;

Lp = self(5,r);
M1 = muta(5,theta);
M2 = muta(5,2*theta);


w =  1e5;
R = 0;

Zs = [R+j*w*Lp 0 0;
   0 R+j*w*Lp 0;
   0 0 R+j*w*Lp];

Zm = j*w*[0 M1 M2;
```

```
   M1 0 M1;
   M2 M1 0];

Z = (Zs+Zm);

Z = Z^-1;

V = ones(3,1);

I = Z*V;

Zt(n) = 1/sum(I);
Lt(n) = imag(Zt(n))/w;

end



% plotting
ang = 1:1:45;

figure(3), plot(ang,Lt/1e-6,ang,Lt1/1e-6), grid on, xlabel('Angle (degrees)'),ylabel('Inductance ({\mu H})'),legend('Angled Conductors','Parallel Conductors'),print('foot.png','-dpng','-r300')

function [Mpa] = muta(l,theta) % Mutual partial inductance - Angled conductor

R = sqrt(2*l^2-2*l^2*cosd(theta));
Mpa = 1e-7*cosd(theta)*2*log((R+2*l)/R);

end

function [Mp] = muts(l,d) % Mutual partial inductance - Parallel conductor

Mp = 2e-7*l*(log(l./d+sqrt((l./d).^2+1))-sqrt(1+(d./l).^2)+d./l);

end
```

```
function [Lp] = self(l,r)


Lp = 2e-7*l*(log(2*l/r-1));


end
```